DEVELOPMENT OF A MATHEMATICAL MODEL OF THE THERMAL DECOMPOSITION OF HYDRAZINE IN AN ENGINE

by

J.R. Sanmartín
E. Fraga
A. Liñán
A. Crespo

Instituto Nacional de Técnica Aeroespacial "Esteban Terradas".
MADRID. (Spain).

Technical Management by:

H.A. Pfeffer

MARCH 1978

ABSTRACT

An overall chemical kinetics for the decomposition of hydrazine has been found for temperatures near 800°K and 1000°K which can be used in the gas-dynamic equations of the engine when the mechanical or residence time of the engine is large compared with the radicals relaxation time. This overall kinetics is used for an steady state analysis using the approximation of perfectly stirred reactor, for times both shorter and larger than the time for wall temperature to reach a steady condition; the validity of these approximations is studied. An alternative plug flow model in which heat is conducted upstream by solid bars is analyzed. In the last chapter a review is made of the results and criteria useful for the experimentalist interested only in the application of the conclusions of this report.

TABLE OF CONTENTS

INTRODUCTION

Low thrust, monopropellant engines based on the catalytic decomposition of hydrazine have been operational on board spacecrafts for some time, for station keeping, attitude and spin rate control, etc. In spite of problems such as aging and poisoning these engines have been found to operate satisfactorily above a certain thrust level. On the other hand, for thrust below 0.1 lbf say, it is difficult to achieve reliable catalytic engines. For that thrust range, propulsion systems based on thermal decomposition (aided by electrical heating) of hydrazine have been lately proposed [1-10].

A basic aspect of such systems is a homogeneous, gas phase, complex kinetics. In an engine this chemical kinetics is coupled to fluid dynamic processes, and as a consequence, basic analyses of thruster performance become difficult. Fortunately, a single, overall reaction (stoichiometry and reaction rate) can substitute for the entire kinetic mechanism under some conditions: If all intermediate radicals produced in the decomposition reach equilibrium with hydrazine in times much shorter than the overall chemical time for transformation of hydrazine into products, radical concentrations become fixed functions of hydrazine concentration, temperature and pressure, in the slower evolution of these variables. If, then, the characteristic residence or mechanical time for the engine is large compared with the radicals relaxation time (in particular, if mechanical and overall chemical times are comparable) an overall kinetics may be used in the gas dynamics equations for the engine. This problem is treated in Chap. I.

A step previous to the gas phase chemical kinetics is the vaporization of hydrazine, since this is injected into the combustion chamber as liquid. To speed up that process, the use of heated screens or grids appears convenient [5-7]. As the

hydrazine jet impinges upon the heated surface of the screen a spray of hot, small droplets is produced, leading to back-flow and near-homogeneity in the chamber; consequently the reactor may be assumed to approximately operate as a perfectly stirred reactor [11-13]. A steady-state analysis of the engine, based in this approximation, is developed in Chap. II for times both shorter and larger than the time for wall temperature to reach a steady condition (pulsed and steady regimes).

The conditions for which the analysis of Chap. II is valid are discussed in chapter III. In particular we study the vaporization process (droplet vaporization time and vaporization rate) and the transients appearing after the start of the engine: chamber filling, and gas heating and ignition.

Chapter IV deals with a plug flow model of the reactor, (an analysis both alternative, and complementary[13] to the study developed in Chap. II). We shall assume that heat is conducted along solid bars, from a region downstream where combustion occurs, toward the chamber entrance; the gas is assumed to reach the bars at the temperature of a grid where it is vaporized.

In Chap. V we review all the results obtained in previous chapters; we also give the criteria useful to the experimentalist which follow from those results. Thus, the reader only interested in the practical application of the conclusions attained in this report, may entirely ship Chaps. I-IV.

R E F E R E N C E S

1. SCHREIB, R.R. and PUGMIRE, T.K. — "AIAA Paper No 69-946" (1969)

2. PUGMIRE, T.K. O'CONNOR, T. and DAVIS, W. — "AIAA Paper No 71-760" (1971)

3. MURCH, C.K. and HUNTER, C.R. — "AIAA Paper No 72-451" (1972)

4. REIN GRABBI and MURCH, C.K. — "AIAA Paper No 76-656" (1976)

5. MURCH, C.K. SACKHEIM, R.L. and KUENZLY, J.D. — "AIAA Paper No 76-658" (1976)

6. VALENTINI, R. — "Propriétés de l'hydrazine et ses applications comme source d'energie" P.331 CENTRE NATIONAL D'ETUDES SPATIALES (1974)

7. MURCH, C.K. — "Propriétés de l'hydrazine et ses applications comme source d'energie" P.341 CENTRE NATIONAL D'ETUDES SPATIALES (1974)

8. TWARDY, H. — "XXVI Congress of International Astronautical Federation" (1975)

9. PUGMIRE, T.K. — "Propriétés de l'hydrazine et ses applications comme source d'energie" P.351 CENTRE NATIONAL D'ETUDES SPATIALES (1974)

10. PUGMIRE, T.K. and O'CONNOR — "AIAA Paper 76-660" (1976)

11. ESSENHIGH, R.H. — "An Introduction to Stirred Reactor Theory Applied to Design of Combustion Chambers" H.B. PALMER and J.M. BEER, Academic (New York) (1974)

12. BRAGG, S.L. — "Brit. Aeronaut. Res. Council" Paper No 16170

13. VULIS, L.A. — "Thermal Regimes of Combustion" MC GRAW-HILL (New York) (1961)

CHAPTER I

CHEMICAL KINETICS OF THERMAL HYDRAZINE DECOMPOSITION

Author

Prof. J.R. Sanmartín*

*Presently at the School of Aeronautics Polytecnic University of Madrid.

CHAPTER I

CHEMICAL KINETICS OF THERMAL HYDRAZINE DECOMPOSITION

The thermal decomposition of hydrazine has been studied extensively in the past [1-10].

For temperatures above 1000°K an overall kinetics has been found to exist [6-8]. If pressure is above 3 atm., say, the initiation reaction for the decomposition is unimolecular, the overall reaction rate being of first order; for such conditions, and for low hydrazine molar fractions, the overall rate constant and stoichiometry are[8]

$$k\left[\text{sec}^{-1}\right] = 2\times10^{13.9}\exp\{-\left[(55\pm2)\text{Kcal/mole}\right]/RT\}$$

$$N_2H_4 \rightarrow NH_3 + \frac{1}{2}N_2 + \frac{1}{2}H_2$$

For temperatures below 1000°K a kinetic mechanism for the decomposition was proposed by Eberstein and Glassman[9], who also determined an overall reaction rate in the limit of a low hydrazine molar fraction. To study ignition conditions, however, we need consider both low temperatures and hydrazine molar fractions of order of unity. Moreover, for sufficiently low temperatures the existence of an overall kinetics (that is, that radicals relaxation times be much shorter that the overall time for transformation of hydrazine into products, as discussed in the Introduction) may be in question.

In this chapter we use the Eberstein-Glassman mechanism under the above mentioned conditions to provide values for the relaxation times. The analysis shows that an overall ki-

netics does indeed exist; we arrive then at analytical expressions for reaction rate and stoichiometry. In a recent paper[10] Urrutia used that mechanism to obtain overall results for the decomposition of highly diluted hydrazine at temperatures near 1000°K.

In the next section we discuss the formulation of the problem. In Secs. 2 and 3 we consider temperatures near 1000°K and 800°K respectively. A discussion of the results obtained is given in Sec. 4. Mathematical details of the analysis are presented in the Appendix.

I. Formulation of the Problem

The kinetic mechanism proposed by Eberstein and Glassman for hydrazine decomposition involves species N_2H_4, NH_2, NH, N_2H_3, H, NH_3, N_2, H_2 (numbered 1 to 8) and ten elementary reactions:

Initiation

1) $N_2H_4 + M \rightarrow 2NH_2 + M$ $\qquad k_1 = ?$

Propagation

2) $N_2H_4 + NH_2 \rightarrow N_2H_3 + NH_3$ $\qquad k_2 = 10^{12}\exp(-7000/RT)$

3) $N_2H_3 + M \rightarrow N_2 + H_2 + H + M$ $\qquad k_3 = 10^{13}\exp(-20000/RT)$

4) $N_2H_4 + H \rightarrow NH_2 + NH_3$ $\qquad k_4 = 10^{13}\exp(-7000/RT)$

Chain branching

5) $N_2H_3 + M \rightarrow NH + NH_2 + M$ $\qquad k_5 = 10^{12.9}\exp(-18000/RT)$

6) $N_2H_4 + NH \rightarrow NH_2 + N_2H_3$ $\qquad k_6 = 10^{14}\exp(-10000/RT)$

Termination

7) $NH_2 + N_2H_3 \rightarrow NH_3 + N_2 + H_2$ $\qquad k_7 = 10^{12.5}$

8) $2N_2H_3 \rightarrow 2NH_3 + N_2$ $\qquad k_8 = 10^{12}$

9) $N_2H_3 + H \rightarrow N_2 + 2H_2$ $\qquad k_9 = 10^{15}$

10) $2NH_2 \rightarrow N_2H_4$ $\qquad k_{10} = 10^{12.5}$

where all k's are measured in cc/mole-sec.

Eberstein and Glassman took, from Gilbert, the value $k_1 = 10^{19}\ e^{-\frac{60}{RT}}$ cc/mole-sec. Actually the initiation reaction appears to be of the Lindeman-Hinshelwood, quasi unimolecular type, so that at sufficiently high and low pressures the reaction is unimolecular and bimolecular respectively; the dividing pressure changes slightly with temperature and is about 3 atm. For this study we shall use the high pressure limit since reacting chamber pressures of the order of 25 atm. contemplated; the initiation rate constant is then

$$k_{1(\infty} = 10^{13.9}\ e^{-\frac{55}{RT}}\ \text{sec.}^{-1}$$

For pressures below 3 atm. experimental results fit well into the RRKM theory assuming that seven effective oscillators contribute energy to the activation of the hydrazine molecule; the initiation rate constant is then

$$k_{1(0} = 10^{15.6}\ e^{(-41/RT)}\ \text{cc/mole-sec.}$$

If $w_{i\alpha}$ is the rate of production (moles per unit time and unit volume) of the i^{th} species due to the α^{th} reaction, which follows from the above mechanism, the continuity equation for the i^{th} species in a general situation reads

$$\frac{DY_i}{Dt} + \frac{1}{\rho}\left(\nabla.\rho Y_i \bar{v}_{di}\right) = \frac{M_i}{\rho} \sum_{\alpha} w_{i\alpha} \qquad (2)$$

where Y_i, $\bar{v}_{di}$ and M_i are the i^{th} mass fraction, diffusion velocity and molar mass respectively. The left-hand side of

Eq.(2) is of the order of Y_{ic}/tm , Y_{ic} being a characteristic value for Y_i and t_m a characteristic mechanical or residence time. The right-hand side contains negative terms arising from the consumption of the i^{th} species in reactions where it enters as a reactant; such terms are of the order of Y_i^n/t_{ci} (n=1 or 2) where t_{ci} is a chemical time which depends on the concentrations of other species. The right side contains also positive terms due to the reactions where the i^{th} species enters as a product; they are of the order of $1/t'_{ci}$ where t'_{ci} is another chemical time. For a very active species t_{ci} is so small that the species is consumed as soon as it is produced -so to speak-, that is,

$$\sum_{\alpha} w_{i\alpha} \simeq 0 \ , \qquad (3)$$

Y_i being very small. Equations (3) then provide expressions for Y_i, for all active species, as functions of reactants and main products. This eliminates the active species of the main evolution of the reaction and leads to simplified kinetics. In the present problem we expect species 2 to 5 to be very active in the above sense, so that an overall reaction would result:

$$N_2H_4 \rightarrow \alpha NH_3 + \beta N_2 + \gamma H_2 \ ,$$
$$\alpha = 2(1-\beta) \ , \quad \gamma = 3\beta - 1 \qquad (4)$$

To find out whether radicals NH_2, NH, N_2H_3 and H are indeed very active, and to determine the values of the various chemical times, it is then simplest to consider a constant volume and temperature, spatially uniform, hydrazine decomposition process. Such analysis would provide also overall results for stoichiometry (β) and reaction rate. Equations (2) then become

$$\frac{dc_i}{dt} = \sum_{\alpha} w_{i\alpha} \qquad (5)$$

where $c_i = \rho Y_i / M_i$ is the i^{th} molar concentration. Especifically we have

$$\frac{dc_1}{dt} = - k_{1\infty} c_1 - k_2 c_1 c_2 - k_4 c_1 c_5 - k_6 c_1 c_3 + k_{10} c_2^2$$

$$\frac{dc_2}{dt} = 2k_{1\infty} c_1 - k_2 c_1 c_2 + k_4 c_1 c_5 + k_5 c c_4 + k_6 c_1 c_3 - k_7 c_2 c_4 - 2k_{10} c_2^2$$

$$\frac{dc_3}{dt} = k_5 c c_4 - k_6 c_1 c_3$$

$$\frac{dc_4}{dt} = k_2 c_1 c_2 - k_3 c c_4 - k_5 c c_4 + k_6 c_1 c_3 - k_7 c_2 c_4 - 2k_8 c_4^2 - k_9 c_4 c_5 \qquad (5')$$

$$\frac{dc_5}{dt} = k_3 c c_4 - k_4 c_1 c_5 - k_9 c_4 c_5$$

$$\frac{dc_6}{dt} = k_2 c_1 c_2 + k_4 c_1 c_5 + k_7 c_2 c_4 + 2k_8 c_4^2$$

$$\frac{dc_7}{dt} = k_3 c c_4 + k_7 c_2 c_4 + k_8 c_4^2 + k_9 c_4 c_5$$

$$\frac{dc_8}{dt} = k_3 c c_4 + k_7 c_2 c_4 + 2k_9 c_4 c_5 \ .$$

Equations (5') are to be solved under initial conditions

$$\frac{dc_8}{dt} = k_3 c c_4 + k_7 c_2 c_4 + 2k_9 c_4 c_5 \ .$$

Equations (5') are to be solved under initial conditions

$$\frac{c_1(t=0)}{c} = 0(1)$$

$$c_i(t=0) = 0 \ , \ i \neq 1. \qquad (6)$$

It may be now notice that, due to the fact that NH_3, N_2 and H_2 enter only as products in the Eberstein-Glassman mechanism, the first five equations in (5') are decoupled from the last three. A further essential simplification arises from the differences, of several orders of magnitude, existing between many rate constants. This allows the use of a perturbation method, essentially a multiple time-scale analysis, by making Eqs (5') nondimensional and ordering the terms in their right-hand sides in powers of a small number ε, equal to 10^{-2} say. The five ordinary differential equations for c_1, c_2 ... c_5 may then be solved asymptotically by letting ε formally go to zero (although at the end of the analysis it must be set equal to 10^{-2}) and retaining dominant terms only.

However, since the rate constants appear multiplying some species concentrations, and these may change substantially as time evolves, it is clear that the relative importance of each term in those equations, changes with time. Thus there will exist several successive stages, different (hopefully few) terms being dominant at each stage. One then proceeds integrating in time the first five Eqs (5'), starting from conditions (6), and at each new stage the results from the previous stage allow to determine the new dominant terms. It should be noticed that the rate constants of some elementary reactions increase steeply from 750°K to 1000°K and therefore the selection of dominant terms, and thus the number and char-

acter of the time stages, will be clarly dependent on temperature.

In the next two sections we give the results of such (singular) asymptotic analysis for temperatures around 1000°K and 800°K. Specifically, we give the characteristic (chemical) times and behaviour of the different stages found, and explicit formulae for β and dc_1/dt as functions of c_1, T and P (pressure). Details of the derivation are given in the Appendix.

II. Temperature near 1000°K

For T ≈ 1000°K and $c_1/c = 0(1)$ in t = 0 five stages are found in the decomposition. The first four stages correspond to chemical relaxation of species NH_2, NH, N_2H_3 and H. Transformation of hydrazine into NH_3, N_2 and H_2 takes place in a fifth, much slower stage. Thus, at T = 1000°K, the Eberstein-Glassman mechanism leads to the existence of an overall kinetics.

There is first a stage with a characteristic time of the order of $(10^{-7}/P)$ sec -where P is measured in atmospheres-, in which NH relaxes to equilibrium through reactions 5 and 6, reaching a quasi-steady state. Next, there occurs relaxation of H through reactions 3 and 4, in a time of the order of $(10^{-6}/P)$ sec. Then, in a time of the order of $(10^{-5}/P)$ sec, NH_2 relaxes through reactions 1 and 2. Finally, for times of the order of $(10^{-4}/P)$ sec, N_2H_3 comes to equilibrium in reactions 2, 3, 5, 6, 8 and 9; simultaneously, reaction 4 becomes negligible and reactions 5 and 6 come into play in the quasi-steady state of NH_2.

Hydrazine decomposes in a much larger time, of the order of $(10^{-1}/P)$ sec, through reactions 1, 2 and 6, we thus have

$$\frac{dc_1}{dt} \simeq w_1 \simeq - k_{1\infty}c_1 - k_2c_1c_2 - k_6c_1c_3 \qquad (7)$$

At this stage, from the preceding results, we also have

$$0 \simeq w_2 \simeq 2k_{1\infty}c_1 - k_2c_1c_2 + k_5cc_4 + k_6c_1c_3$$

$$0 \simeq w_3 \simeq k_5cc_4 - k_6c_1c_3 \qquad (8)$$

$$0 \simeq w_4 \simeq k_2c_1c_2 - k_3cc_4 - k_5cc_4 + k_6c_1c_3 - 2k_8c_4^2 - k_9c_4c_5$$

$$0 \simeq w_5 \simeq k_3cc_4 - k_9c_4c_5.$$

Using (8) in (7) we then find an explicit expression for the overall rate of decomposition of hydrazine $\bar{w}_1$, as function c_1, T and c, or alternatively c_1, T and P(c = P/RT),

$$\frac{dc_1}{dt} \simeq \bar{w}_1 = - 3k_{1\infty}c_1 \left[1 + \frac{1+ (1+2\phi)^{1/2}}{\phi(1- k_3/k_5)} \right]$$

$$= -3 \frac{k_5}{k_8} (k_5-k_3)\, c^2 \frac{1}{2} \left[1+(1+2\phi)^{1/2} +(1-k_3/k_5)\phi \right]$$

$$\simeq -10^{14} \exp\{- \frac{36000}{RT}\} c^2 \frac{1}{2} \left[1+(1+2\phi)^{1/2} + 0.54\phi \right] \qquad (9)$$

where

$$\phi = \frac{2k_{1\infty}k_8}{(k_5-k_3)^2} \frac{c_1}{c^2} \simeq 8.7 \exp\{- \frac{19000}{RT}\} \frac{c_1}{c^2} . \qquad (10)$$

We also find

$$\frac{c_2}{c} = 0(10^{-4}),\ \frac{c_3}{c} = 0(10^{-6}),\ \frac{c_4}{c} = 0(10^{-3}),\ \frac{c_5}{c} = 0(10^{-6}). \quad (11)$$

In an engine we would then use $\bar{w}_1$ in

$$\frac{DY_1}{Dt} + \frac{1}{\rho}\nabla.(\rho Y_1 \vec{V}_{d1}) = \frac{M_1}{\rho}\bar{w}_1 .$$

According to (4) the overall rates of production of NH_3, N_2 and H_2 would be

$$\bar{w}_6 = -2(1-\beta)\bar{w}_1 \qquad \bar{w}_7 = -\beta\bar{w}_1 \qquad \bar{w}_8 = -(3\beta-1)\bar{w}_1 . \quad (12)$$

The dominant reactions in the productions of these species are found to be 2 and 8; 3, 8 and 9; and 3 and 9, respectively. Hence, we finally arrive at

$$\beta \simeq \frac{1+k_3/k_5}{3}\ \frac{1+(1+2\phi)^{1/2}+(k_5-k_3)\phi/(k_5+k_3)}{1+(1+2\phi)^{1/2}+(1-k_3/k_5)\phi} \quad (13)$$

$$\simeq 0.49\ \frac{1+(1+2\phi)^{1/2}+0.37\phi}{1+(1+2\phi)^{1/2}+0.54\phi}$$

Equation (13) leads to overall rates of production of NH_3, N_2 and H_2, and overall heat of decomposition.

The preceding results are valid as long as $c_1/c = 0(1)$. Equations (8) show however that as $c_1/c \to 0$, both c_2 and c_3 become singular as $1/c_1$, and the analysis needs modification. For $c_1/c = 0(10^{-1})$, reaction 1 may be neglected, while reactions 7 and 10 must be taken into account, the quasi-steady state of NH_2 and N_2H_3 being modified. We obtain

$$\bar{w}_1 \simeq -3\,\frac{k_5}{k_8}\,(k_5-k_3)c^2\left[1+\frac{k_7(3k_5-k_3)}{k_2k_8}\,\frac{c}{c_1}+4\frac{k_3k_5k_{10}}{k_2^2k_8}\,\frac{c^2}{c_1^2}\right]^{-1}$$

$$\simeq -10^{14}\exp\{-\frac{36000}{RT}\}c^2\left[1+64\exp\{-\frac{11000}{RT}\}\,\frac{c}{c_1}+10^3\exp\{-\frac{24000}{RT}\}\frac{c^2}{c_1^2}\right]^{-1} \qquad (14)$$

$$\beta \simeq \frac{1+k_3/k_5}{3}\,\frac{1+2k_7(3k_5-k_3)c/k_2k_8(1+k_3/k_5)c_1}{1+k_7(3k_5-k_3)c/k_2k_8c_1}$$

$$\simeq 0.49\,\frac{1+87\exp(-11000/RT)c/c_1}{1+64\exp(-11000/RT)c/c_1}\quad , \qquad (15)$$

$$\frac{c_2}{c} = 0(10^{-3})\ ,\ \frac{c_3}{c} = 0(10^{-5}),\ \frac{c_4}{c} = 0(10^{-3}),\ \frac{c_5}{c} = 0(10^{-6}) \qquad (16)$$

Both c_2 and c_3 pass through a large maximum in this range of values of c_1, and the characteristic time for the overall reaction is now much shorter, $(10^{-2}/P)$ sec.

For $c_1/c = 0(10^{-2})$, the overall kinetics changes again. Reactions 7 and 8 may now be neglected, while reaction 1 must again be taken into account. The overall reaction time is again $(10^{-1}/P)$ sec. We obtain

$$\frac{c_2}{c} = 0(10^{-4}),\ \frac{c_3}{c} = 0(10^{-6}),\ \frac{c_4}{c} = 0(10^{-5}),\ \frac{c_5}{c} = 0(10^{-6}), \qquad (17)$$

$$\beta \simeq 2/3 \qquad (18)$$

$$\bar{w}_1 \simeq -\frac{3}{4}\frac{k_2^2}{k_{10}}\left\{\frac{k_5}{k_3}-1\right\}c_1^2\,\frac{1}{2}\left[1+\left\{1+\frac{16k_1k_{10}k_3^2}{k_2^2(k_5-k_3)^2}\,\frac{c}{c_1}\right\}^{1/2}\right]$$

$$\simeq -10^{11}\exp\left\{-\frac{12000}{RT}\right\}c_1^2\,\frac{1}{2}\left[1+\left\{1+2.7\times10^9\exp\left(-\frac{50000}{RT}\right)\frac{c}{c_1}\right\}^{1/2}\right] \quad (19)$$

It may be noticed that the limits of (9) and (14), for decreasing c_1/c and c/c_1 respectively, match each other smoothly as they should. Similarly the limits of (14) and (19), for decreasing c_1/c and c/c_1 respectively, match smoothly too. Similar statements may be made about (13) and (15), and (15) and (18). The results in (18) and (19) agree with those given by Urrutia in Ref. 10 for $c_1/c = 0(10^{-2})$.

III. Temperature near 800°K

For $T \simeq 800°K$ and $c_1/c \simeq 0(1)$ in $t = 0$ we find four stages in the decomposition. First, NH and H reach a quasi-steady state in a time of the order of $(10^{-6}/P)$sec, through reactions 5 and 6, and 3 and 4 respectively. Next, in a time of order of $(10^{-5}/P)$sec, NH_2 comes to a quasi-steady state through reactions 1 and 2. That state is modified by reactions 4, 5 and 6 in a third stage, whose characteristic time is $(10^{-3}/P)$sec. Simultaneously there is exponential growth of N_2H_4, leading to a quasi-steady state through reactions 2, 3, 5, 6, 8 and 9, while reaction 8 modifies the equilibrium of H.

Transformation of hydrazine into products proceeds in a (10/P) sec time scale through reactions 2, 4 and 6; in this final stage reaction 1 may be neglected. The results for the overall reaction are

$$\frac{c^2}{c} = 0(10^{-6}),\quad \frac{c_3}{c} = 0(10^{-7}),\quad \frac{c_4}{c} = 0(10^{-4}),\quad \frac{c_5}{c} = 0(10^{-7}),\quad (20)$$

$$\bar{w}_1 \simeq -3\,\frac{k_5}{k_8}\,(k_5-k_3)c^2\left[1+\frac{k_3(5k_5-2k_3)}{3k_5(k_5-k_3)}\left\{1+\frac{k_5-k_3}{k_8}\,\frac{k_9}{k_4}\,\frac{c}{c_1}\right\}^{-1}\right]$$

$$\simeq -1.2\times10^{14}\exp\{-\frac{36000}{RT}\}c^2\left[1+0.8\{1+5.1\times10^{2}\exp\{-\frac{11000}{RT}\}\,\frac{c}{c_1}\}^{-1}\right] \qquad (21)$$

$$\beta \simeq \frac{1+k_3/k_5}{3}\left[1+\frac{2k_3/3k_5}{1+k_9(k_5-k_3)c/k_4k_8c_1}\right]^{-1}$$

$$\simeq 0.45\left[1+\frac{0.24}{1+5.1\times10^{2}\exp(-11000/RT)c/c_1}\right]^{-1} \qquad (22)$$

When $c_1 \to 0$, the overall kinetics changes because c_2 and c_3 become singular. For $c_1/c = 0(10^{-1})$ reaction 7 must be taken into account, while reaction 4 may be neglected. We arrive at

$$\frac{c_2}{c} = 0(10^{-5}),\ \frac{c_3}{c} = 0(10^{-6})\ \frac{c_4}{c} = 0(10^{-4}),\ \frac{c_5}{c} = 0(10^{-7}), \qquad (23)$$

$$\bar{w}_1 \simeq -3\,\frac{k_5}{k_8}\,(k_5-k_3)c^2\left[1+\frac{k_7(3k_5-k_3)}{k_2k_8}\,\frac{c}{c_1}\right]^{-1}$$

$$\simeq -1.2\times10^{14}\,\exp\{-\frac{36000}{RT}\}c^2\left[1+66\exp\{-\frac{11000}{RT}\}\,\frac{c}{c_1}\right]^{-1} \qquad (24)$$

$$\beta \simeq \frac{1+k_3/k_5}{3}\,\frac{1+2k_7(3k_5-k_3)c/k_2k_8(1+k_3/k_5)c_1}{1+k_7(3k_5-k_3)c/k_2k_8c_1}$$

$$\simeq 0.45\,\frac{1+97\exp(-11000/RT)c/c_1}{1+66\exp(-11000/RT)c/c_1} \qquad (25)$$

$$\simeq 0.45\ \frac{1+97\exp(-11000/RT)c/c_1}{1+66\exp(-11000/RT)c/c_1} \qquad (25)$$

As in the 1000°K case, both c_2 and c_3 pass through a large maximum in this range of values of c_1, and the overall characteristic time decreases sharply, to a (1/P) sec value.

For $c_1/c = 0(10^{-2})$, reaction 8 may be neglected but reaction 10 must be taken into account. The overall reaction time is again (10/P)sec. We also find

$$\beta \simeq 2/3\ , \qquad (26)$$

$$\overline{w}_1 \simeq -3\ \frac{k_5}{k_8}\ (k_5-k_3)c^2\left[\frac{k_7(3k_5-k_3)}{k_2k_8}\ \frac{c}{c_1} + 4\ \frac{k_3k_5k_{10}}{k_2^2k_8}\ \frac{c^2}{c_1^2}\right]^{-1}$$

$$\simeq -1.8\times 10^{12}\exp\{-\frac{25000}{RT}\}cc_1\left[1+15\exp\{-\frac{13000}{RT}\}\ \frac{c}{c_1}\right]^{-1}, \qquad (27)$$

$$\frac{c_2}{c} = 0(10^{-5}),\ \frac{c_3}{c} = 0(10^{-6}),\ \frac{c_4}{c} = 0(10^{-5}),\ \frac{c_5}{c} = 0(10^{-7}). \qquad (28)$$

Notice again the smooth matching of Eqs.(21), (24) and (27), and (22), (25) and (26).

IV. Discussion

Using an asymptotic analysis based on large differences among the rate constants of several elementary reactions, we have shown that the Eberstein-Glassman mechanism for the thermal decomposition of hydrazine at fixed temperatures near 800°K

and near 1000°K leads to an overall kinetics: Relaxation of the active radicals appearing in the decomposition occurs in several stages involving times extremely short compared with the characteristic time for the overall process of decomposition. This last time is of the order of $(10^{-1}/P)$sec (the pressure P being measured in atmospheres) for temperature, T, near 1000°K, and hydrazine molar fraction, c_1/c, of the order of either unity or 10^{-2}; that time is $(10^{-2}/P)$sec for $c_1/c \simeq 0(10^{-1})$. For given c_1/c between unity and values $0(10^{-2})$, the overall time at $T \simeq 800°K$ is about 10^2 times larger than the overall time at 1000°K.

We have found explicit expressions (see Secs. 3 and 2) for the rate of decomposition of hydrazine $|\bar{w}_1|$, and the stoichiometric coefficient β, in the overall reaction

$$N_2H_4 \rightarrow 2(1-\beta)NH_3 + \beta N_2 + (3\beta-1)H_2.$$

Once β is known, the heat of decomposition can be found from thermodynamic tables. At either 800 or 1000°K the expressions for w_1 (and β) change in form when c_1/c decreases from unity down to values $0(10^{-1})$ and $0(10^{-2})$; we have shown however that the expressions for the different ranges of c_1/c match smoothly. Furthermore, it may be verified that for given $0(c_1/c)$, the expressions for $\bar{w}_1$ (and β) at $T \simeq 800°K$ and $T \simeq 1000°K$ match smoothly each other at intermediate temperatures*. Thus it is possible to write down patched formulae for $\bar{w}_1$ and β, valid for, say, $750°K < T < 1050°K$ and $1 \geq c_1/c > 10^{-3}$. It should be noticed however that such formulae are quite complex and

---

*Compare Eqs.(9), (13)-(15), (18) and (19) in Sec.2 with Eqs. (21), (22), (24)-(27) in Sec.3, respectively. Differences between factors 10^{14} and 1.2×10^{14}, 0.45 and 0.49, etc. are due to our having approximated factors $(1-k_3/k_5)$, $(1+k_3/k_5)$, etc. by numbers independent of T, changing slightly from the neighborhood of 800°K to the neighborhood of 1000°K.

involve errors of the order of 10 or 20%.

It should be noticed that in an engine the combustion will not be isothermal since heat is evolved in the reaction. However if the characteristic time for temperature changes is large compared with the radicals relaxation times, the adicals will reach local equilibrium at each value of T, and it will be possible to make use of the results found above.

Appendix

Detailed analysis for temperature near 1000°K

We define

$$X_i = \frac{c_i}{c} \qquad ; \qquad t_* = k_9 c t$$

$$\frac{k_{1\infty}}{k_9 c} = \frac{\varepsilon^4}{P} K_{1\infty} \quad ,, \quad \frac{k_2}{k_9} = \varepsilon^{2.5} K_2 \quad ,, \quad \frac{k_3}{k_9} = \varepsilon^3 K_3$$

$$\frac{k_4}{k_9} = \varepsilon^2 K_4 \quad ,, \quad \frac{k_5}{k_9} = \varepsilon^3 K_5 \quad ,, \quad \frac{k_6}{k_9} = \varepsilon^{1.5} K_6$$

$$\frac{k_7}{k_9} = \varepsilon^{1.5} K_7 \quad ,, \quad \frac{k_8}{k_9} = \varepsilon^{1.5} K_8 \quad ,, \quad \frac{k_{10}}{k_9} = \varepsilon^{1.5} K_{10}$$

where P is measured in atm., $K_i = 0(1)$ and $\varepsilon \equiv 10^{-2}$; for P of the order of 20, the case of interest here, $\varepsilon^4/P = 0(\varepsilon^{4.5})$. Then, as long as c does not change sensibly, Eqs. (5') become

$$\frac{dX_1}{dt_*} = -\frac{\varepsilon^4}{P} K_{1\infty} X_1 - \varepsilon^{2.5} K_2 X_1 X_2 - \varepsilon^2 K_4 X_1 X_5$$

$$-\varepsilon^{1.5} K_6 X_1 X_3 + \varepsilon^{1.5} K_{10} X_2^2 \qquad \text{(A1.a)}$$

$$\frac{dX_2}{dt_*} = -\frac{\varepsilon^4}{P} K_{1\infty} X_1 - \varepsilon^{2.5} K_2 X_1 X_2 + \varepsilon^2 K_4 X_1 X_5 + \varepsilon^3 K_5 X_4 + \varepsilon^{1.5} K_6 X_1 X_3$$

$$- \varepsilon^{1.5} K_7 X_2 X_4 - \varepsilon^{1.5} 2K_{10} X_2^2 \qquad \text{(A1.b)}$$

$$\frac{dX_3}{dt_*} = \varepsilon^3 K_5 X_4 - \varepsilon^{1.5} K_6 X_1 X_3 \qquad \text{(A1.c)}$$

$$\frac{dX_4}{dt_*} = \varepsilon^{2.5} K_2 X_1 X_2 - \varepsilon^3 K_3 X_4 - \varepsilon^3 K_5 X_4 + \varepsilon^{1.5} K_6 X_1 X_3 +$$

$$- \varepsilon^{1.5} K_7 X_2 X_4 - \varepsilon^{1.5} 2K_8 X_4^2 - X_4 X_5 \qquad \text{(A1.d)}$$

$$\frac{dX_5}{dt_*} = \varepsilon^3 K_3 X_4 - \varepsilon^2 K_4 X_1 X_5 - X_4 X_5 \qquad \text{(A1.e)}$$

$$\frac{dX_6}{dt_*} = \varepsilon^{2.5} K_2 X_1 X_2 + \varepsilon^2 K_4 X_1 X_5 + \varepsilon^{1.5} K_7 X_2 X_4 + \varepsilon^{1.5} 2K_8 X_4^2 \qquad \text{(A1.f)}$$

$$\frac{dX_7}{dt_*} = \varepsilon^3 K_3 X_4 + \varepsilon^{1.5} K_7 X_2 X_4 + \varepsilon^{1.5} K_8 X_4^2 + X_4 X_5 \qquad \text{(A1.g)}$$

$$\frac{dX_8}{dt_*} = \varepsilon^3 K_3 X_4 + \varepsilon^{1.5} K_7 X_2 X_4 + 2X_4 X_5 \ . \qquad \text{(A1.h)}$$

For small enough t_*, condition

$$\left| \int_0^{t_*} \left(\frac{dX_1}{dt_*} \right) dt_* \right| << X_1(t=0) \equiv X_1^\circ \qquad \text{(A2)}$$

is obviously satisfied so that

$$X_1 = X_1^\circ \qquad c \simeq c_1(t = 0) \ . \qquad \text{(A3)}$$

Then, eq. (A1.b, e) show that the first term in the right hand side of each of those eqs. is dominant. Therefore, as $t_* \to 0$, we may write

$$X_2 \simeq 2K_{1\infty}X_1^o \frac{\varepsilon^4}{P} t_* \qquad X_4 \simeq K_{1\infty}K_2(X_1^o) \frac{\varepsilon^{6,5}}{P} t_*^2 \tag{A4}$$

$$X_3 \simeq \frac{1}{3} K_{1\infty}K_2K_5(X_1^o)^2 \frac{\varepsilon^{9,5}}{P} t_*^3 \quad X_5 \simeq \frac{1}{3} K_{1\infty}K_2K_3(X_1^o)^2 \frac{\varepsilon^{9,5}}{P} t_*^3 \ .$$

These simple growth laws lead to the "first" stage of the reaction attained when either condition (A2) is violated or some other term becomes comparable to the first one in the R.H.S. of any of eqs. (A1.b-A1.e).

1st Stage

Equations (A1.b-A1.e) and (A3), (A4) show that in this first stage $t_* = 0(\varepsilon^{-1.5})$, when the second term in the R.H.S. of eqs. (A1.c) becomes comparable to the first one. Defining $t_1 = t_*\varepsilon^{1.5}$ we have

$$X_1 \simeq X_1^o \ ,, \quad \frac{dX_2}{dt_1} \simeq 2K_{1\infty}X_1 \frac{\varepsilon^{2.5}}{P} \ ,, \quad \frac{dX_4}{dt_1} \simeq K_2X_1X_2\varepsilon \tag{A5}$$

$$\frac{dX_3}{dt_1} \simeq K_5X_4\varepsilon^{1.5} - K_6X_1X_3 \ ,, \quad \frac{dX_5}{dt_1} \simeq K_3X_4\varepsilon^{1.5} \ .$$

The asymptotic behaviour of this system for $t_1 \to \infty$ is

$$X_1 = X_1^o \ , \quad X_2 = 2K_{1\infty}X_1^o \frac{\varepsilon^{2.5}}{P} t_1 \ , \quad X_4 = K_{1\infty}K_2(X_1^o)^2 \frac{\varepsilon^{3,5}}{P} t_1^2$$

$$X_3 = (K_{1\infty}K_2K_5/K_6)X_1^o \frac{\varepsilon^5}{P} t_1^2 \qquad X_5 = \frac{1}{3} K_{1\infty}K_2K_3(X_1^o)^2 \frac{\varepsilon^5}{P} t_1^3 \quad (A6)$$

2nd Stage

Eqs. (A6) show that a second stage of the reaction is reached for times $t_1 = 0(\varepsilon^{-0.5})$ when the second term in the R.H.S. of eq. (A1.e) becomes comparable to the first one. Defining $t_2 = t_*\varepsilon^2$ we arrive at

$$X_1 \simeq X_1^o \;,\; \frac{dX_2}{dt_2} \simeq 2K_{1\infty}X_1 \frac{\varepsilon^2}{P} \;,\; \frac{dX_4}{dt_2} \simeq K_2X_1X_2\varepsilon^{0.5}$$

$$\frac{dX_3}{dt_2} \simeq K_5X_4\varepsilon - K_6X_1X_3\varepsilon^{-0.5} \simeq 0 \;,\; \frac{dX_5}{dt_2} \simeq K_3X_4\varepsilon - K_4X_1X_5$$

Notice that X_3 is already in a steady-state condition. For $t_2 \to \infty$ we find

$$X_1 \simeq X_1^o \;,\; X_2 \simeq 2K_{1\infty}X_1^o \frac{\varepsilon^2}{P} t_2 \;,\; X_4 \simeq K_{1\infty}K_2(X_1^o)^2 \frac{\varepsilon^{2.5}}{P} t_2^2$$

$$X_3 \simeq (K_5X_4/K_6X_1^o)\varepsilon^{1.5} \;,\; X_5 \simeq (K_{1\infty}K_2K_3/K_4)X_1^o \frac{\varepsilon^{3.5}}{P} t_2^2$$

3rd Stage

In a 3rd stage the second term in the R.H.S. of eq.(A1.b) and the last term of eq(A1.e) become simultaneously dominant while X_5 reaches steady state. Defining $t_3 = t_*\varepsilon^{2.5}$ we find

$$X_1 \simeq X_1^o \;,\; \frac{dX_2}{dt_3} \simeq 2K_{1\infty}X_1 \frac{\varepsilon^{1.5}}{P} - K_2X_1X_2 \;,\; \frac{dX_4}{dt_3} \simeq K_2X_1X_2$$

$$\frac{dX_3}{dt_3} \simeq K_5 X_4 \varepsilon^{0.5} - K_6 X_1 X_3 \varepsilon^{-1} \simeq 0$$

$$\frac{dX_5}{dt_3} \simeq K_3 X_4 \varepsilon^{0.5} - K_4 X_1 X_5 \varepsilon^{-0.5} - X_4 X_5 \varepsilon^{-2.5} \simeq 0,$$

As $t_3 \to \infty$

$$X_1 \simeq X_1^o \quad ,, \quad X_2 \simeq \frac{2K_{1\infty}}{K_2} \frac{\varepsilon^{1.5}}{P}$$

$$X_4 \simeq 2K_{1\infty} X_1^o \frac{\varepsilon^{1.5}}{P} t_3 \quad ,, \quad X_3 \simeq (K_5 X_4 / K_6 X_1^o)\varepsilon^{1.5} \quad ,, \quad X_5 \simeq K_3 \varepsilon^3$$

4^{th} Stage

A 4^{th} stage is reached when the fourth and fifth terms, and the second, third, fourth, sixth and last terms in the R.H.S. of eqs. (A1.b, A1.d) respectively become dominant, while X_2 reaches steady state, and the middle term in (A1.e) becomes negligeable. Defining $t_4 \simeq t_* \varepsilon^3$ we obtain

$$X_1 \simeq X_1^o \quad ,, \quad \frac{dX_2}{dt_4} \simeq 2K_{1\infty} X_1 \frac{\varepsilon}{P} - K_2 X_1 X_2 \varepsilon^{-0.5} + K_5 X_4 + K_6 X_1 X_3 \varepsilon^{-1.5} \simeq 0$$

$$\frac{dX_3}{dt_4} \simeq K_5 X_4 - K_6 X_1 X_3 \varepsilon^{-1.5} \simeq 0$$

$$\frac{dX_4}{dt_4} \simeq K_2 X_1 X_2 \varepsilon^{-0.5} - K_3 X_4 - K_5 X_4 + K_6 X_1 X_3 \varepsilon^{-0,5} - 2K_8 X_4^2 \varepsilon^{-1,5} +$$

$$- X_4 X_5 \varepsilon^{-3} \quad .$$

$$\frac{dX_5}{dt_4} \simeq K_3 X_4 - X_4 X_5 \varepsilon^{-3} \simeq 0 \quad ,$$

As $t_4 \to \infty$

$$X_1 \simeq X_1^o \;, \quad X_2 \simeq 2\,\frac{K_{1\infty}}{K_2}\,\frac{\varepsilon^{1.5}}{P} + 2\,\frac{K_5 X_4}{K_2 X_1^o}\,\varepsilon^{0,5}$$

$$X_3 \simeq (K_5 X_4 / K_6 X_1^o)\varepsilon^{1.5} \;,$$

$$X_4 \simeq \frac{K_5 - K_3}{2}\,\varepsilon^{1.5}\left[1+\{1+\frac{4K_{1\infty}X_1^o}{(K_5-K_3)^2}\,\frac{\varepsilon^{-0.5}}{P}\}^{1/2}\right], \quad X_5 \simeq K_3\varepsilon^3$$

5th Stage

Condition (A2) is finally violated for $t_4 = O(\varepsilon^{-1,5})$ when the first, second and fourth terms of (A1,a) become simultaneously dominant while X_4 reaches a steady-state. Going back to dimensional variables we arrive at eqs. (7) and (8) of section 2. From eqs. (8) it follows that

$$X_2 \simeq 2(k_{1\infty}/ck_2) + 2(k_5 c_4 / k_2 c_1) \qquad (A7)$$

$$X_3 \simeq k_5 c_4 / k_6 c_1$$

$$X_4 \simeq \frac{k_5 - k_3}{2k_9}\left|1+\{1+\frac{4k_{1\infty}k_9 c_1}{c(k_5-k_3)^2}\}^{1/2}\right|$$

$$X_5 \simeq \frac{k_3}{k_9} \;;$$

using (A7) in eq. (7) of section 2, eqs. (9) and (10) follow. Eqs. (A7) yield $X_2 \simeq 0(\varepsilon^2)$, $X_3 \simeq 0(\varepsilon^3)$, $X_4 \simeq 0(\varepsilon^{1.5})$ and $X_5 \simeq 0(\varepsilon^3)$ then the last three eqs. in eq. (5') become

$$\frac{dc_6}{dt} \simeq k_2 c_1 c_2 + 2k_8 c_4^2$$

$$\frac{dc_7}{dt} \simeq k_3 c c_4 + k_8 c_4^2 + k_9 c_4 c_5$$

$$\frac{dc_8}{dt} \simeq k_3 c c_4 + 2k_9 c_4 c_5$$

whence eq. (13) for $\beta(\equiv -dc_7/dc_1)$.

A similar analysis for $X_1 = 0(\varepsilon^{0.5})$ and $0(\varepsilon)$, or for $T \simeq 800°K$ leads to the remaining results of the Chapter I.

REFERENCES

1. GILBERT, M. "Combustion and Flame" 2 . 137 (1958).

2. ADAMS, G.K. and STOCKS, G.W. "IV Symposium (International) on Combustion" P. 239, Williams and Wilkins, (1953).

3. SZWARC, M "Proc. Roy. Soc." (London) A 198, 267, (1949).

4. DIESEN, R.W. "J. Chem. Phys". 39, 2121 (1963).

5. MOBERLY, W.H. "J. Phys. Chem." 66, 366 (1962).

6. McHALE, E.T. KNOX, B.E. and PALMER, H.B. "X Symposium (International) on Combustion" P. 341. The Combustion Institute (1965).

7. MICHEL, K.W. and WAGNER, R.G. "X Symposium (International) on Combustion" P. 353. The Combustion Institute (1965).

8. MEYER, E. OLSCHEWSKI, H.A.P. TROE, J. and WAGNER, H.G. "XII Symposium (International) on Combustion" 345, The Combustion Institute (1969).

9. EBERSTEIN, I.J. and GLASSMAN, I. "X Symposium (International) on P. 365, The Combustion Institute (1965).

10. URRUTIA, J.L. "Report ESTEC Contract 1121/70 AA".

CHAPTER II

PERFECTLY STIRRED HYDRAZINE REACTOR.

Authors

Prof, J.R. Sanmartín*

Dr. E. Fraga

*Presently at the School of Aeronautics Polytecnic University of Madrid.

CHAPTER II

PERFECTLY STIRRED HYDRAZINE REACTOR

Inside a continuous flow reactor with appropriate stirring, conditions may be assumed homogeneous and equal to those holding at the exit opening (perfectly stirred reactor). Since the grids used in thermal hydrazine engines, to heat and break into drops the entering liquid hydrazine, result in back-flow and turbulence, those engines might be analyzed, in a first approximation as perfectly stirred reactors.

I. General equations

We shall consider two limiting cases: a short pulse regime such that the wall temperature remains frozen at its initial value T_{wo} and a long pulse regime or steady regime, such that T_w reaches equilibrium conditions. Thus a time-dependent equation for T_w must be considered, in order to determine its final steady value. On the other hand we consider a steady flow for either case. A discussion of the characteristic times for changes in both T_w and the flow is carried out in Chapter III.

The steady-state mass conservation equations for N_2H_4, NH_3, N_2, H_2 and liquid N_2H_4 (indexed 1 to 4 and 1L respectively) read

$$\dot{m}_v - \dot{m}Y_1 + M_1 V \delta_1 \overline{W}_1 = 0 \qquad (1)$$

$$-\dot{m}Y_j + M_j V \delta_1 \overline{W}_1 = 0 \quad (j = 2,3,4) \qquad (2)$$

$$\dot{m} - \dot{m}Y_{1L} - \dot{m}_v = 0 \qquad (3)$$

where $\dot{m}_v$, $\dot{m}$ and V are the evaporation mass rate, the mass flow rate and the reactor volume respectively, and Y_i is the i^{th} mass fraction inside and at the exit of the chamber. The stoichiometric coefficients are

$$\delta_1 = 1, \quad \delta_2 = -2(1-\beta), \quad \delta_3 = -\beta, \quad \delta_4 = -(3\beta-1), \qquad (4)$$

From Chapter I, β is found to lie between about 0.40 and 0.65 for typical pressures around 20 atm. and temperatures from, say, 700 to 1100°K; for temperatures above 1100°K and low hydrazine molar fractions, $\beta \simeq 0.5$ (see references 6-8 in Chapter I). An approximate expression for the overall molar rate of production of hydrazine per unit volume $\bar{w}_1$, as function of P, T and X_1, valid for temperatures lying between 700 and 1100°K, may be taken from the analysis of Chapter I,

$$\bar{w}_1 \simeq -\frac{1.8\times10^{10}P^2}{T^2}\left[X_1^2 + \frac{0.8X_1^3}{X_1+510\exp(-5500/T)}\right]$$

$$X\left[X_1^2+66X_1\exp(-5500/T)+10^3\exp(-12000/T)\right]^{-1}\exp(-18000/T) \qquad (5)$$

where P is measured in atmospheres and T in °K. For temperatures above 1100°K and low hydrazine molar fractions (references 6-8 of Chapter I),

$$\bar{w} \simeq -1.9 \times 10^{12}\frac{PX_1}{T}\exp(-27500/T) \qquad (6)$$

The energy balance equation reads

$$\frac{\dot{m}h^{e}_{1L}}{M_1} - \dot{m}\left[\sum_{i=1}^{4} Y_i \frac{h_i}{M_i} + Y_{1L}\frac{h_{1L}}{M_1}\right] + \dot{Q} = 0 \qquad (7)$$

where h stands for molar enthalpy and h^{e}_{1L} is the molar enthalpy of liquid hydrazine at the entrance. The external heating rate of the mixture within the combustion chamber, Q, may be written as

$$\dot{Q} = K(T_w - T) \qquad (8)$$

where T_w is a mean temperature of grids and chamber walls.

The energy equation for walls and grids is

$$C_w \frac{dT_w}{dt} = \dot{Q}_h - K(T_w - T) - \sigma_w A_w T_w^4 \qquad (9)$$

where C_w is their heat capacity; $\dot{Q}_h$ is the constant power input provided by the heater element and $\sigma_w A_w T_w^4$ is the power assumed to be radiated to the vacuum by a surface of aera A_w and emissivity σ_w. If, however, the chamber is shielded by an external heat shield, energy equations for both shield and walls should be considered instead of (9)

$$C_s \frac{dT_s}{dt} = \dot{Q}_s - \sigma_s A_s T_s^4 \qquad (10a)$$

$$C_w \frac{dT_w}{dt} = \dot{Q}_h - K(T_w - T) - \dot{Q}_s \qquad (10b)$$

where C_s and T_s are the shield heat capacity and temperature, and $\dot{Q}_s(T_s, T_w)$ is the power lost by the chamber to the shield. In steady-state, before the opening of the control valve ($t<0$), the heating term $\dot{Q}$ is missing and we have from (9) and (10) respectively.

$$T_w = T_{wo} = (\dot{Q}_h/\sigma_w A_w)^{1/4} \propto \dot{Q}_h^{1/4}, \tag{11}$$

$$\dot{Q}_h = \dot{Q}_s(T_{so}, T_{wo}) = \sigma_s A_s T_{so}^4$$

$$T_{wo} \sim T_{so} \propto \dot{Q}_h^{1/4} \tag{12}$$

Equation (9) may then be rewritten as

$$C_w \frac{dT_w}{dt} = \dot{Q}_h(1 - T_w^4/T_{wo}^4) - K(T_w - T) \tag{9'}$$

II. Nondimensional variables and parameters

From eqs. (1) to (3) we find

$$Y_{1L} = 1 - \dot{m}_v/\dot{m} \tag{13}$$

$$Y_1 = \dot{m}_v/\dot{m} + (M_1 V\overline{W}_1/\dot{m})\delta_1 \tag{14}$$

$$\frac{M_1}{M_j} Y_j = (M_1 V\overline{W}_1/\dot{m})\delta_j \, . \tag{15}$$

Since

$$X_1 = \frac{Y_1}{\Sigma Y_i M_1/M_i} \tag{16}$$

equations (14) and (15) yield

$$X_1 = (\dot{m}_v + M_1 V\bar{W}_1)/(\dot{m}_v + M_1 V\bar{W}_1 \Sigma\delta_i) \quad , \quad \Sigma\delta_i = -2\beta \tag{17}$$

and using equations (13)-(15), equations (7) becomes

$$\frac{M_1 K(T_w - T)}{\dot{m}} + h^e_{1L} - \frac{M_1 V\bar{W}_1}{\dot{m}} \Sigma h_i \delta_i - \frac{\dot{m}_v}{\dot{m}} h_1 - Y_{1L} h_{1L} = 0 \, . \tag{18}$$

Defining now

$$Q = \Sigma\delta_i h_i \tag{19}$$

which is the molar heat of reaction at constant pressure, we finally get

$$-\frac{M_1 V\bar{M}_1}{\dot{m}} = -\frac{M_1 K(T_w - T)}{\dot{m} Q} + \frac{h_1 - h^e_{1L}}{Q} - \frac{h_1 - h_{1L}}{Q}\left(1 - \frac{\dot{m}_v}{\dot{m}}\right) \, . \tag{20}$$

For Q we have

$$Q = \Delta H^0_{f(N_2H_4)} - 2(1-\beta)\Delta H^0_{f(NH_3)}$$

where $\Delta H^0_f(T)$ is the heat of formation, which can be taken from tables in reference 1; for $0.40<\beta<0.65$ and $700°K<T<1400°K$ we find

$$Q \simeq 35 \, \frac{Kcal}{mole} \quad ,$$

within an error of about 3% or less.

For $h_1 - h_{1L}^e$ we have from Fig. 1

$$h_1(T) - h_{1L}(T^e) \equiv h_D - h_A \approx h_C - h_B = L^e + \int_{T^e}^{T} C_p dT \qquad (21)$$

where L^e is the heat of vaporization at the entrance temperature T^e and C_p is the hydrazine molar heat capacity; in (21) we have neglected both $h_B - h_A$ (because the liquid molar volume and the coefficient of thermal expansion are very small) and $h_D - h_C$ (which is exactly zero for an ideal gas).

Under conditions to be determined in the next chapter we may set

$$\frac{\dot{m}_v}{\dot{m}} = 1 \qquad (22)$$

Then, defining

$$\sigma = \frac{M_1 K}{\dot{m} C_{pm}} + 1 \qquad (23)$$

$$\theta = \frac{C_{pm} T}{Q} \qquad (24)$$

we write equation (20) in the form

$$- \frac{M_1 V \bar{W}_1}{\dot{m}} = - (\sigma - 1) (\theta_w - \theta) + \frac{L^e}{Q} + (\theta - \theta^e) \qquad (25)$$

where the last term in (21) has been approximated by $C_{pm}(T - T^e)$. Here C_{pm} is an appropriate middle value of the hydrazine molar heat capacity at constant pressure C_p; choosing $C_{pm} = C_p(730°K) \approx 20.3 \frac{cal}{mole}$ the error in the approximation for equation (21) does not exceed 5% if, say, $\sigma > 5$ (smaller values of σ will later be shown unacceptable).

Finally equations (17) and (25) become

$$-\frac{M_1 V\bar{W}_1}{\dot{m}} \equiv \lambda f(X_1,\theta)\exp(-\frac{\theta_a}{\theta}) = \frac{1-X_1}{1+2\beta X_1} \qquad (26)$$

$$\lambda f(X_1,\theta)\exp(-\frac{\theta_a}{\theta}) = \sigma(\theta-\theta^*) \qquad (27)$$

where

$$\theta^* = \theta_w - \frac{\theta_w-\theta^e+L^e/Q}{\sigma} \qquad (28)$$

and 2β will be taken equal to unity.

If equation (5) is used we have

$$\lambda=\bar{\lambda}\equiv \frac{1.8\times10^{10}P^2M_1VC_{pm}^2}{\dot{m}Q^2} \simeq 19.4\times10^4\ \frac{V(cm^3)}{\dot{m}(g/s)}\left[P(atm)\right]^2 ,$$

$$\theta_a = \bar{\theta}_a \simeq 10.4 , \qquad (29)$$

$$f=\bar{f}\equiv \frac{1}{\theta^2}\left(X_1^2+\frac{0.8X_1^3}{X_1+510\exp(-3.2/\theta)}\right)\left[X_1^2+66X_1\exp(-3.2/\theta)+\right.$$

$$\left.+10^3\exp(-6.9/\theta)\right]^{-1} ;$$

similarly, from Eq(6)

$$\lambda = \bar{\bar{\lambda}} \simeq 1.9\times10^{12} \frac{PM_1 VC_{pm}}{\dot{m}Q} \simeq 3.5\times10^{10} \frac{V(cm^3)}{\dot{m}(g/s)} P(atm) \ , \tag{30}$$

$$\theta_a = \bar{\bar{\theta}}_a \simeq 16 \quad , \quad f = \bar{\bar{f}} \equiv X_1/\theta$$

Equation (9') may now be written as

$$\frac{d\theta_w}{ds} = \varepsilon\left(1 - \frac{\theta_w^4}{\theta_{wo}^4}\right) - (\sigma - 1)(\theta_w - \theta) \tag{31}$$

where

$$\varepsilon = \frac{M_1}{\dot{m}} \frac{\dot{Q}_h}{Q} \quad , \quad s = t \frac{\dot{m}C_{pm}}{M_1 C_w} \tag{32}$$

Equations (26)-(28) and (31) yield X_1, θ and θ_w as functions of λ, σ, θ^e, ε, θ_{wo} and s.

III. Frozen wall temperature

Consider first a pulse of duration τ such that

$$\tau << \frac{M_1 C_w}{\dot{m}C_{pm}} \tag{33}$$

Then $s << 1$ during the entire pulse, and therefore[a]

---

[a] As shown in the next chapter, Eq.(34) is valid under condition (33) even though σ will usually be large (ε, on the contrary, is usually small for typical engines).

$$\theta_w \simeq \theta_{wo} \tag{34}$$

Then Eqs. (26)-(28) yield X_1 and θ as functions of λ, σ, θ_{wo} and θ^e. The molar fraction X_1 lies between 0 (total combustion) and 1 (no combustion); the respective values of θ are $\theta^*+\sigma^{-1}$ and θ^* where now

$$\theta^* = \theta_{wo} - \frac{\theta_{wo}-\theta^e+L^e/Q}{\sigma} \quad . \tag{35}$$

Figure 2a represents X_1 versus $\bar{\lambda}$ for several values of $\sigma(5,10,20,40,\infty)$ and $T_{wo}=700°K$. Values of σ less than about 5 need not be considered since then $T^* \equiv Q\theta^*/C_{pm}$ would not be larger than the boiling temperature. On the other hand, for σ above 5, the maximum temperature, $(\theta^*+\sigma^{-1})Q/C_{pm}$, is about 1000°K or less, if T_{wo} does not exceed 900°K. Thus, in drawing Fig. 2a and following, we have used Eq.(29). Finally T^e has been set equal to 300°K; some results for different T^e are given at the end of the chapter.

It may be noticed that all curves in Fig. 2a cross one another at an unique point. To understand this, notice that, from Eqs. (26), (27) and (35)

$$\frac{1-X_1}{1+X_1} = \sigma\left(\theta-\theta_{wo} + \frac{\theta_{wo}-\theta^e+\frac{L^e}{Q}}{\sigma}\right) \tag{36}$$

Thus for $\theta=\theta_{wo}$,

$$X_1 = \frac{1-(\theta_{wo}-\theta^e+\frac{L^e}{Q})}{1+(\theta_{wo}-\theta^e+\frac{L^e}{Q})} \equiv X_{cr}(\theta_{wo}) \tag{37a}$$

$$\bar{\lambda} = \frac{\theta_{wo} - \theta^e + \frac{L^e}{Q}}{\bar{f}\{X_{cr}(\theta_{wo}), \theta_{wo}\}} \exp(\bar{\theta}_a/\theta_{wo}) \equiv \bar{\lambda}_{cr}(\theta_{wo}) \ . \qquad (37b)$$

It may also be noticed that curves $X_1(\bar{\lambda})$ change in shape with σ.

For large enough σ, X_1 decreases monotonically with increasing $\bar{\lambda}$. As σ decreases, however, a value σ_{inf} (about 20) is reached for which $X_1(\bar{\lambda})$ presents an inflexion point; below σ_{inf}, $\bar{\lambda}(X_1)$ presents both a minimum and a maximum and these values get farther apart as σ decreases,

Figure 2b represents θ versus $\bar{\lambda}$ for T_{wo}=700°K, T^e= =300°K and σ=5,10,20,40,∞. As in Fig. 2a all curves cross one another at a point $\{\theta=\theta_{wo}$, $\bar{\lambda}=\bar{\lambda}_{cr}(\theta_{wo})\}$. Moreover, from (36),

$$\frac{d\theta}{dX_1} = \frac{-2\sigma^{-1}}{(1+X_1)^2} \neq 0 \ , \quad \frac{d^2\theta}{dX_1^2} = \frac{4\sigma^{-1}}{(1+X_1)^3} \neq 0 \ ;$$

it follows that $\theta(\bar{\lambda},\sigma)$ and $X_1(\bar{\lambda},\sigma)$ present maxima and minima simultaneously and that, for $\sigma > \sigma_{inf}$, θ increases monotonically with σ. Also, from (35) we have

$\theta^* \to \theta_{wo}$, $\theta^* + \sigma^{-1} \to \theta_{wo}$ as $\sigma \to \infty$; thus, as seen in Fig, 2b, $\theta(\bar{\lambda},\sigma)$ collapses to $\theta=\theta_{wo}$ as $\sigma \to \infty$.

Figures 3a to 6a represent $X_1(\bar{\lambda},\sigma)$ for T^e = 300°K and T_{wo} = 750,800,850 and 900°K respectively; similarly Figs. 3b to 6b represent $\theta(\bar{\lambda},\sigma)$. The figures prove that the value of σ_{inf} decreases as θ_{wo} increases.

In Chapter III we will show that if $\sigma < \sigma_{inf}(\theta_{wo})$ and

$\bar{\lambda}$ lies between the above mentioned minimum and maximum, the actual solution will lie on the upper branch of Figs. 2a-6a (lower branch in Figs. 2b-6b). Then, as seen in the figures, we have approximatly

$$X_1 \simeq 0 \quad , \quad \theta \simeq \theta^* + \frac{1}{\sigma}$$

if $\bar{\lambda} > \bar{\lambda}_{max}(\theta_{wo},\sigma)$, where $\lambda_{max}(\theta_{wo},\sigma)$ is the maximum of $\bar{\lambda}$, while if $\bar{\lambda} < \bar{\lambda}_{max}(\theta_{wo},\sigma)$ we have

$$X_1 \simeq 1 \quad , \quad \theta \simeq \theta^* \ ;$$

clearly $\bar{\lambda}_{max}$ is an ignition value of $\bar{\lambda}$. On the other hand if $\sigma > \sigma_{inf}(\theta_{wo})$, there is no such clear-cut criterion for ignition; one may say, however, that if $\bar{\lambda} > \bar{\lambda}_{cr}(\theta_{wo})$ the unburned fraction X_1 will not exceed 0.3 (see Figs. 2a-6a).

$\bar{\lambda}_{max}$ may be estimated analytically for σ not too large (clearly, we must have $\sigma < \sigma_{inf}$ anyway). At $\bar{\lambda}_{max}$, we have $\frac{d\lambda}{d\theta} = 0$ while $X_1 \simeq 1$ and $\theta \simeq \theta^*$; then $\bar{f} \simeq 1.8\theta^{-2}$ and Eq.(27) becomes

$$\bar{\lambda} = \frac{\sigma\theta^2}{1.8}(\theta-\theta^*)\exp(\frac{\theta_a}{\theta}) \qquad (38)$$

To first order in $\theta^*/\bar{\theta}_a$, which is small due to the large activation energy of the overall reaction, we find

$$\bar{\lambda}_{max} \simeq \frac{\sigma}{1.8}(\theta^{*4}/\bar{\theta}_a)(1+3\theta^*/\bar{\theta}_a)\exp(\frac{\theta_a}{\theta^*} - 1) \ , \qquad (39)$$

$$\theta(\bar{\lambda}_{max}) \simeq \theta^*(1+\theta^*/\bar{\theta}_a), \qquad (40)$$

$$X_1(\bar{\lambda}_{max}) \simeq 1-2\sigma\,\theta^{*2}/\bar{\theta}_a, \qquad (41)$$

IV. Equilibrium wall temperature

If the pulse duration τ is such that

$$\tau >> \frac{M_1 C_w}{\dot{m} C_{pm}}$$

one may assume that a steady wall temperature has been reached. Then Eqs. (26)-(28) together with Eq. (31) (where $d\theta_w/ds$ is neglected) yield X_1, θ and θ_w as functions of λ, σ, θ_{wo}, θ^e and ε. We get therefore

$$\frac{1-X_1}{1+X_1} = \varepsilon\left(\frac{\theta}{\theta_{wo}^4} - 1\right) + \theta + \frac{L^e}{Q} - \theta^e, \tag{42}$$

$$\lambda f e^{-\frac{\theta_a}{\theta}} = \frac{1-X_1}{1+X_1}, \tag{43}$$

$$\theta_w = \theta - \frac{\varepsilon}{\sigma-1}\left(\frac{\theta_w^4}{\theta_{wo}^4} - 1\right). \tag{44}$$

For typical values of ε and for acceptable $\sigma(\sigma>5)$, Eq.(44) gives $\theta_w \simeq \theta$. Then Eqs. (42) and (43) will give $X_1(\lambda)$ (a typical curve obtained is shown schematically in fig.7) and $\theta(\lambda)$.

Since X_1 is a two-valued function of λ, we must discuss on which branch the steady-state lies. Consider then the time evolution until that state is reached; that is, consider Eqs. (26)-(28) and (31), the initial condition being $\theta_w = \theta_{wo}$ (pulsed regime conditions). To simplify the discussion, neglect the first term on the right hand side of Eqs. (31), and (42), which represents a small correction; then

$(X_{cr}, \bar{\lambda}_{cr})$, as given in Eqs. (37), satisfy Eqs. (42) and (43) when using Eq. (29) [$(X_{cr}, \bar{\lambda}_{cr})$ lies on the upper branch in Fig. 7 for all reasonable values of θ_{wo}].

Now, let us first assume $\sigma>\sigma_{inf}(\theta_{wo})$. If $\bar{\lambda}=\bar{\lambda}_{II}>\bar{\lambda}_{cr}(\theta_{wo})$ (see Fig. 7), then from Figs. 2a to 6b, $\theta(s=0)>\theta_{wo}$ and $X_1(s=0)<X_{cr}$. Consequently, first, $(d\theta_w/ds)_{s=0}>0$ (see Eq. (31)) and clearly $d\theta_w/ds$ will remain positive until the steady-state is reached. Since the flow remains steady as s grows and θ_w changes, both X_1 and θ are given, for each θ_w, by Eqs. (26)-(28); their evolution, clearly, may be followed from Figs. 2a-6b, for given σ and λ. Then $dX_1/d\theta_w<0$ since X_1 in Figs. 2a to 6a is a decreasing function of θ_{wo}; thus $dX_1/ds<0$. Therefore, since $X_1(s=0) < X_{cr}$ [$X_1(s=0)$ lies between both branches (Point B of Fig. 7)], the steady state will correspond to point D in the lower branch. If, on the other hand $\bar{\lambda}=\bar{\lambda}_I<\bar{\lambda}_{cr}(\theta_{wo})$, then $\theta(s=0)<\theta_{wo}$ and $X_1(s=0)>X_{cr}$; now $X_1(s=0)$ lies above the upper branch in Fig. 7 (Point C) while $dX_1/ds>0$, and therefore combustion will decrease until extinction.

Let now $\sigma<\sigma_{inf}(\theta_{wo})$. It can be shown, in a way similar to that of case $\sigma>\sigma_{inf}(\theta_{wo})$, that if $\bar{\lambda}=\bar{\lambda}_{III}>\bar{\lambda}_{max}(\theta_{wo},\sigma)$ the steady state will lie on the lower branch while if $\bar{\lambda}=\bar{\lambda}_I<\bar{\lambda}_{cr}(\theta_{wo})$, X_1 will increase until extinction. On the other hand, if $\bar{\lambda}_{cr}(\theta_{wo})<\bar{\lambda} = \bar{\lambda}_{II}<\bar{\lambda}_{max}(\theta_{wo},\sigma)$ then X_1 will increase until either steady state on the upper branch [for $X_1(s=0)$ below the upper branch] or extinction [for $X_1(s=0)$ above that branch] are reached; since, however, $X_1(s=0)$ would be close to unity, combustion will be negligible in either case.

Quantitative results for X_1 and θ versus λ, for several T_{wo} (and T^e), are given in Figs. 8a and 8b. Since, however, lower branch temperatures are too large to use Eq. (29) (that is, $\bar{\lambda}$), these figures have been computed using Eq. (30) (that

is $\bar{\bar{\lambda}}$.

V. Discussion of results

The analysis carried out in sections III and IV leads to clear cut conclusions about the performance of thermal hydrazine engines. There we introducedthe functions

$$\sigma_{inf}(T_{wo}, T^e) ,$$

$$\bar{\lambda}_{cr}(T_{wo}, T^e) ,$$

$$\bar{\lambda}_{max}(\sigma, T_{wo}, T^e)$$

Let us now define

$$\bar{\lambda}_{ign}(\sigma, T_{wo}, T^e) = \bar{\lambda}_{cr}(T_{wo}, T^e), \quad \text{if} \quad \sigma>\sigma_{inf}(T_{wo}, T^e)$$

$$= \bar{\lambda}_{max}(\sigma, T_{wo}, T^e) \quad \text{if} \quad \sigma<\sigma_{inf}(T_{wo}, T^e);$$

$\bar{\lambda}_{ign}$ is shown versus σ for several values of T_{wo} and T^e in Figs. 9. The points where the straight and curved parts of the lines meet, correspond to σ_{inf} and $\bar{\lambda}_{cr}$ for each pair of T_{wo} and T^e values. An alternative representation of $\bar{\lambda}_{ign}(\sigma, T_{wo}, T^e)$ is given in Figs. 10.

Now, we showed in sections III and IV that for both pulsed and steady regimes, and given $\bar{\lambda}$, σ, T_{wo} and T^e, if $\bar{\lambda}>\bar{\lambda}_{ign}(\sigma, T_{wo}, T^e)$ there is near full combustion ($X_1 \simeq 0$) while if $\bar{\lambda}<\bar{\lambda}_{ign}$ the opposite conclusion follows ($X_1 \simeq 1$). Actually, for the pulsed regime the above statement is a clear cut conclusion only for $\sigma<\sigma_{inf}(T_{wo}, T^e)$; for $\sigma>\sigma_{inf}$, a more precise conclusion is that for $\bar{\lambda}>\bar{\lambda}_{ign}\equiv\bar{\lambda}_{cr}$, then X_1 is less than about 0.3.

If near full combustion occurs ($\bar{\lambda}>\bar{\lambda}_{ign}$) engine performances may be determined using Figs. 2a-6b for the pulsed regime and Figs. 8 for the steady regime.

Notice that for σ less than about 5, $\bar{\lambda}$ becomes extremely large, confirming that $\sigma<5$ values are unaceptable. On the other hand, for given T_{wo} and T^e, increasing σ beyond $\sigma_{inf}(T_{wo}, T^e)$ is useless since then λ_{ign} does not depend on σ; σ_{inf} is shown in Fig. 11. Finally, Fig. 12 shows $\bar{\lambda}_{cr}(T_{wo}, T^e)$ (the minimum $\bar{\lambda}$ value for ignition to occur).

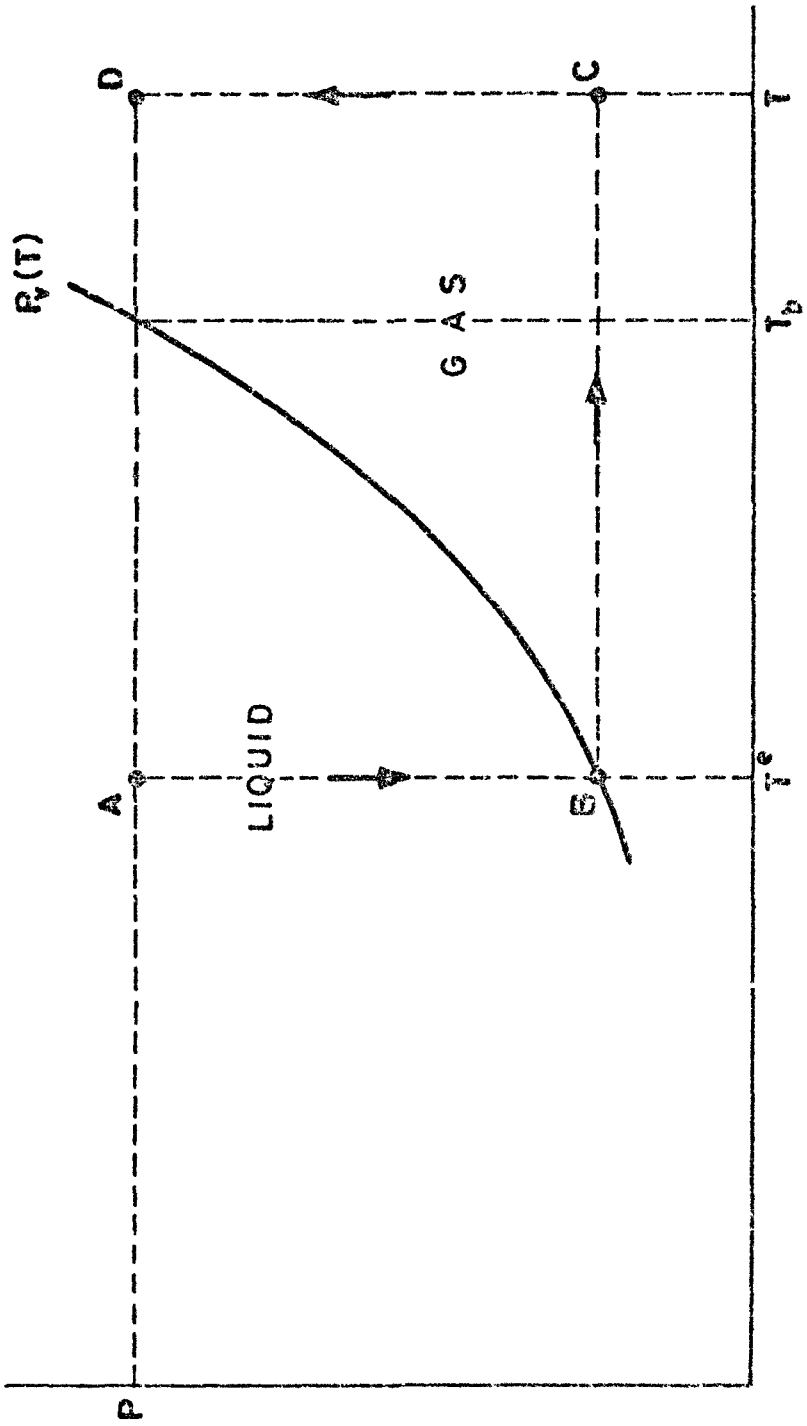

Fig.1 Schematic diagram showing the approximation in Eq.(21)

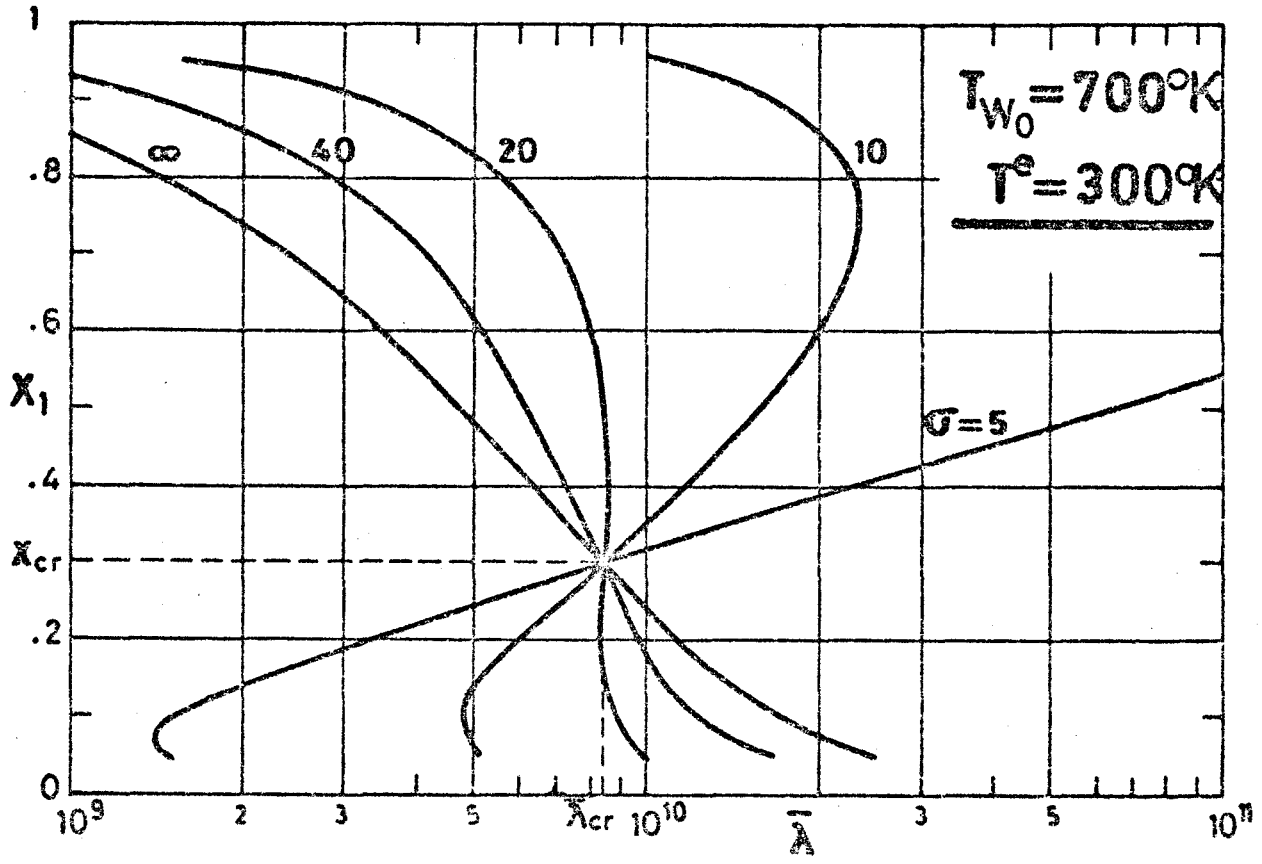

Fig.2a Hydrazine molar fraction X_1 at the chamber exit, versus parameters σ and $\bar{\lambda}$, defined in Eqs.(23) and (29); entrance temperature $T^e=300°K$.

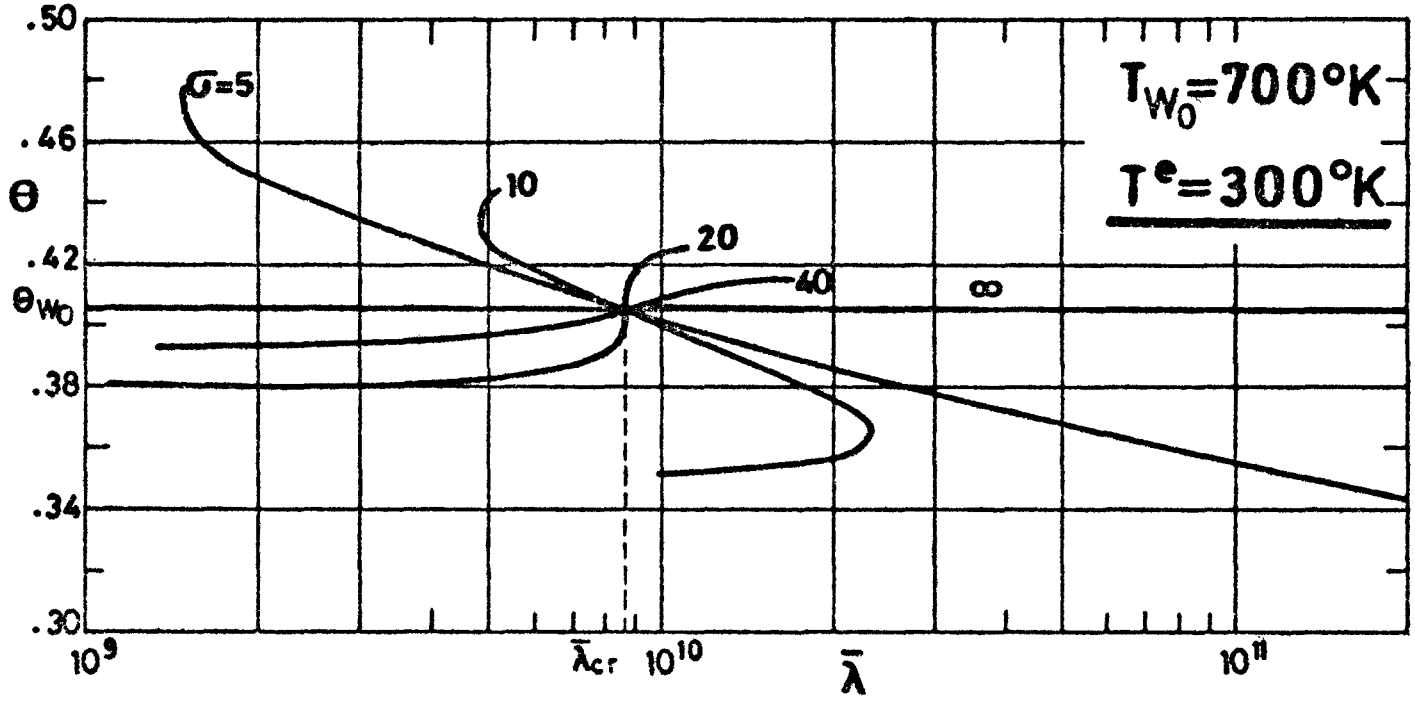

Fig.2b Dimensionless temperature $\theta \equiv TC_{pm}/Q$ at the chamber exit, versus parameters σ and $\bar{\lambda}$ defined in Eqs.(23) and (29); entrance temperature T^e=300°K.

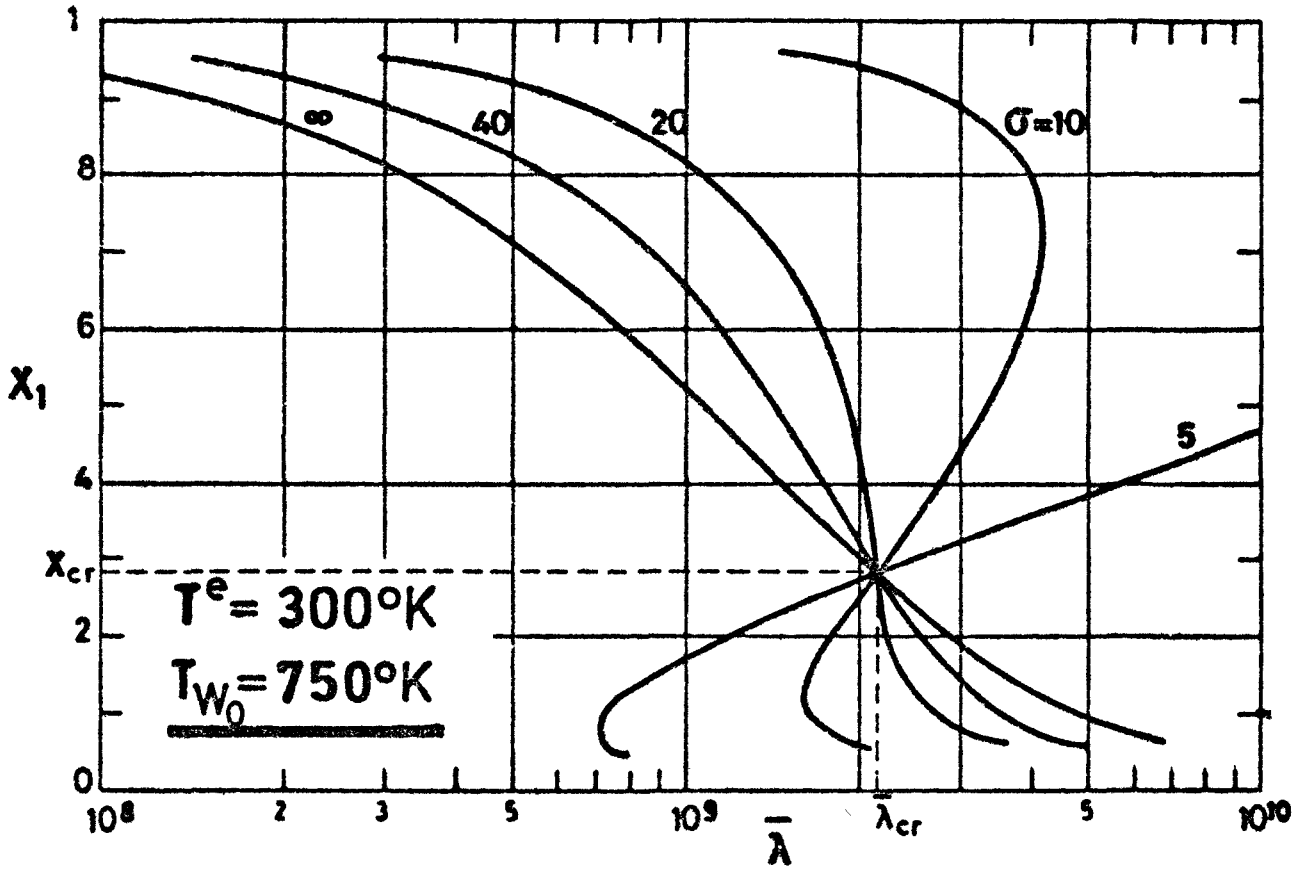

Fig.3a Hydrazine molar fraction X_1 at the chamber exit, versus parameters σ and $\bar{\lambda}$, defined in Eqs.(23) and (29); entrance temperature T^e=300°K.

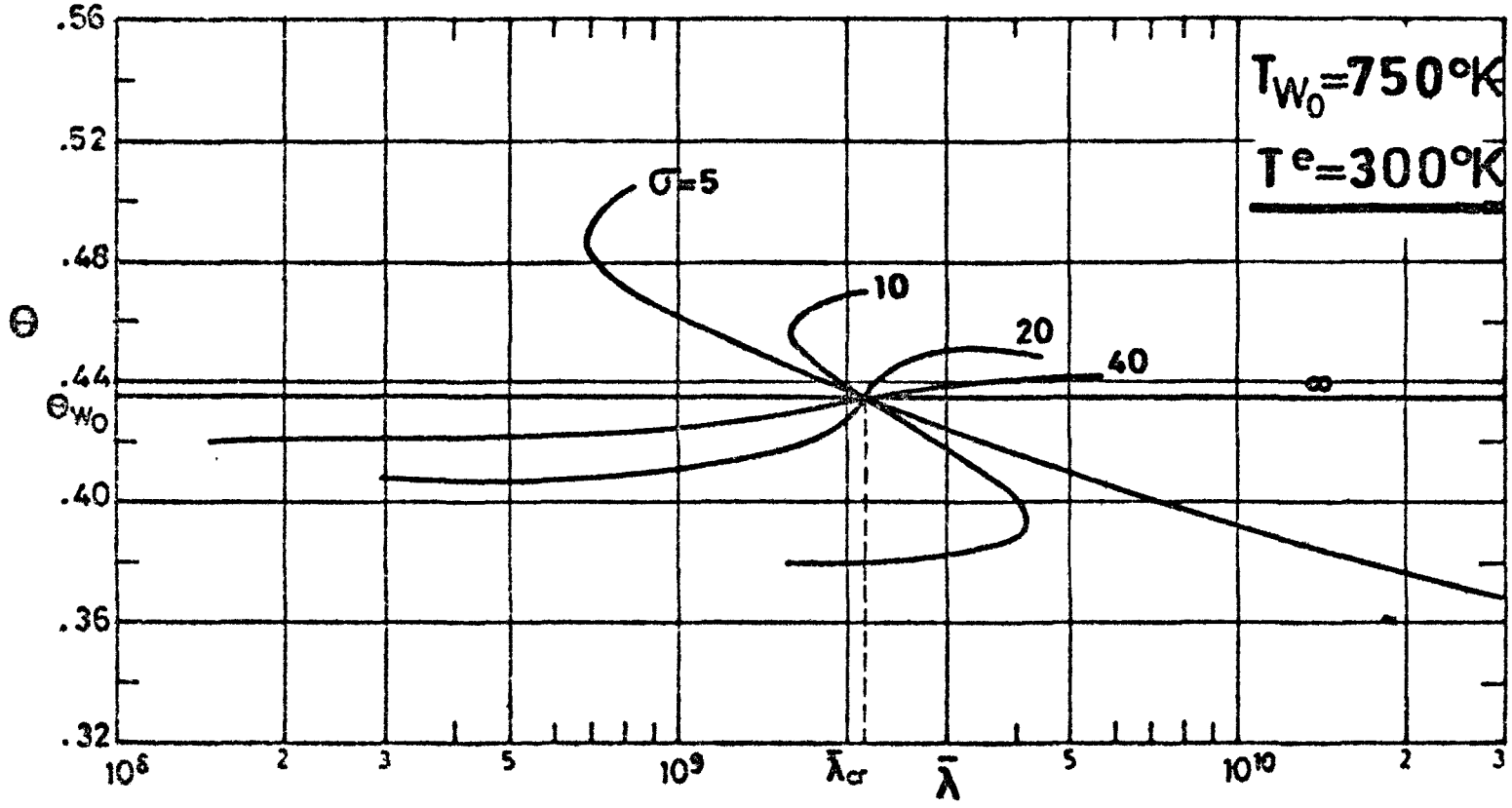

Fig.3b Dimensionless temperature $\theta \equiv TC_{pm}/Q$ at the chamber exit, versus parameters σ and $\bar{\lambda}$ defined in Eqs.(23) and (29); entrance temperature $T^e = 300°K$.

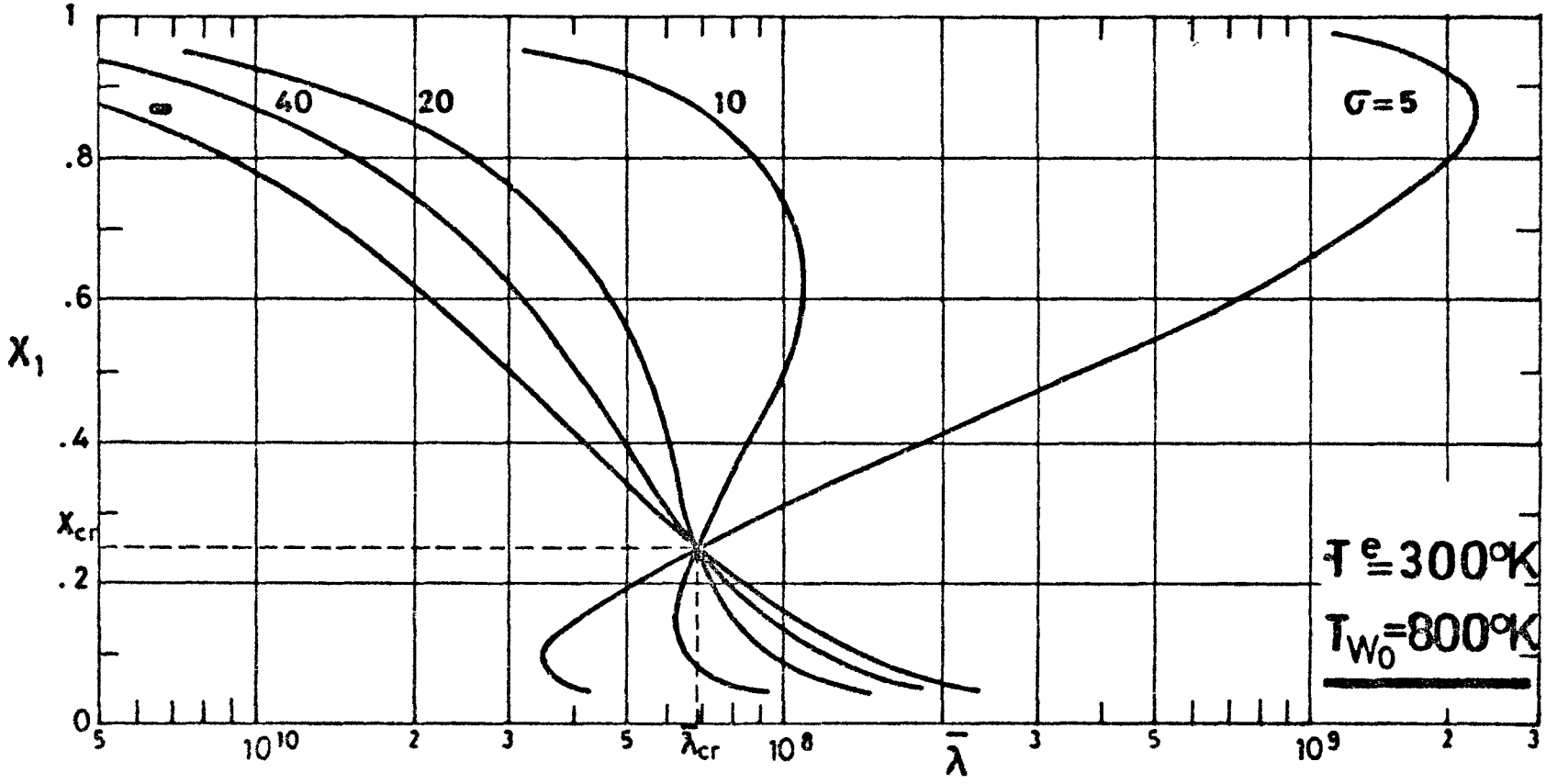

Fig.4a Hydrazine molar fraction X_1 at the chamber exit, versus parameters σ and $\bar{\lambda}$, defined in Eqs.(23) and (29); entrance temperature T^e=300°K.

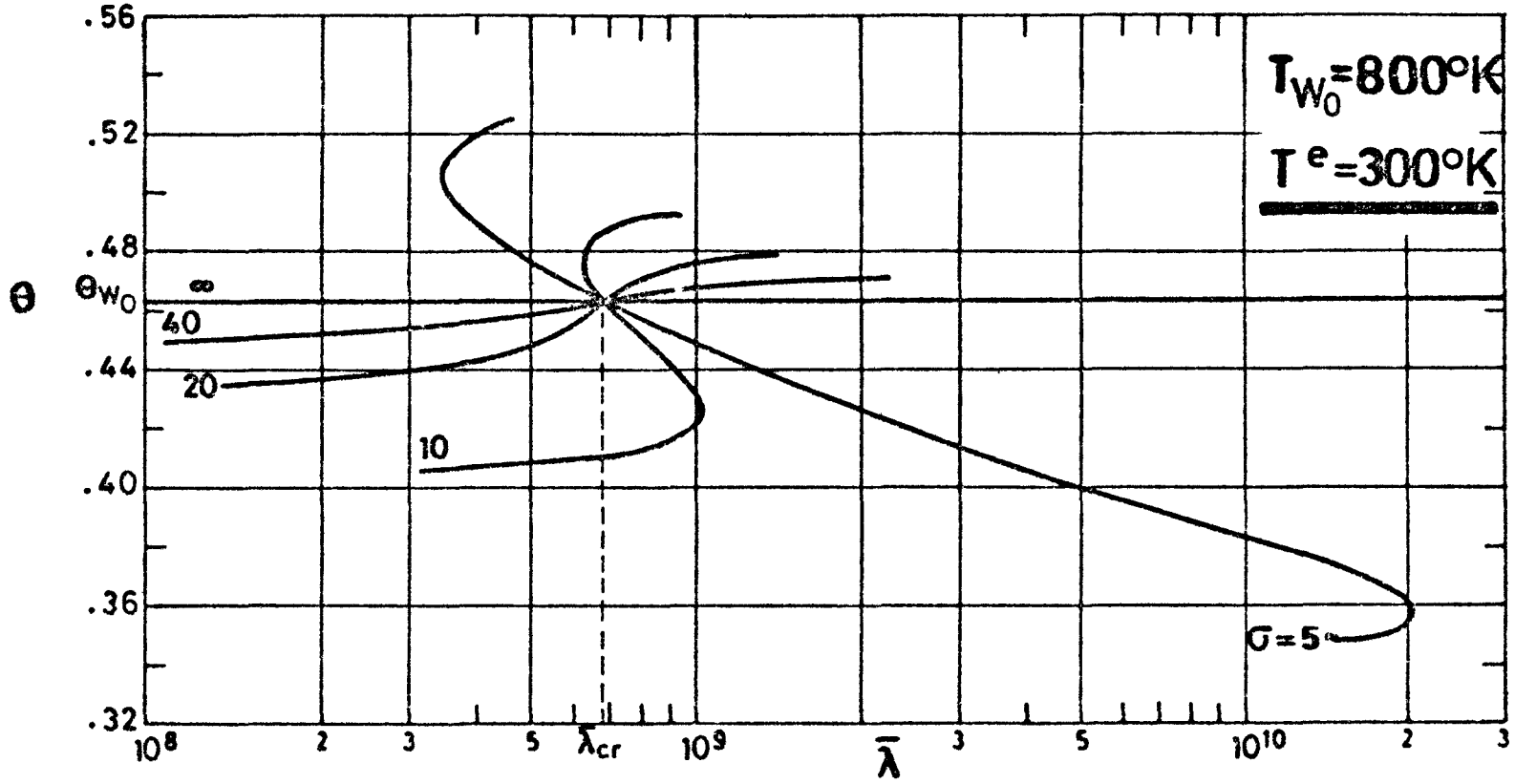

Fig.4b Dimensionless temperature $\theta \equiv TC_{pm}/Q$ at the chamber exit, versus parameters σ and $\bar{\lambda}$ defined in Eqs.(23) and (29); entrance temperature $T^e = 300°K$.

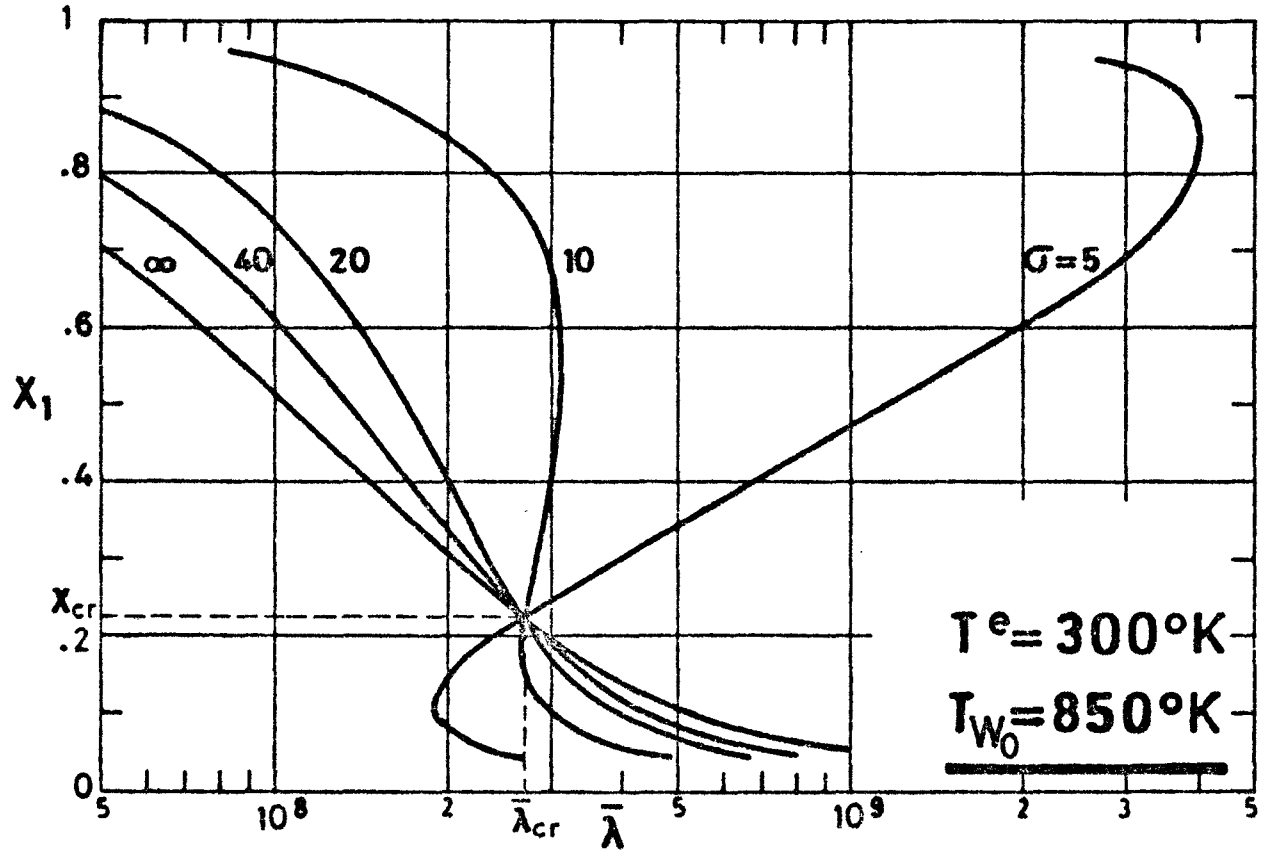

Fig.5a Hydrazine molar fraction X_1 at the chamber exit, versus parameters σ and $\bar{\lambda}$, defined in Eqs.(23) and (29); entrance temperature T^e=300°K.

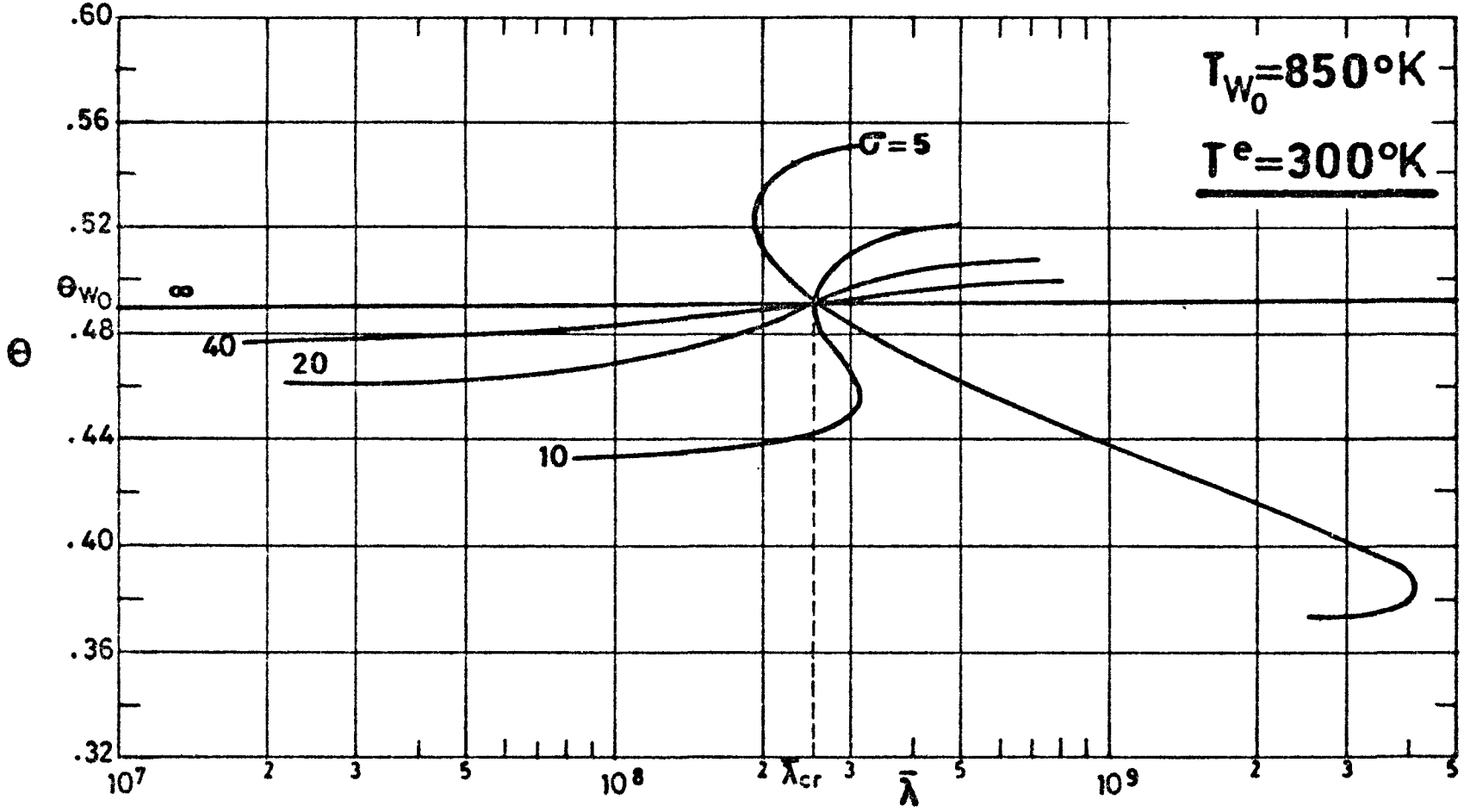

Fig.5b Dimensionless temperature $\theta \equiv TC_{pm}/Q$ at the chamber exit, versus parameters σ and $\bar{\lambda}$ defined in Eqs.(23) and (29); entrance temperature T^e=300°K.

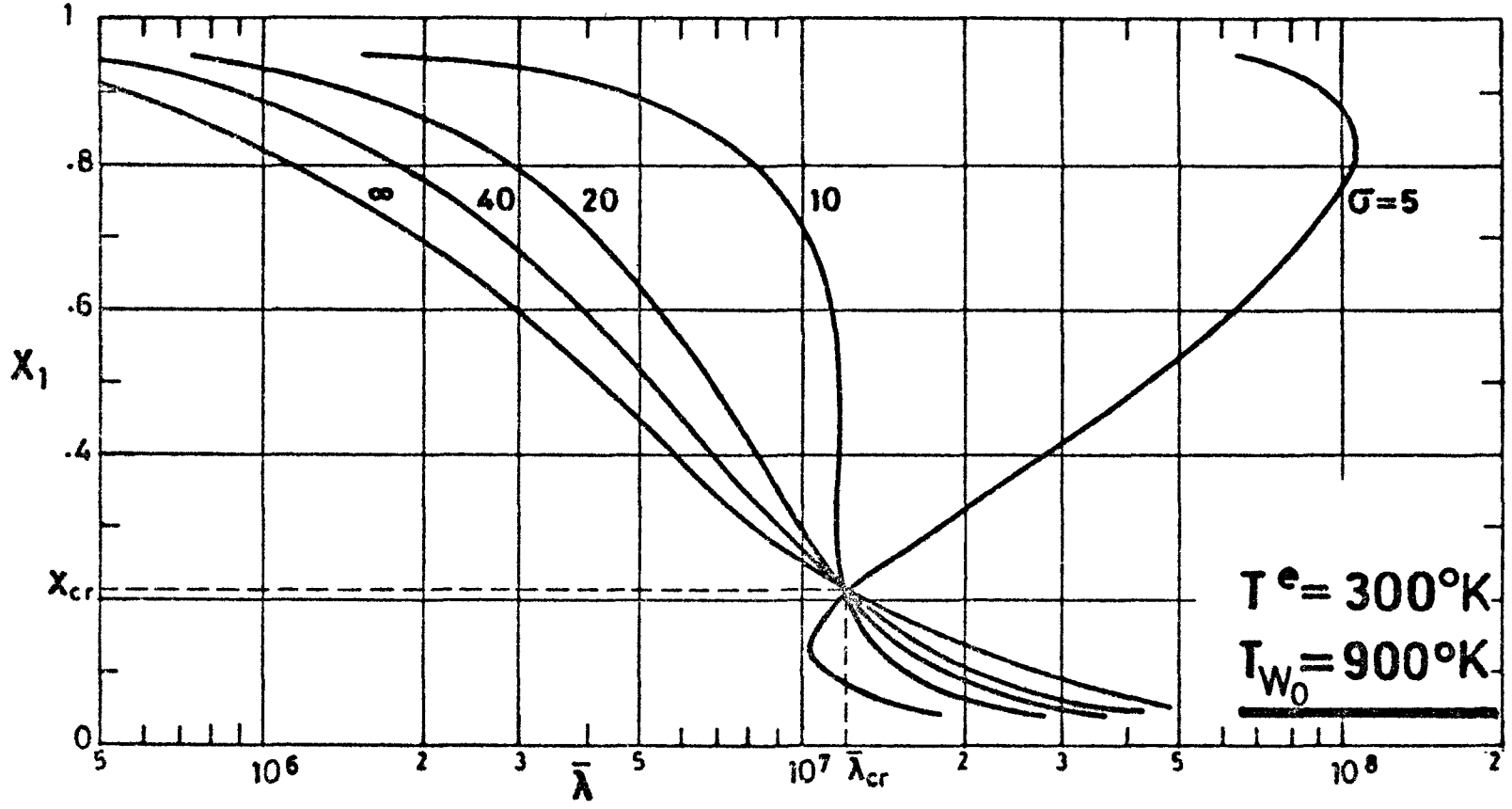

Fig.6a Hydrazine molar fraction X_1 at the chamber exit, versus parameters σ and $\bar{\lambda}$, defined in Eqs.(23) and (29); entrance temperature T^e=300°K.

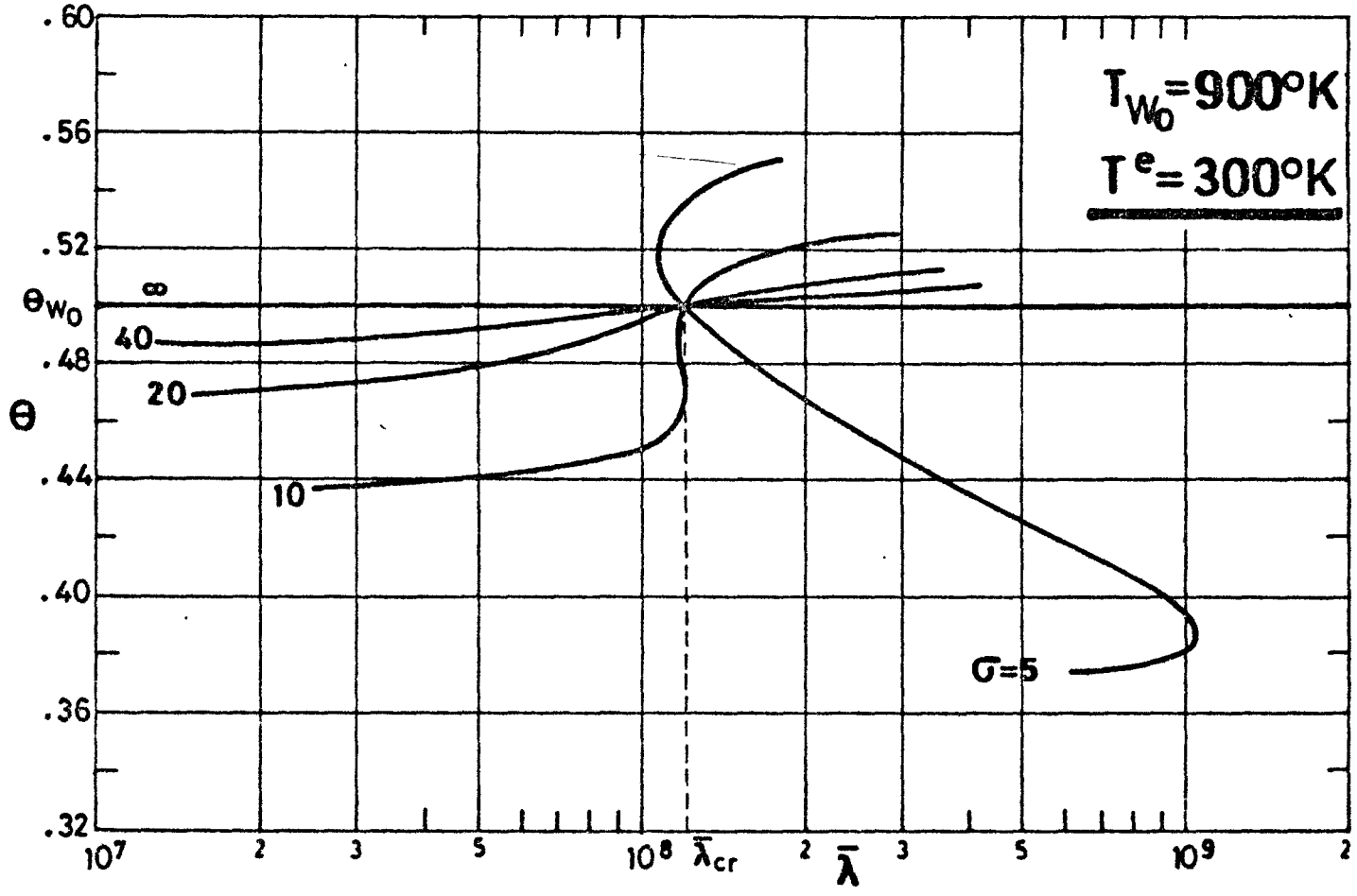

Fig.6b Dimensionless temperature $\theta \equiv TC_{\bar{p}m}/Q$ at the chamber exit, versus parameters σ and $\bar{\lambda}$ defined in Eqs.(23) and (29); entrance temperature T^e=300°K.

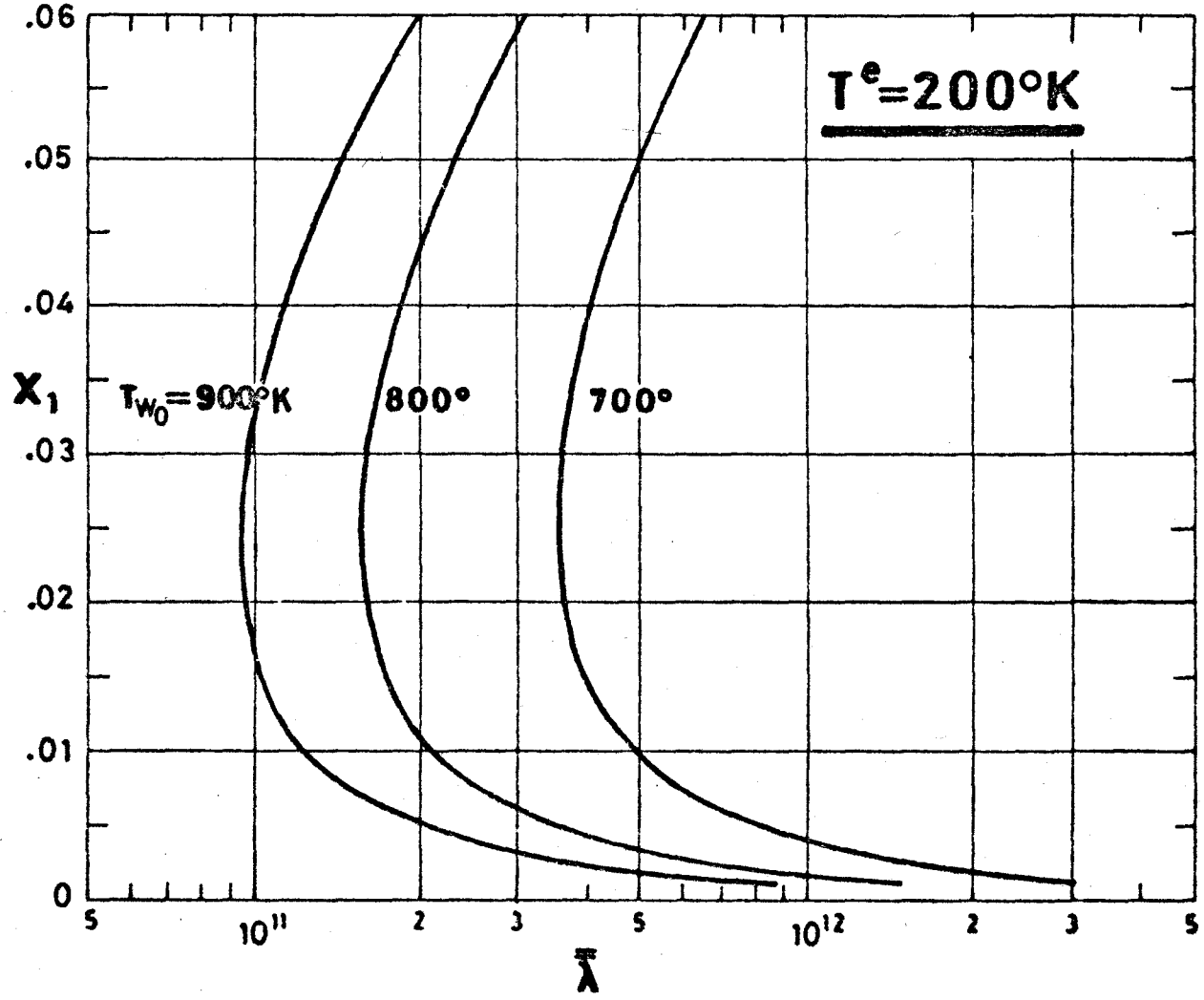

Fig.8a, Hydrazine molar fraction X_1 at the chamber exit, versus $\bar{\lambda}$ for different T_{wo} and T^e=200°K (steady regime).

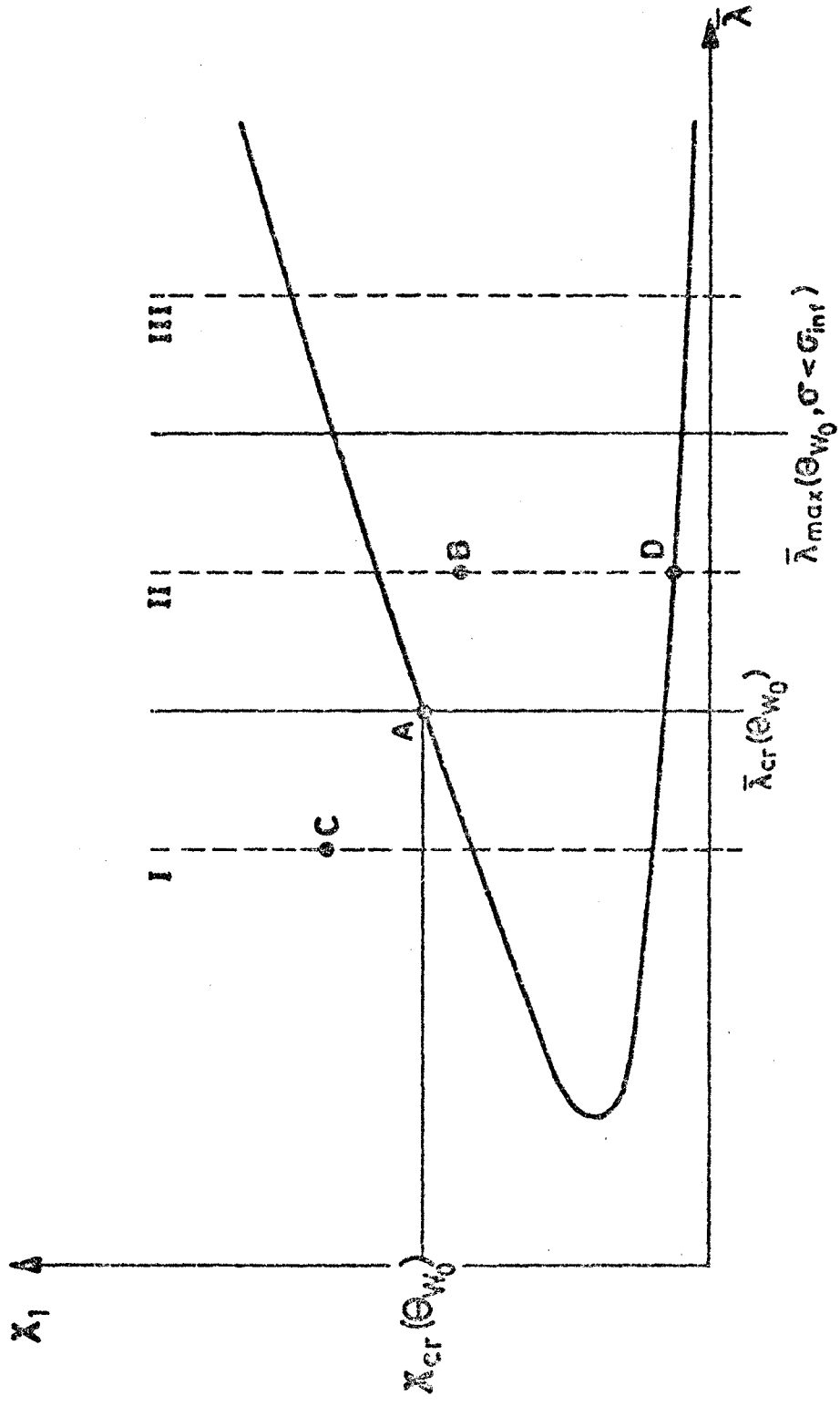

Fig.7 Schematic diagram showing the steady regime solution for $X_1(\bar{\lambda})$.

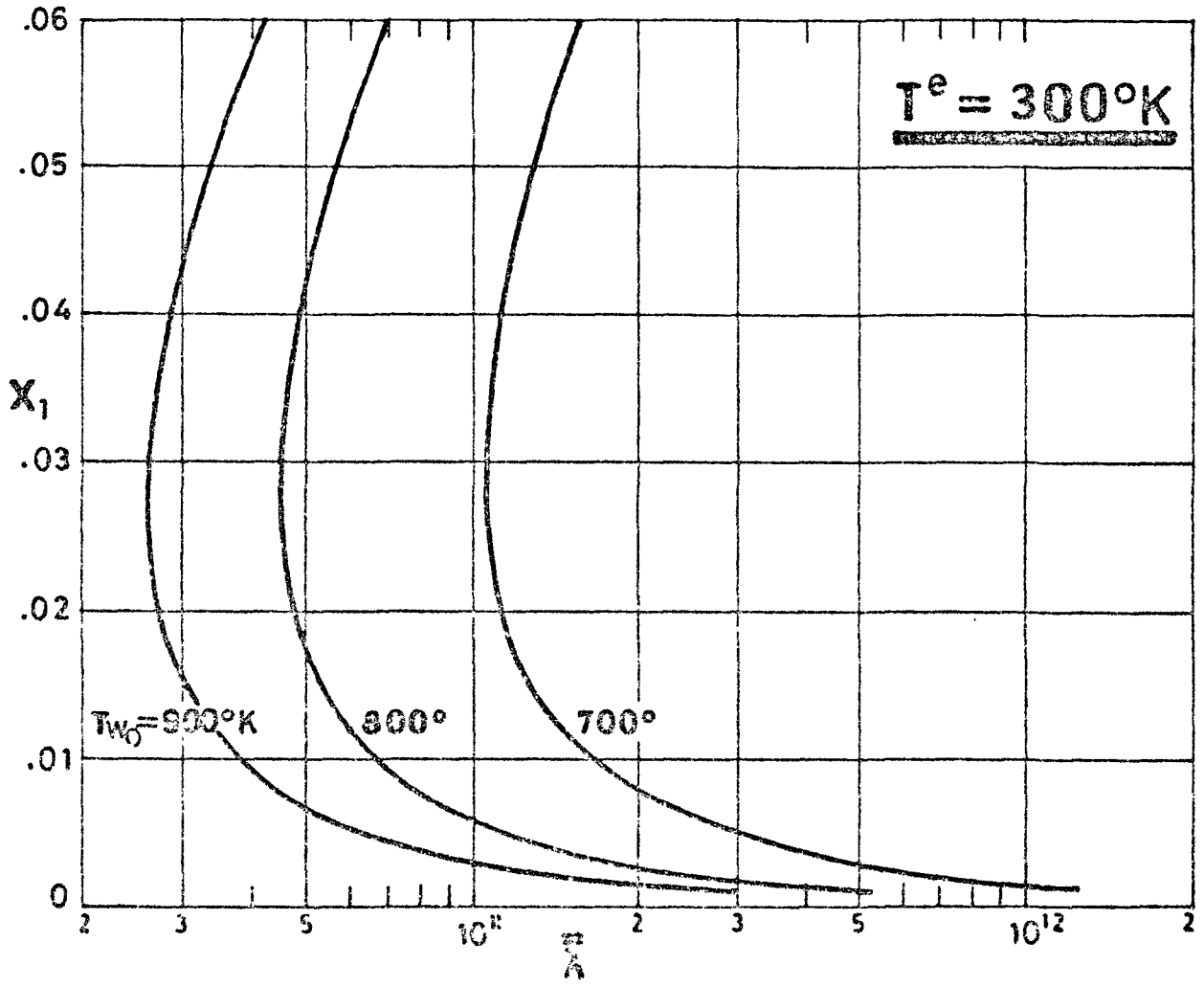

Fig.8a$_2$ Hydrazine molar fraction X_1 at the chamber exit, versus $\bar{\lambda}$ for different T_{wo} and T^e=300°K (steady regime).

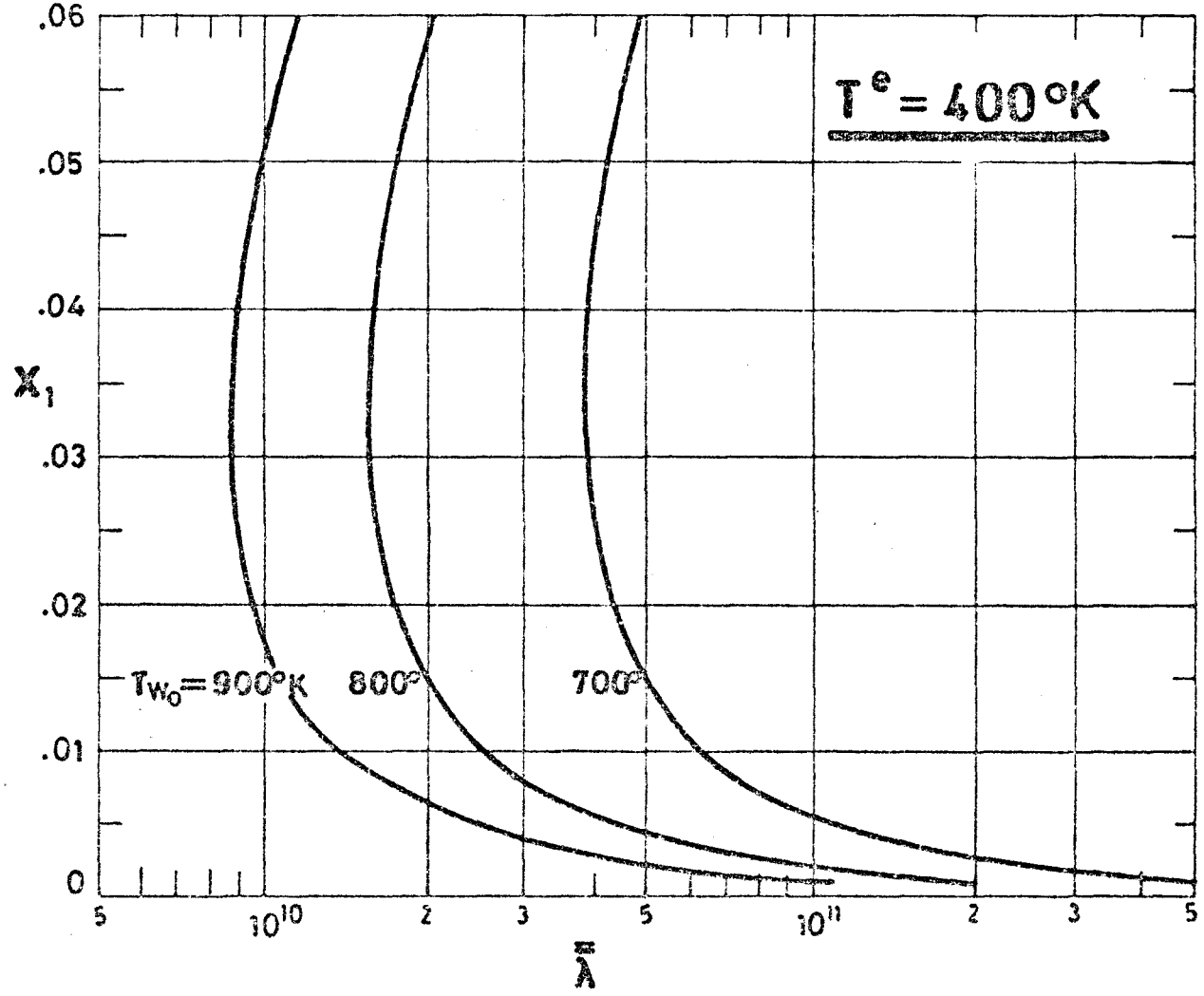

Fig.8a$_3$ Hydrazine molar fraction X_1 at the chamber exit, versus $\bar{\lambda}$ for different T_{wo} and T^e=400°K (steady regime).

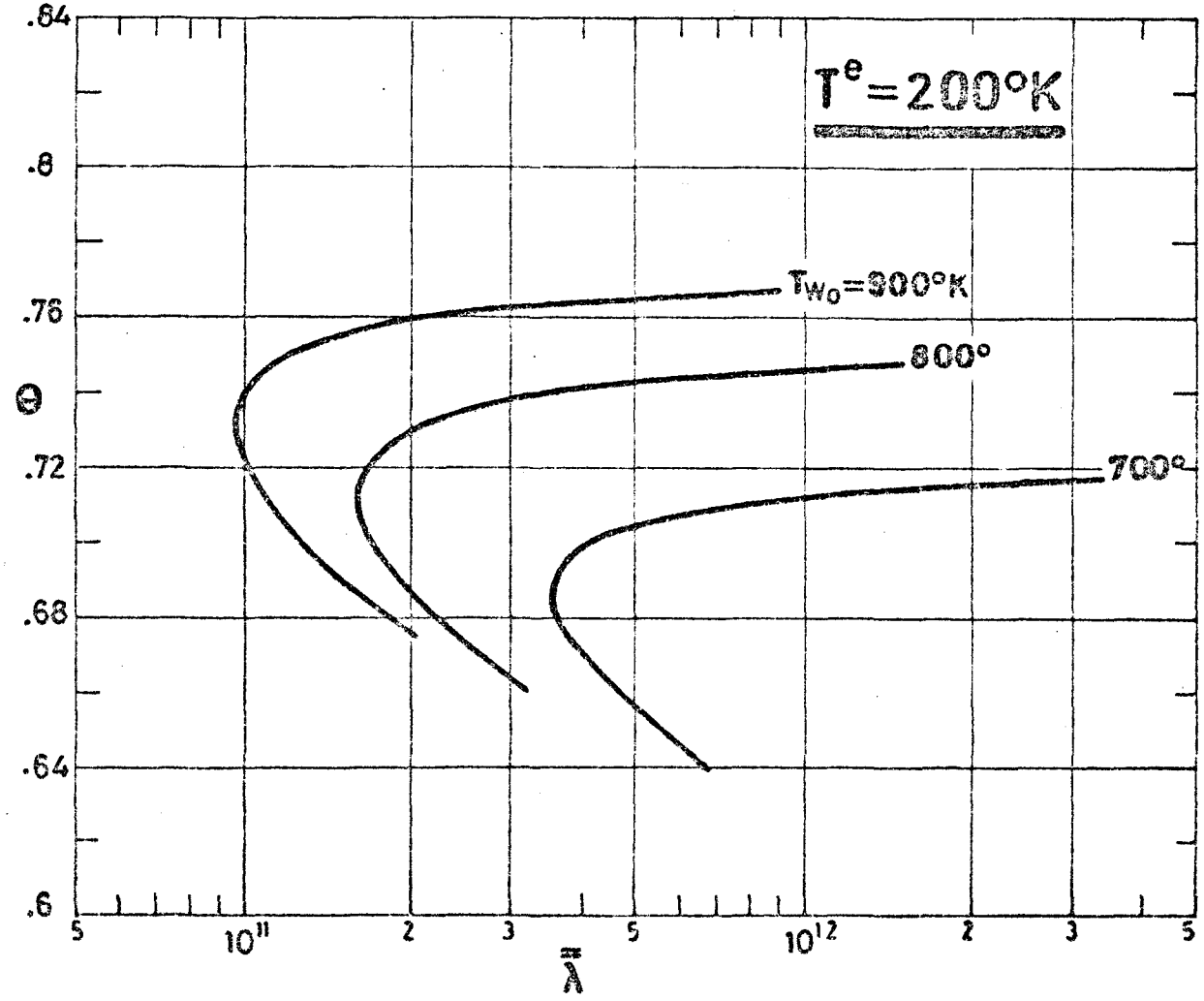

Fig.8b, Dimensionless temperature $\theta \equiv TC_{pm}/Q$ at the chamber exit, versus $\bar{\lambda}$ for different T_{wo} and $T^e = 200°K$ (steady regime).

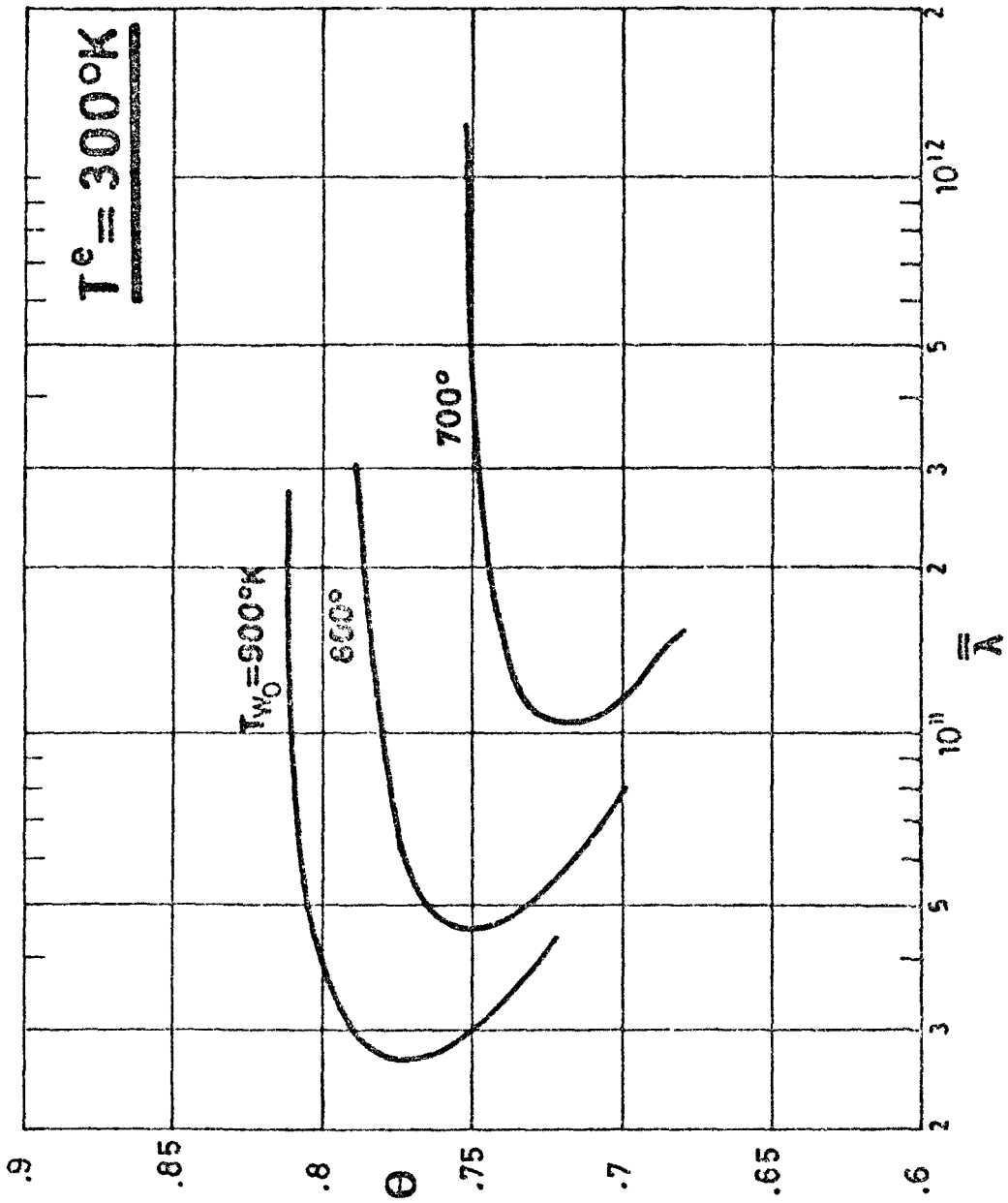

Fig.8b$_2$ Dimensionless temperature $\theta \equiv TC_{pm}/Q$ at the chamber exit, versus $\bar{\bar{\lambda}}$ for different T_{wo} and T^e=300°K (steady regime).

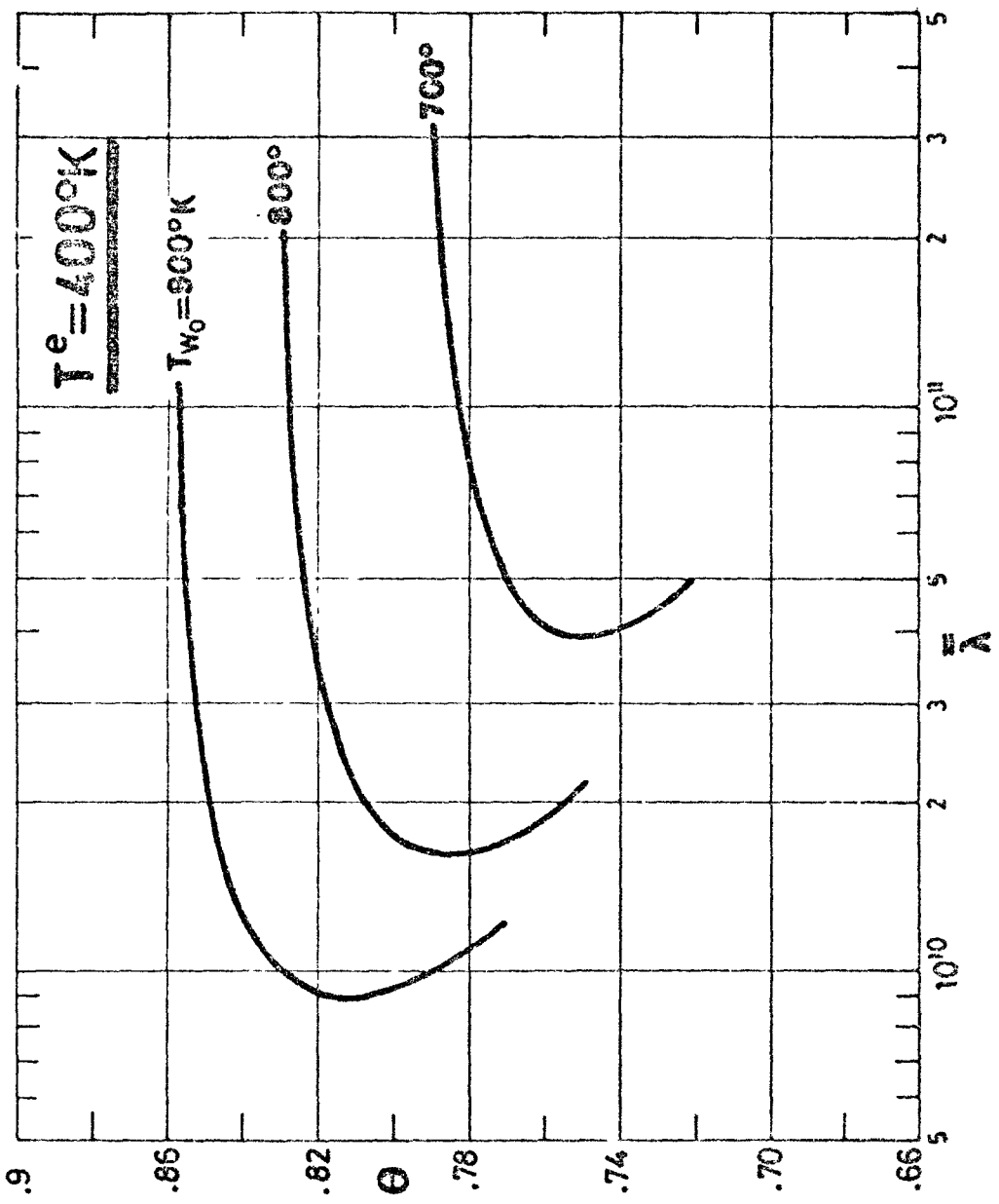

Fig.8b$_3$ Dimensionless temperature $\theta = T/T_{p_n}$ at the chamber exit, versus $\bar{\lambda}$ for different T_{w_0} and T^e=400°K (steady regime).

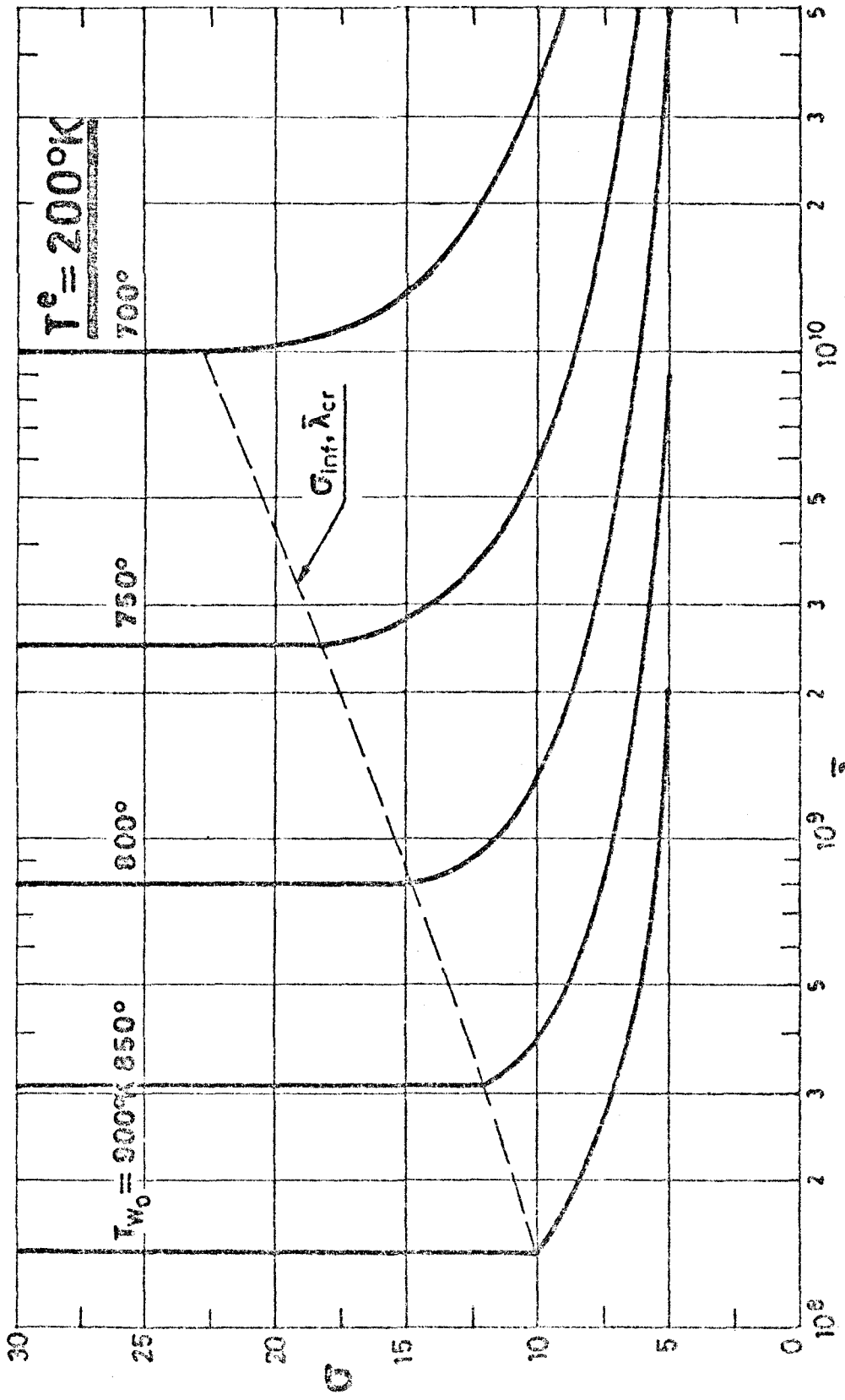

Fig. 9a $\bar{\lambda}_{ign}$ versus σ for several T_{wo} and $T^e = 200°K$.

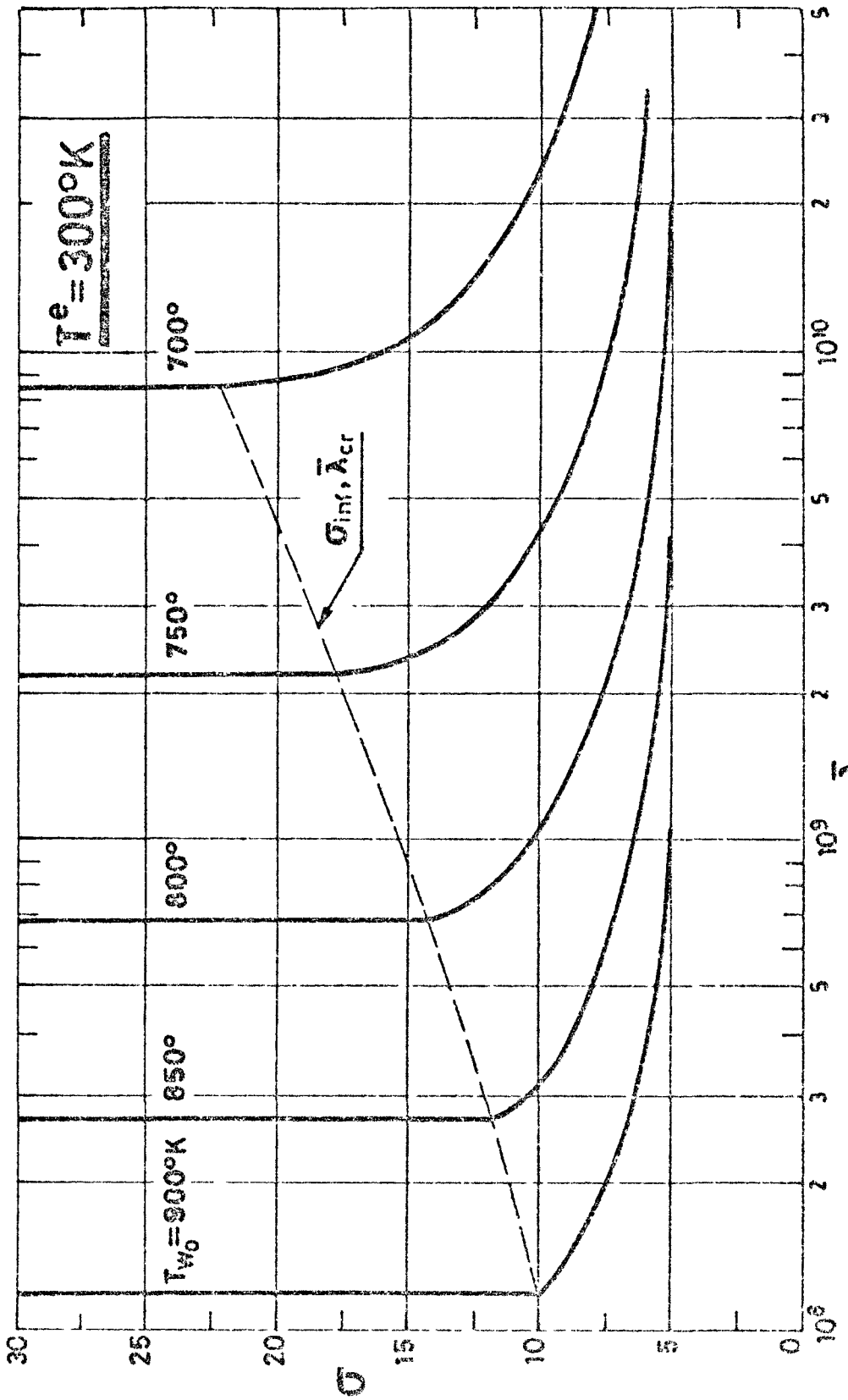

Fig.9b $\bar{\lambda}_{ign}$ versus σ for several T_{wo} and T^e=300°K.

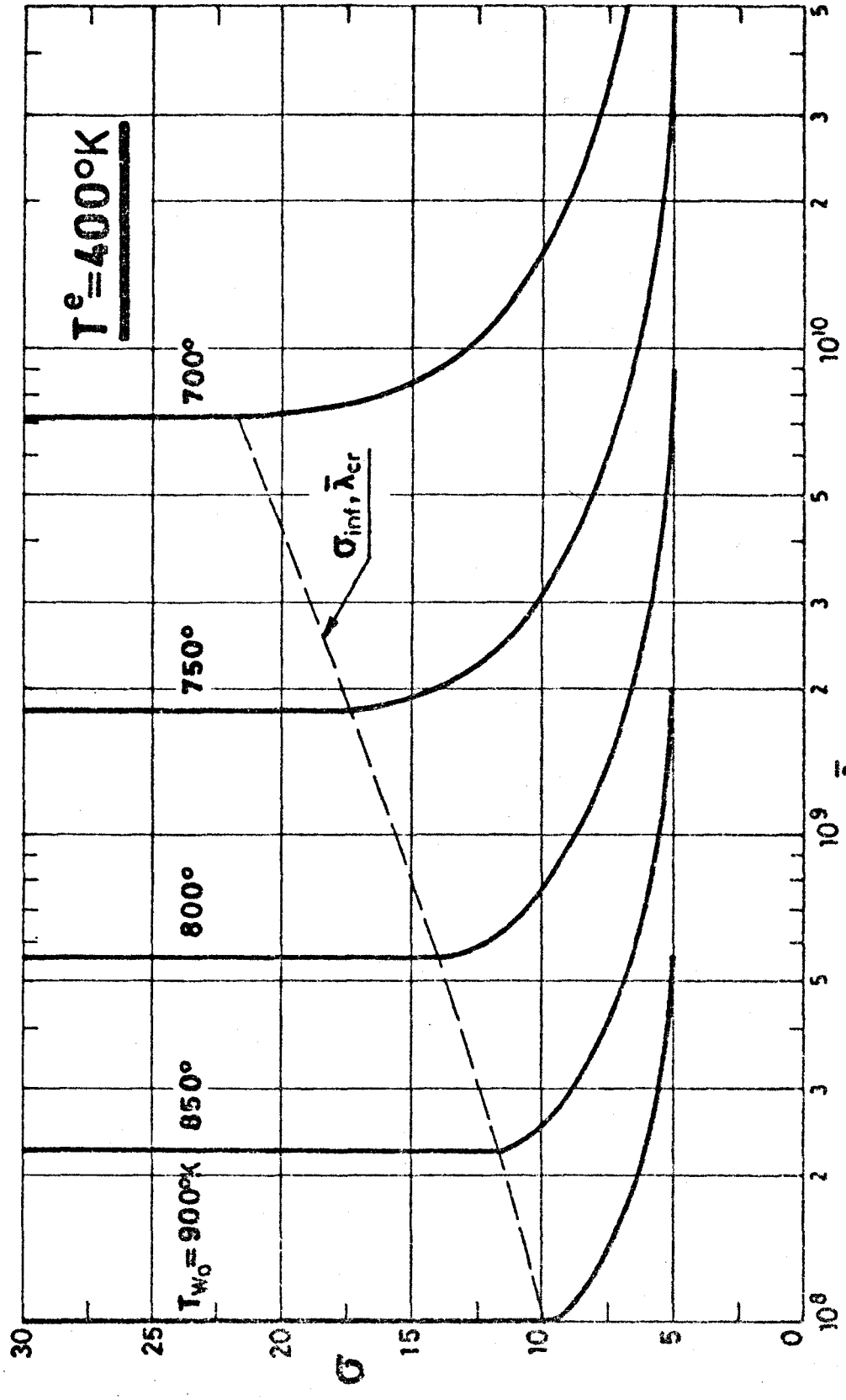

Fig.9c $\bar{\lambda}_{ign}$ versus σ for several T_{wo} and T^e=400°K.

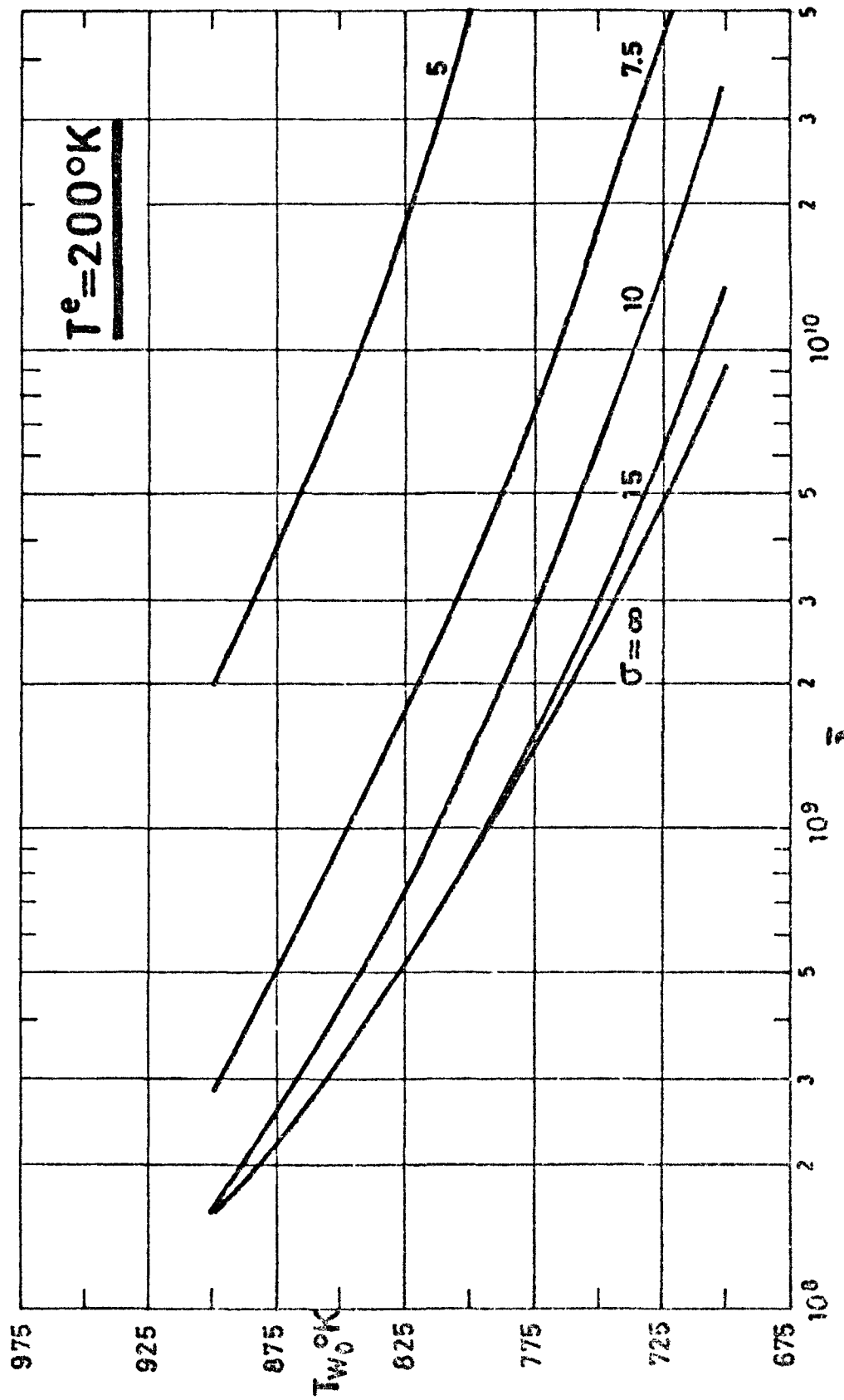

Fig.10a $\bar{\lambda}_{ign}$ versus T_{w_0} for several σ and T^e=200°K.

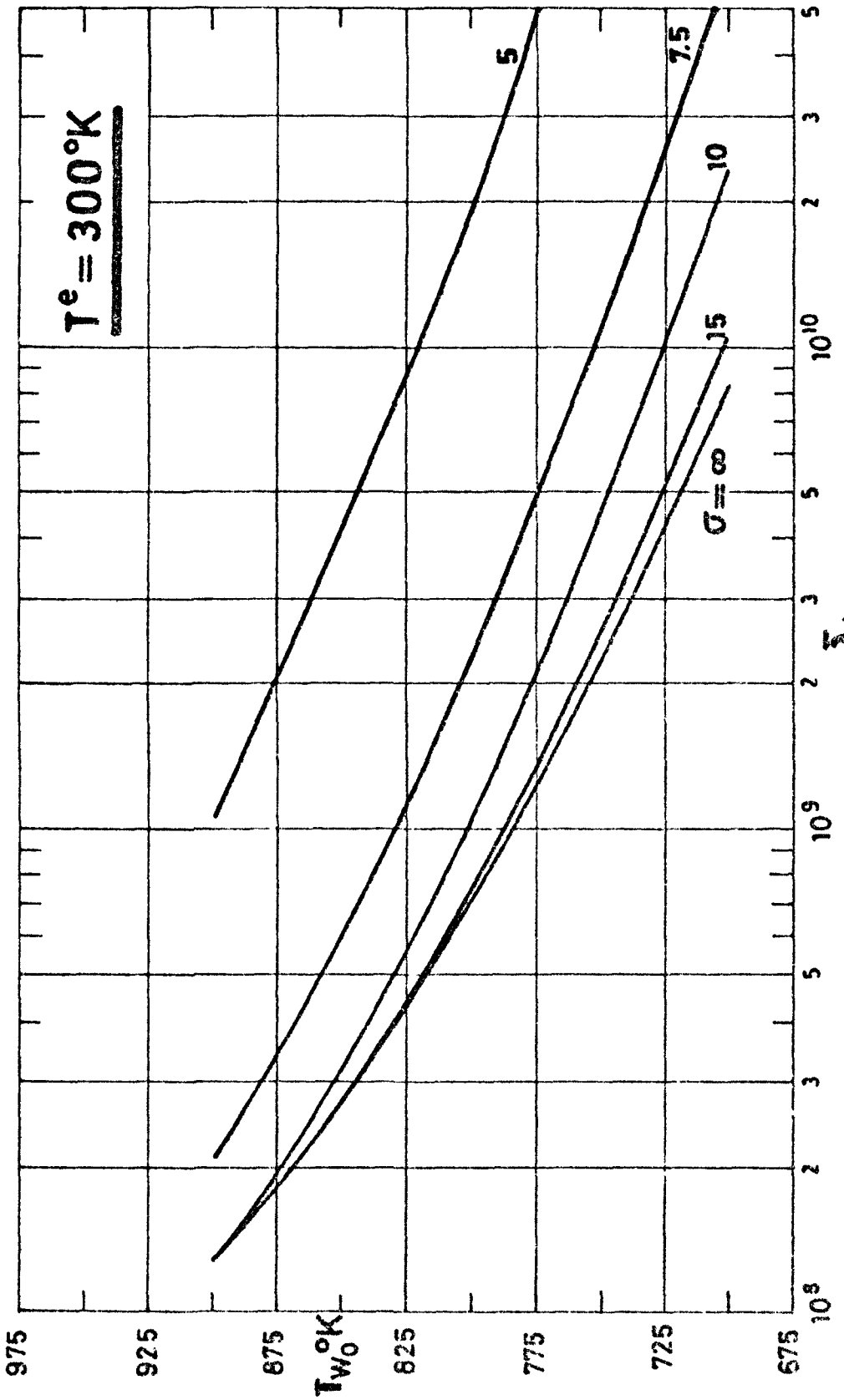

Fig.10b $\bar{\lambda}_{ign}$ versus T_{wo} for several σ and $T^e = 300°K$.

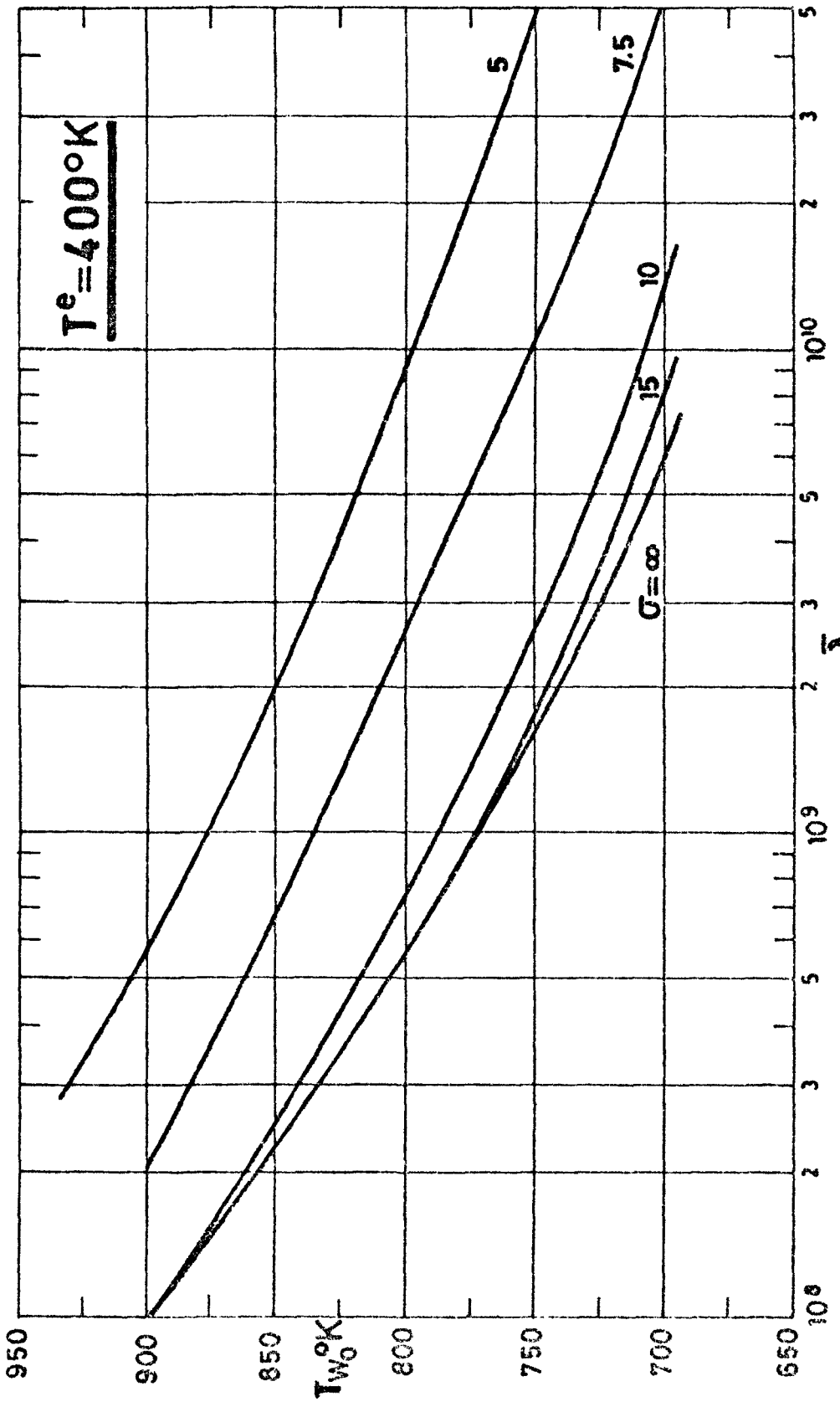

Fig.10c $\bar{\lambda}_{ign}$ versus T_{wo} for several σ and T^e=400°K.

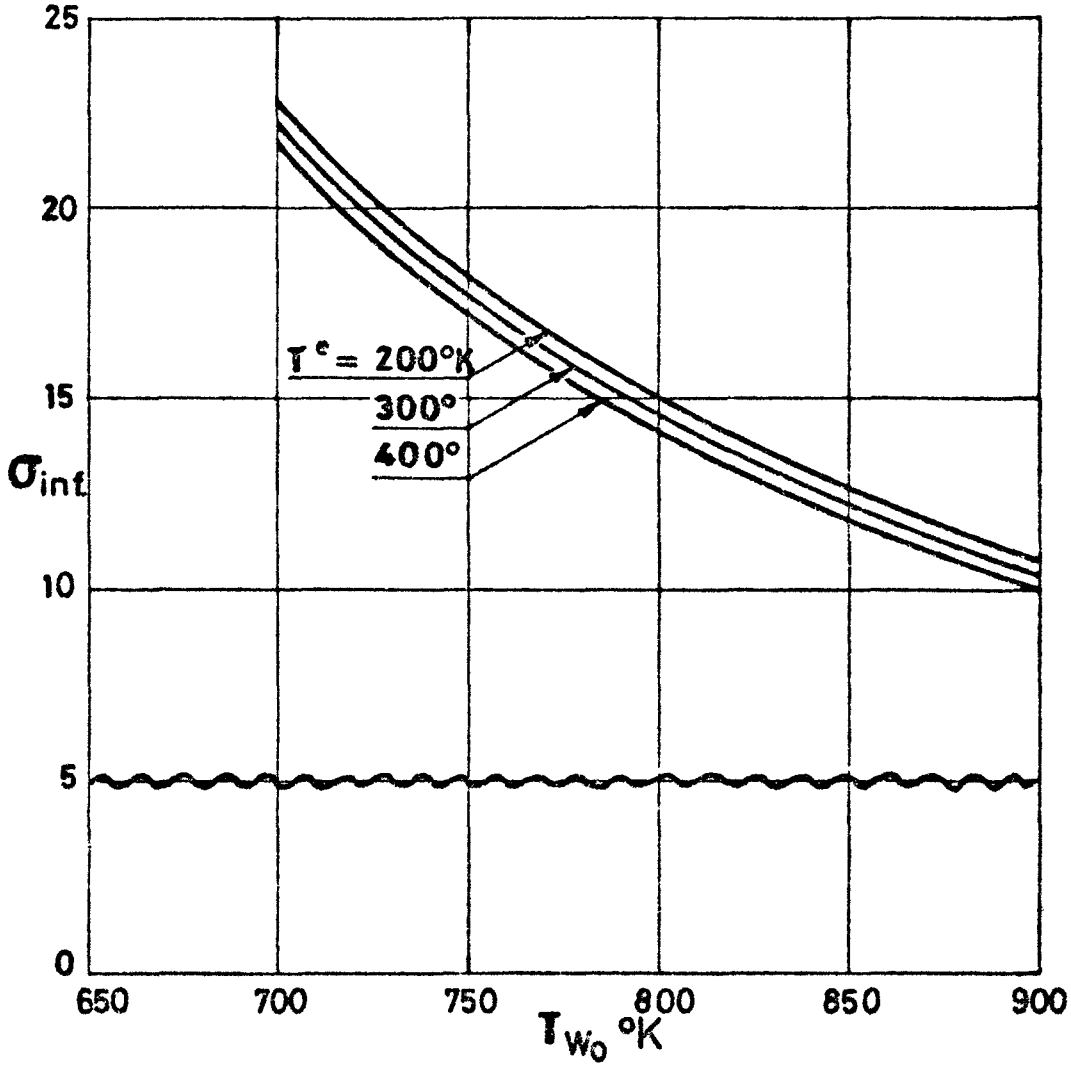

Fig.11 σ_{inf} versus T_{wo} for several values of T^e.

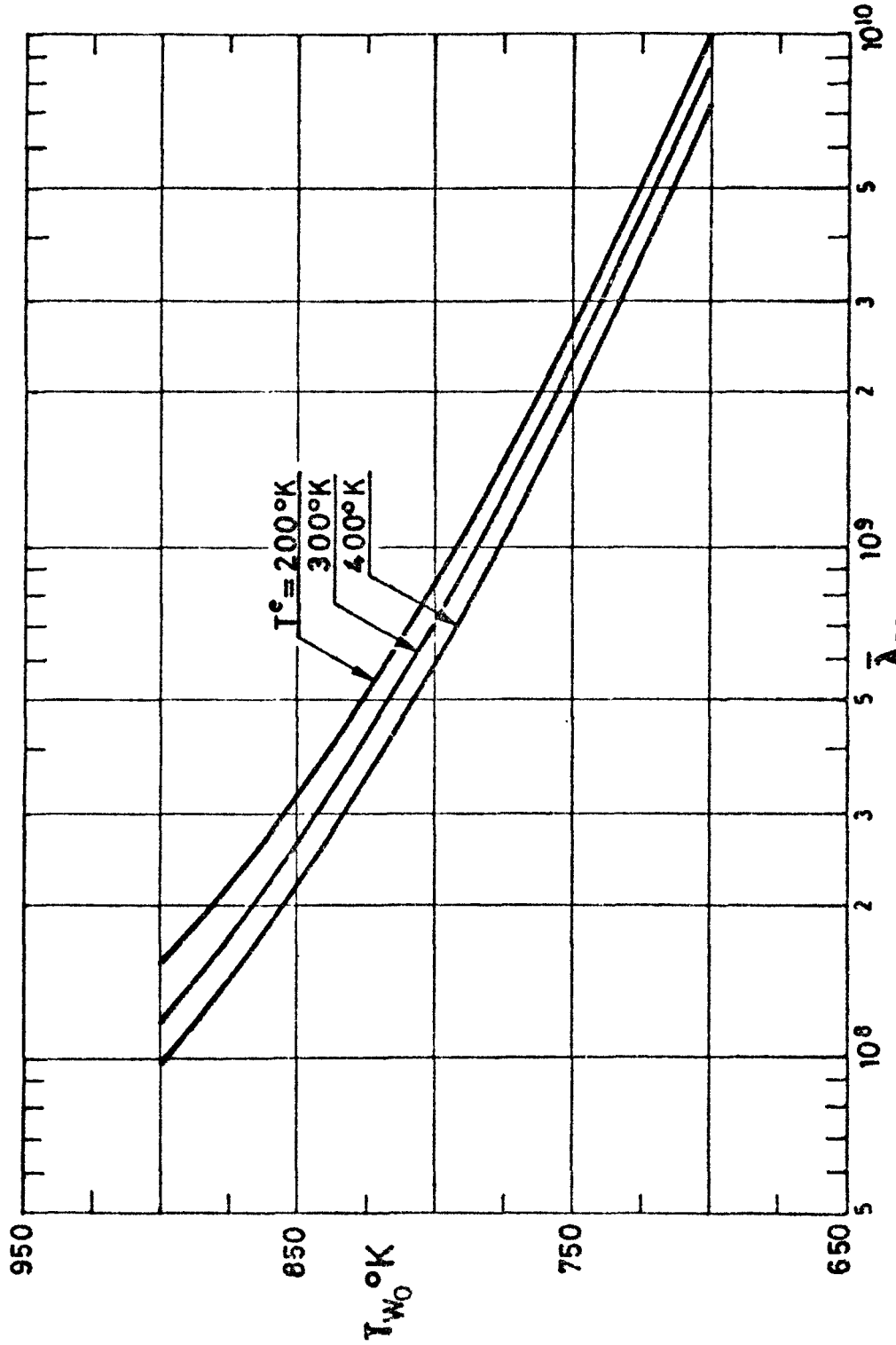

Fig.12 T_{wo} versus $\bar{\lambda}_{cr}$ (minimum value of $\bar{\lambda}$ for ignition to occur) for different values of T^e.

CHAPTER III.

DISCUSSION OF TRANSIENT EFFECTS.

Authors

Prof. J.R. Sanmartín*

Dr. E. Fraga

*Presently at the School of Aeronautics Polytecnic University of Madrid.

CHAPTER III

DISCUSSION OF TRANSIENT EFFECTS

- - - - -

In order to determine the conditions for which the analysis of Chapter II is valid, we study here the transient effects that appear after the start of the engine. We shall be concerned with the vaporization process, and filling, heating and chemical transients.

I. Droplet vaporization time.

Right at the start of the engine, vaporization of the droplets produced by the grids will take place in near vacuum. Then, the rate of vaporization of a droplet of radius r_s and temperature T^e is[1]

$$\dot{m}_d = cP_v(T^e)\sqrt{\frac{M_1}{2\pi RT^e}}\,4\pi r_s^2 \qquad (1)$$

where P_v is the vapor pressure and c is a constant of the order of unity. In addition

$$\dot{m}_d = -\frac{d}{dt}\left(\frac{4}{3}\pi r_s^3\rho_L\right); \qquad (2)$$

then

$$r_s = r_{so} - \frac{cP_v\sqrt{\frac{M_1}{2\pi RT^e}}}{\rho_L}\,t$$

where r_{so} is the initial droplet radius. Thus, the time required for r_s to reduce to λr_{so} ($\lambda<1$) is

$$t_\gamma \sim \frac{r_{so}\rho_L(T^e)}{P_v(T^e)} \quad \frac{2\pi RT^e}{M_1}(1-\gamma). \qquad (3)$$

Since the gas density inside the chamber will grow with time, a point will arrive when the mean free path will be smaller than r_s and equation (1) will cease to be valid. The vaporization would be then diffusion limited. Thus if t_γ, as given in equation (3), is too large, diffusion limited vaporization should be considered.

In monopropellants with large activation energies, (the case of hydrazine), and sufficiently high temperatures, the diffusion limited vaporization of droplets is greatly influenced by the combustion, which occurs in a thin region close to the surface.[2] At lower temperatures, when combustion is negligible (in particular, to study ignition conditions), vaporization will require a longer time. Thus, to estimate a vaporization time we may neglect combustion and therefore particle diffusion, since there would be a negligible amount of products. Consequently, the vaporization process will be limited by heat conduction.

Consider then a hydrazine droplet vaporizing in a hydrazine atmosphere at a given uniform pressure P (convection being negligible), the temperature far enough from the droplet being T_∞.[3] Due to the large density ratio of condensed to gaseous phases, the process may be, as usually, taken to be quasisteady. In this case the energy equation for the gaseous phase reads

$$\dot{m}_d \frac{h_1(T)}{M_1} - 4\pi r^2 \kappa \frac{dT}{dr} = \dot{m}_d \frac{h_{1L}(T_s)}{M_1} \qquad (4)$$

where r is the distance to droplet center, T_s the temperature at $r = r_s$, and κ the thermal conductivity of gaseous hy-

drazine.

From equation (4) we have immediately

$$\int_{T_s}^{T_\infty} \frac{M_1 \kappa(T) dT}{h_1(T) - h_{1L}(T_s)} = \int_{r_s}^{\infty} \frac{\dot{m}_d dr}{4\pi r^2} = \frac{\dot{m}_d}{4\pi r_s} \quad . \tag{5}$$

Defining $z \equiv T/T_b$ and

$$I(T_\infty, T_s) \equiv \frac{C_p(T_s)}{M_1 \kappa(T_s)} \int_{T_s}^{T_\infty} \frac{M_1 \kappa(T) dT}{h_1(T) - h_{1L}(T_s)} \quad , \tag{6}$$

and assuming

$$\kappa(T) = \kappa(T_s)(T/T_s)^{\alpha}$$

$$h_1(T) - h_1(T_s) = \bar{C}_p(T - T_s)$$

where $\bar{C}_p$ is an appropriate value of C_p between T_s and T_∞. We get

$$I = \int_1^{T_\infty/T_s} \left[\frac{\bar{C}_p}{C_p(T_s)} (z-1) + \frac{L(T_s)}{C_p(T_s) T_s} \right]^{-1} z^{\alpha} dz \; ;$$

thus

$$\dot{m}_d = 4\pi r_s \frac{M_1 \kappa(T_s)}{C_p(T_s)} I(T_\infty, T_s). \tag{7}$$

From equations (2) and (7) we obtain

$$t = \frac{\rho_L(T_s)C_p(T_s)}{2M_1\kappa(T_s)I(T_\infty,T_s)}\,(r_{so}^2 - r_s^2); \qquad (8)$$

then

$$t_\gamma = \frac{\rho_L(T_s)C_p(T_s)(1-\gamma^2)r_{so}^2}{2M_1\kappa(T_s)I(T_\infty,\,T_s)} \qquad (9)$$

where the fraction of mass vaporized is $(1-\gamma^3)$.

For entrance temperature $T^e \sim 300°K$, equation (3) gives

$$t_\gamma(\text{sec}) \sim .02\,(1-\gamma)r_{so}(\text{cm}) \qquad (10)$$

On the other hand setting $T_\infty \sim T_{wo} \sim 800°$ and $T_s \sim T^e \sim 300°K$ equation (9) gives

$$t_\gamma(\text{sec}) \sim 2.10^3(1-\gamma^2)r_{so}^2(\text{cm}^2). \qquad (11)$$

To estimate the numerical coefficients in equations (10) and (11) we set $\alpha = 1$ (a simple reasonable value from kinetic theory) and $\bar{C}_p/C_p = 1.2$ (a good approximation obtained from Ref 4); values of hydrazine properties were taken in Refs 4 and 5. Clearly, for $r_{so} \sim 10^{-4}$ cm or larger the vaporization would be diffusion limited. Furthermore, for pulses as short as 10^{-2} sec. r_{so} should not be larger than 10^{-3} cm; thus the injection system and the grids should be such as to break the liquid hydrazine into droplets of that size

II. Vaporization rate

Equations (2) and (7) allow now to determine the conditions for which the liquid mass fraction inside the chamber and at the exit, Y_{1L}, is very small so that the assumption

$\dot{m}_v/\dot{m} \simeq 1$ used in chapter II is satisfied. To this end we find the drop size distribution function. Let $F(r_s, t)dr_s$ be the number of drops in the chamber with radii lying between r_s and $r_s + dr_s$. Obviously F obeys a Boltzmann-like equation

$$\frac{\partial F}{\partial t} + \frac{\partial}{\partial r_s}\left(F \frac{dr_s}{dt}\right) = \left(\frac{\partial F}{\partial t}\right)_s \qquad (12)$$

where the right-hand side represents the rate of change of F due to drops of size r_s entering the chamber (sources) or leaving the chamber (sink); with neither sources nor sinks, (12) is a continuity equation of the usual type. We have

$$\left(\frac{\partial F}{\partial t}\right)_s = \frac{\dot{m}}{m_{so}} \delta(r_s - r_{so}) - \frac{F}{t_s} . \qquad (13)$$

In the source term m_{so} is the mass of the drops "entering the chamber" (drops produced by the grids), which all have radius r_{so}; $\dot{m}/m_{so}$ is then the number of drops produced per unit time. We have written the sink term introducing an appropriate time t_s, in general dependent on r_s.

In steady state we obtain

$$\frac{d}{dr_s}\left(F \frac{dr_s}{dt}\right) = \frac{\dot{m}}{m_{so}} \delta(r_s - r_{so}) - \frac{F}{t_s} \qquad (14)$$

To solve (14) we make the approximation of taking t_s independent of r_s. Using equation (8) we get

$$\frac{dr_s}{dt} = - \frac{M_1 \kappa I}{\rho_L C_p} \frac{1}{r_s} \equiv \frac{-\chi}{r_s} ; \qquad (15)$$

introducing now

$$g = \frac{F}{r_s} \exp\left(-\frac{r_s^2}{2\chi t_s}\right) \tag{16}$$

the equation for g reads

$$\frac{dg}{dr_s} = \frac{-\dot{m}}{\chi m_{so}} \exp\left(\frac{-r_{so}^2}{2\chi t_s}\right) \delta(r_s - r_{so}). \tag{17}$$

Since $F(r_s > r_{so}) \equiv 0$, equations (16) and (17) finally yield

$$F = \frac{\dot{m}}{\chi m_{so}} \exp\left(\frac{-r_{so}^2}{2\chi t_s}\right) r_s \exp\left(\frac{r_s^2}{2\chi t_s}\right). \tag{18}$$

To obtain now the liquid mass fraction Y_{1L} we notice that the liquid mass inside the chamber is

$$m_L = \int_o^{r_{so}} m_s F dr_s$$

while the liquid mass leaving the chamber per unit time is

$$Y_{1L}\dot{m} = \int_o^{r_{so}} m_s t_s^{-1} F dr_s = \frac{m_L}{t_s} \tag{19}$$

Thus

$$Y_{1L} = \frac{1}{\dot{m} t_s} \int_o^{r_{so}} m_s F dr_s$$

$$= \int_o^{r_{so}} \frac{1}{\chi t_s} \frac{r_s^3}{r_{so}^3} \exp\left(\frac{-r_{so}^2}{2\chi t_s}\right) r_s \exp\left(\frac{r_s^2}{2\chi t_s}\right) dr_s. \tag{20}$$

Defining now

$$q = r_s/r_{so}, \quad \mu = r_{so}^2/\chi t_s$$

equation (20) becomes

$$Y_{1L} = \mu \exp(-\mu/2) \int_o^1 q^4 \exp(\mu q^2/2) dq; \qquad (21)$$

clearly

$$Y_{1L} \to 1 \quad \text{as} \quad \mu \to \infty$$

$$Y_{1L} \to \mu/5 \quad \text{as} \quad \mu \to 0.$$

Therefore, we conclude that assumption $\dot{m}_v/\dot{m} \simeq 1$ ($Y_{1L} << 1$) requires that μ (actually $\mu/5$) be small. Now, the time for total vaporization {$t(\gamma=0)$ in equation (11)} is $r_{so}^2/2\chi$, while t_s, according to (19), is a mechanical time:

$$t_s = \frac{m_L}{Y_{1L}\dot{m}} = \frac{m_T}{\dot{m}} \qquad (22)$$

where m_T is the total mass in the chamber (liquid+gas); we have

$$m_T \simeq \rho V = \frac{PM_1}{RT} V.$$

Thus, for Y_{1L} small

$$Y_{1L} = 1 - \dot{m}v/\dot{m} \sim 2/5 \, \frac{t(\gamma=0)}{t_s} .$$

Condition $Y_{1L} << 1$ reads

$$\text{(vaporization time)}\ \frac{r_{so}^2 \rho_L C_p}{5 M_1 \kappa I} << \frac{P M_1 v}{R T \dot{m}}\ \text{(mechanical time)}.$$

For $V \sim 1\ cm^3$, $P \sim 20$ atm, $T \sim T_b(P) \sim 500°K$, $\dot{m} \sim 1$g/sec, $r_{so} \sim 10^{-3}$cm, we get

$$Y_{1L} \sim 1/25;$$

$T_b(P)$ is the boiling temperature at pressure P.

III. Filling stage

To estimate a characteristic time for the filling of the chamber we write

$$V \frac{d\rho}{dt} = \dot{m}_v = \int_o^{r_{so}} \dot{m}_d F dr_{so} \qquad (23)$$

neglecting the gas leaving the chamber in this stage. To obtain the distribution function F from equations (12) and (13) we notice that for the values considered at the end of the last section

$$\dot{m}/m_{so} \sim 10^8\ sec^{-1},$$

while

$$\frac{1}{r_s}\frac{dr_s}{dt} \sim t(\gamma=0) \sim .02 r_{so}(cm) \qquad \text{(Eq.10)}$$

$$\frac{1}{r_s}\frac{dr_s}{dt} \sim t(\gamma=0) \sim 2.10^3 r_{so}^2(cm^2) \qquad \text{(Eq.11)}$$

$$t_s^{-1} = \dot{m}/m_T \sim 10^2\ sec^{-1}. \qquad (24)$$

Thus for $t << 10^{-3}$ sec, we may write

$$\frac{\partial F}{\partial t} = \frac{\dot{m}}{m_{so}} \delta(r_s - r_{so})$$

so that

$$F = \frac{\dot{m}}{m_{so}} t\delta(r_s - r_{so}). \qquad (25)$$

Then, from equation (23) we obtain

$$\rho = \frac{\dot{m}_d \dot{m}}{m_{so} V} \frac{t^2}{2}. \qquad (26)$$

For mean free path λ less than r_s, that is,

$$\lambda \sim \frac{\kappa M_1}{\rho C_p} \sqrt{\frac{M_1}{RT}} < r_s ,$$

equation (1) should be used for $\dot{m}_d$. Then we find that when $r_s \sim \lambda$

$$t \propto \left[V/\dot{m} P_v(T^e) \right]^{1/2}$$

$$\sim 10^{-5} \text{ sec } (T^e \sim 300^\circ K).$$

Thus to determine the time for filling the chamber equation (7) must be used in (26). Setting then $\rho = M_1 P/RT$, and taking the steady state value of pressure ($P \sim 20$atm) and $T \sim 500^\circ K$, we arrive at

$$t_f = \left(\frac{2Vm_{so}}{\dot{m}_d \dot{m}} \frac{M_1 P}{RT}\right)^{1/2} \sim 10^{-3} \text{ sec.} \qquad (27)$$

The value of t_f is of the order of the time for droplet vaporization.

IV. Heating transient

To discuss the transients corresponding to gas heating and combustion, and wall heating, we assume here $\dot{m}_v/\dot{m} \simeq 1$, and that a steady mass flow has been reached. Then retaining the time derivatives in the mass conservation equations for all species. Equations (1) and (2) of chapter II would become

$$\frac{d(mY_1)}{dt} = \dot{m}-\dot{m}Y_1+M_1V\delta_1\overline{W}_1 \tag{28}$$

$$\frac{d(mY_j)}{dt} = -\dot{m}Y_j+M_jV\delta_j\overline{W}_1\,;\ (j=2,3,4) \tag{29}$$

then, using $mY_i=N_iM_i$, $N_i=X_1N$, and Eq(16) of Chap. II, we get, after tedious transformatios

$$\frac{M_1N}{\dot{m}}\frac{dX_1}{dt}= 1-X_1+ \frac{M_1V\overline{W}_1\delta_1}{\dot{m}} \left(1- \frac{\Sigma\delta_i}{\delta_1} X_1\right). \tag{30}$$

Similarly the time dependent energy balance equation becomes

$$\frac{d}{dt}\ \Sigma N_i(h_i-RT)= \frac{\dot{m}h^e_{1L}}{M_1} - \dot{m}\Sigma\ \frac{Y_ih_i}{M_i}+K(T_W-T) \tag{31}$$

h_i-RT being the molar internal energy. At constant pressure ΣN_iRT is constant, while

$$\Sigma h_i\ \frac{dN_i}{dt} = \Sigma\ \frac{h_i}{M_i}\ \frac{d(mY_i)}{dt}\ .$$

Then Eq(31) becomes

$$M_1 \frac{\Sigma N_i C_{pi}}{Q\dot{m}} \frac{dT}{dt} = - \frac{C_{pm}(T-T^e)+L^e}{Q} + \frac{KM_1}{Q\dot{m}}(T_w-T) - \frac{V\bar{W}_1 M_1}{\dot{m}}. \qquad (32)$$

Defining now, as in Chap.II, $\delta, \sigma, \theta, \lambda, s$, and θ^*, Eqs. (30) and (32) become

$$\frac{NC_{pm}}{C_w} \frac{dX_1}{ds} = 1-X_1-(1+X_1)\lambda f \exp(-\theta_a/\theta), \qquad (33)$$

$$\frac{\Sigma N_i C_{pi}}{C_w} \frac{d\theta}{ds} = -\sigma(\theta-\theta^*)+\lambda f \exp(-\theta_a/\theta), \qquad (34)$$

and for θ_w we have from Chap. II

$$\frac{d\theta_w}{ds} = \varepsilon\left(1- \frac{\theta_w^4}{\theta_{wo}^4}\right)-(\sigma-1)(\theta_w-\theta). \qquad (35)$$

We shall now assume

$$\frac{NC_{pm}}{C_w} << 1 , \qquad (36)$$

$$\lambda f(1, \theta)e^{-\theta_a/\theta} << \sigma \qquad (37)$$

Where θ is some value between θ^c and θ_{wo} [say $\theta_b(P)$]. Equations

(33)-(35) show then that gas heating occurs in a time t_h much shorter than the time for combustion t_c and wall heating t_w. Clearly

$$t_h \sim \frac{NM_1}{\dot{m}\sigma} \qquad \left(s \sim \frac{NC_{pm}}{\sigma C_w}\right) \tag{38}$$

For $t/t_h \to \infty$, $\theta \to \theta^*$.

For large σ, $\theta_{No} - \theta^* = 0(1/\sigma)$. Thus

$$t_w \sim \frac{M_1 C_w}{\dot{m} C_{pm}} \qquad (s \sim 1), \tag{39}$$

as pointed out in chapter II section III. If furthermore,

$$\frac{NC_{pm}}{C_w} >> \lambda f(1,\theta_{wo}) \exp(-\theta_a/\theta_{wo}) \tag{40}$$

then $t_e << t_w$; we have

$$t_e \sim \frac{NM_1}{\dot{m}}\left[\lambda f(1,\theta_{wo})\exp(-\theta_a/\theta_{wo})\right]^{-1} \tag{41}$$

Thus under conditions (36), (37) and (40) gas heating, combustion and wall heating occur in three succesive stages. The analysis of chapter II corresponds to $t >> t_c$ and $t << t_w$ (pulsed regime) or $t >> t_w$ (steady regime).

V. Chemical kinetics transient

To discuss ignition in the combustion stage we consider

Eqs (33) and (34) with $\theta_w=\theta_{wo}$, and $X_1=1$, $\theta=\theta^*$ at s=0. Expanding θ and X_1 in the form

$$\theta = \theta^* + \frac{\phi}{\sigma} , \tag{42}$$

$$X_1 = 1 - \frac{\chi}{\sigma} ,$$

we get

$$\frac{d\chi}{d(sC_w\sigma/NC_{pm})} \simeq 2\lambda f(1,\theta^*)\exp(\frac{-\theta_a}{\theta^*})\exp(\frac{\theta_a\phi}{\theta^{*2}\sigma}) \tag{43}$$

$$\frac{d\phi}{d(sC_w\sigma/NC_{pm})} \simeq -\phi + \lambda f(1,\theta^*)\exp(\frac{-\theta_a}{\theta^*})\exp(\frac{\theta_a\phi}{\theta^{*2}\sigma}). \tag{44}$$

The right hand side of Eq(44), written as

$$K_1(e^{K_2\phi} - \frac{1}{K_1K_2} K_2\phi)$$

is positive for small ϕ. If it never vanishes, $\phi \to \infty$ as $cC_w\sigma/NC_{pm} \to \infty$ so that expansion (42) will finally cease to be valid; then crearly, there will be ignition. On the other hand, no ignition will occur for K_1K_2 small enough, since $d\phi/d(sC_w\sigma/NC_{pm})$ will vanish at some ϕ. The critical condition for ignition will be given by

$$e^{K_2\phi} - \frac{1}{K_1K_2} K_2\phi = 0,$$

$$e^{K_2\phi} - \frac{1}{K_1K_2} = 0,$$

that is

$$K_1 K_2 = e^{-1}, \text{ or}$$

$$\lambda f(1,\theta^*)\exp(-\theta_a/\theta^*)\ \frac{\theta_a}{\theta^{*2}\sigma} = \frac{1}{e}$$

which, to lowest order in θ^*/θ_a, agrees with Eq.(39) of chapter II, with the approximation $f(1,\theta^*) \simeq 1.8/\theta^{*2}$.

These results confirm that for $\sigma<\sigma_{inf}$ and $\lambda<\lambda_{max}$ the actual solution will lie on the lower branch in Figs. 3b-6b of Chap.II. Additional confirmation, is provided by checking that for any given $\lambda<\lambda_{max}$ all points in the phase space X_1, θ, corresponding to this branch are nodal points. From Eqs(33) and (34), we write

$$\frac{dX_1}{d\theta} = \frac{\Sigma N_i C_{pi}}{NC_{pm}}\ \frac{(1-X_1)-(1+X_1)\lambda f\exp(-\theta_a/\theta)}{-\sigma(\theta-\theta^*)+\lambda f\exp(-\theta_a/\theta)}$$

and linearize around a point in that branch, $\hat{X}_1$, $\hat{\theta}$,

$$X_1 = \hat{X}_1 + \varepsilon,\ \theta = \hat{\theta} + \omega\ , \tag{45}$$

to obtain

$$\frac{d\varepsilon}{d\omega} = \frac{\Sigma N_i C_{pi}}{NC_{pm}}\ x$$

$$\frac{\varepsilon\left[1+\lambda f\exp(-\theta_a/\hat{\theta})\right]+(1+\hat{X}_1)\lambda f\exp(-\theta_a/\hat{\theta})\left[(-2/\hat{\theta})+(\theta_a/\hat{\theta}^2)\right]\omega}{\omega\left[\sigma-\lambda f\exp(-\theta_a/\hat{\theta})(-2/\hat{\theta})+(\theta_a/\hat{\theta}^2)\right]} \tag{46}$$

$$\equiv \frac{A\varepsilon+B\omega}{C\varepsilon+D\omega}$$

where we have used the approximation $f\simeq 1.8/\theta^2$ since X_1 is close to unity and θ is low. In a nodal point

$$(A+D)^2 > 4(AD-BC) > 0;$$

since here $C=0$ and $A>0$ it will suffice to show that

$$0<D=\sigma\left[1-\frac{\lambda f}{\sigma}\exp(-\theta_a/\hat{\theta})(-2/\hat{\theta}+\theta_a/\hat{\theta}^2)\right]=\sigma\left[1-\frac{(\hat{\theta}-\theta^*)(\theta_a-2\hat{\theta})}{\hat{\theta}^2}\right]. \quad (47)$$

Now $\theta(\lambda_{max})$satisfies Eq(38) of Chap.II, that is, the bracket in Eq(47) vanishes for $\hat{\theta}=\theta(\lambda_{max})$; it is then easy to verify that for $\hat{\theta}<\theta(\lambda_{max})$ the case for the branch here considered) the bracket is positive if $0.28\ \theta_a>\theta^*$, a condition clearly satisfied.

REFERENCES

1. LANDAU L., LIFCHITZ E. "Physique statistique" Editions Mir Moscu 1967.

2. LIÑAN A. "Monopropellant droplet decomposition for large activation energies" Acta Astronautica Vol 2. 1975.

3. LAW C.K. "Quasi-steady droplet vaporization theory with property variations" Physics of Fluids Vol 18 No 11. 1975.

4. JANAF. "Thermochemical Tables" Office of Standards Reference Data National Bureau of Standards 1971.

5. AUDRIETH L.F., ACKERSON B. "The Chemistry of Hydrazine" John Wiley and Sons 1951.

CHAPTER IV

PLUG-FLOW HYDRAZINE REACTOR.

Authors

Prof. J.R. Sanmartín*
Prof. A. Liñán*
Prof. A. Crespo
Dr. E. Fraga

*Presently at the School of Aeronautics Polytecnic University of Madrid.

Chapter IV

PLUG-FLOW HYDRAZINE REACTOR

As an alternative model to the stirred reactor idealization carried out previously, we shall present in this chapter a plug-flow analysis of a hydrazine reactor; such analysis would, in fact, be more appropriate for some types of engines.

We shall assume, in particular, that heat is conducted through solid bars, from a region downstream where appreciable decomposition occurs, toward the chamber entrance. We shall also assume that the hydrazine reaches the bars at the temperature of a grid (T_G) where it is vaporized.

I Steady state equations

Let $T_B(x)$ be the bars temperature and x the distance along the reactors from the bars origin. Then the conservation of energy for the gas is

$$NC_{pm}u_o \frac{dT}{dx} + K(T-T_B) = -Q\bar{V}\bar{W}_1 \qquad (1)$$

where u_o is the gas velocity. The conservation of energy for the bars reads

$$k_B \frac{d^2T_B}{dx^2} + h(T-T_B) = 0 \qquad (2)$$

where k_B is the heat conductivity of the solid and h is

the heat transfer coefficient from the gas to the solid; clearly conservation of energy at the interface between gas and solid requires that

$$h = K/S_B L.$$

L and S_B are the length and the total cross section area of the bars. Finally, the conservation equation for hydrazine is

$$N u_o \frac{dY_1}{dx} = V\bar{W}_1. \qquad (3)$$

We have neglected upstream diffusion and gas conduction.

We assume that the bars are thermally isolated from the walls. Then the boundary conditions are:

At $x = 0$

$$Y_1 = 1 \quad , \quad T = T_G \quad , \quad dT_B/dx = 0 \qquad (4)$$

and at

$$x = L \qquad dT_B/dx = 0 \qquad (5)$$

Defining now the dimensionless variables of Chapter II together with

$$\xi = x/l_c \quad , \quad l_c^{-1} = \sqrt{h/k_B} \quad , \quad \nu = \frac{KM_1 l_c}{C_{pm}\dot{m}L} \qquad (6)$$

Eqs. (1)-(3) become

$$\theta - \theta_B + d^2\theta_B/d\xi^2 = 0 \qquad (7)$$

$$d\theta/d\xi + \nu\,(\theta-\theta_B) = \frac{\lambda}{\xi_L} f(Y_1, \theta) \exp(-\theta_a/\theta) \qquad (8)$$

$$dY_1/d\xi = -\frac{\lambda}{\xi_L} f(Y_1, \theta)\exp(-\theta_a/\theta) \qquad (9)$$

with the boundary conditions

$$\theta(o) = \theta_G \quad , \quad Y_1(o) = 1 \quad , \quad (d\theta_B/d\xi)_{\xi\approx 0} = 0 \qquad (10)$$

$$d\theta_B/d\xi = 0 \quad \text{at} \quad \xi = \xi_L \equiv L/l_c \qquad (11)$$

where λ/ξ_L is the Damkohler number.

From Eqs. (7)-(9), taking into account boundary conditions (10), we obtain the following general relation

$$Y_1 + \theta - \nu\, d\theta_B/d\xi = 1 + \theta_G \qquad (12)$$

which may be used to calculate Y_1 in terms of θ and θ_B. When this relation is substituted into Eq. (8), the resulting equation together with Eq. (7) and the boundary conditions (10) and (11) will determine $\theta(\xi)$ and $\theta_B(\xi)$.

In particular

$$\theta_L \equiv \theta(\xi_L) \quad \text{and} \quad Y_{1L} \equiv Y_1(\xi_L)$$

will be determined as functions of the following parameters

$$\theta_G \quad , \quad \xi_L \quad , \quad \nu \quad , \quad \lambda \quad , \quad \theta_a$$

characteristic of the initial temperature, the chamber length, the heat exchange between gas and bars, the reaction rate and the activation energy of the reaction. Another important characteristic of the reactor is the maximum temperature θ_m and its location ξ_m which are functions of the five parameters mentioned above.

We shall look in the following for the asymtotic form of the relations between θ_L, Y_L, θ_m and the five parameters θ_G, ξ_L, ν, λ, θ_a taking into account that θ_a is large for hydrazine.

II Asymptotic solution for large activation energies

For sufficiently large θ_a, and appropriately large Damköler numbers, the flow will be frozen upstream of a certain ξ_t and in equilibrium for $\xi > \xi_t$. That is

$$Y = 1 \qquad \text{for} \qquad \xi < \xi_t \tag{13a}$$

and

$$Y = 0 \qquad \xi > \xi_t \tag{13b}$$

The transition value ξ_t of ξ is a function of λ, θ_a, etc., to be determined later.

If Eq.(13) is substituted into Eq.(12) we obtain

$$\theta = \theta_G + \nu \, d\theta_B/d\xi \qquad \text{for} \qquad \xi < \xi_t \tag{14a}$$

and

$$\theta = 1 + \theta_G + \nu \, d\theta_B/d\xi \quad \text{for} \qquad \xi > \xi_t \tag{14b}$$

In particular we obtain in this limit

$$\theta_L = 1 + \theta_G \quad , \quad Y_{1L} = 0 \tag{15}$$

From Eqs.(14) and (7) we obtain the equations

$$\theta_G - \theta_B + \nu \frac{d\theta_B}{d\xi} + \frac{d^2\theta B}{d\xi^2} = 0 \quad \text{for } \xi < \xi_t \tag{16a}$$

and

$$1 + \theta_G - \theta_B + \nu \frac{d\theta_B}{d\xi} + \frac{d^2\theta_B}{d\xi^2} = 0 \quad \text{for } \xi > \xi_t \tag{16b}$$

The solution of Eq.(16a) with the boundary condition $d\theta_B/d\xi = 0$ at $\xi = 0$ is

$$\theta_B = \theta_G + A_1 e^{r_1\xi} - (r_1 A_1/r_2) e^{r_2\xi} \qquad (\xi<\xi_t) \tag{17a}$$

where

$$r_{1,2} = -\frac{\nu}{2} \pm \left(\frac{\nu^2}{4} + 1\right)^{1/2}$$

and A_1 is an integration constant to be determined later.

The solution of (16b), using the boundary condition

$$\frac{d\theta_B}{d\xi} = 0 \quad \text{at} \quad \xi = \xi_L, \quad \text{is}$$

$$\theta_B = 1 + \theta_G + A_2 e^{r_1(\xi-\xi_L)} - \frac{r_1 A_2}{r_2} e^{r_2(\xi-\xi_L)} \quad , \ \xi > \xi_t \tag{17b}$$

where A_2 is an integration constant to be determined together with A_1 by means of the conditions that θ_B and $d\theta_B/d\xi$ must be continuous at $\xi=\xi_t$. Notice that both Y_1 and the gas temperature θ have jumps of value 1 at $\xi=\xi_t$

where the chemical reaction occurs suddenly.

The continuity of θ_B and $d\theta_B/d\xi$ at $\xi=\xi_t$ provide the relations.

$$A_1 e^{r_1\xi_t} - (r_1 A_1/r_2) e^{r_2\xi_t} = 1 + A_2 e^{r_1(\xi_t-\xi_L)} - \frac{r_1 A_2}{r_2} e^{r_2(\xi_t-\xi_L)} \qquad (18a)$$

and

$$A_1 r_1 e^{r_1\xi_t} - A_1 r_1 e^{r_2\xi_t} = A_2 r_1 e^{r_1(\xi_t-\xi_L)} - A_2 r_1 e^{r_2(\xi_t-\xi_L)} \qquad (18b)$$

which may be used to calculate A_1 and A_2 explicitly as a function of ξ_t, ξ_L and ν:

$$A_1 = \frac{r_2}{r_2-r_1} e^{-r_2\xi_t} \frac{e^{(r_1-r_2)(\xi_L-\xi_t)} - 1}{e^{(r_1-r_2)\xi_L} - 1} \qquad (18c)$$

where clearly $r_1-r_2=(4+\nu^2)^{1/2}$, and

$$\frac{A_2}{A_1} = \frac{e^{r_1\xi_t} - e^{r_2\xi_t}}{e^{r_1(\xi_t-\xi_L)} - e^{r_2(\xi_t-\xi_L)}} \qquad (18d)$$

The maximum value of the gas temperature θ_m is the value of θ at $\xi=\xi_t^+$, while $\theta_t=\theta_m-1$ is the value of θ at $\xi=\xi_t^-$

$$\theta_m = 1 + \theta_G + \nu A_1 r_1 (e^{r_1\xi_t} - e^{r_2\xi_t}) = \theta_t + 1 \qquad (19)$$

If we assume θ_t to be known, then , ξ_t will also be known,

and the temperature of gas and bars will be given by equations (14) and (17).

The possible solutions of this problem will be discussed in the last part of this Chapter.

III. The ignition region.

Just before ξ_t there is a region (the ignition region) where the incipient effects of the chemical reaction cause the gas phase temperature θ to rise above the frozen flow value $\theta=\theta_I(\xi)$, given by Eq.(14a), by an amount of order θ_a^{-1}. There is then a large increase in the reaction rate, leading to a thermal runaway of the reaction at $\xi=\xi_t$ and equilibrium flow for $\xi > \xi_t$.

Let us define

$$\theta=\theta_I(\xi) + \psi(\xi)\theta_a^{-1} \tag{20}$$

$$Y_1 = 1 - \theta_a^{-1} y \tag{21}$$

and write

$$\theta_I(\xi_t) = \theta_t \quad , \quad (d\theta_I/d\xi)_{\xi=\xi_t^-} = \theta_t' \ . \tag{22}$$

Since the thermal effect of the chemical reaction is small, we obtain in the first approximation the following equation for ψ

$$\theta_a^{-1}\frac{d\psi}{d\xi} = \frac{\lambda f(1,\theta_t)}{\xi_L}\exp(-\theta_a/\theta_t)\exp\{\theta_a(\theta-\theta_t)/\theta_t^2\} =$$

$$\frac{\lambda f}{\xi_L}\exp(-\theta_a/\theta_t)\exp\{\frac{1}{\theta_t^2}\psi + \frac{\theta}{\theta_t^2}(\theta_1-\theta_t)\} \tag{23}$$

where the Arrhenius exponent has been linearized in the way of Frank-Kamenetskii.

The term $\theta_a \theta_t^{-2}(\theta_I-\theta_t)$ in the Arrhenius exponent causes the reaction term to be negligible before the ignition region. The length of the ignition region is associated with the fact that $\frac{\theta_a}{\theta_t^2}(\theta_I-\theta)$ should be of order unity in this region. Then $\theta_I-\theta_t$ is small (of order θ_a^{-1}) and may be approximated by

$$\theta_I-\theta_t = (\xi-\zeta_t)\theta_t' \tag{24}$$

If we introduce the new variables

$$\eta = \psi\theta_t^{-2} \quad \text{and} \quad \zeta = \theta_a(\xi-\xi_t)\theta_t'/\theta_t^2 \tag{25}$$

we obtain the equation

$$d\phi/d\zeta = Ee^{\eta+\zeta} \tag{26}$$

where

$$E = \frac{\lambda f(1,\theta_t)}{\theta_t'\xi_L}\, e^{-\theta_a/\theta_t} \tag{27}$$

However E must be equal to 1 if we want the solution of Eq. (26), with the boundary condition $\eta=0$ at $\zeta\to-\infty$, to give $\eta\to\infty$ at $\zeta=0$.

Then

$$1 - e^{-\eta} = e^{\zeta} \tag{28}$$

gives the rise in temperature above the frozen flow value associated with the chemical reaction effects.

Condition E = 1 yields

$$\frac{\lambda f(1,\theta_t)}{\xi_L} \exp(-\theta_a/\theta_t) = \theta_t' = \nu\left[\theta_B(\xi_t)-\theta_t\right] \qquad (29)$$

Equation (29) together with equation (19), provide the values of θ_t an ξ_t as function of θ_G, ν, ξ_L, and λ.

The asymptotic analysis for this ignition region ceases to be valid for ξ so close to ξ_t, that ϕ becomes of order θ_a large compared with 1. The structure of the reaction region is described by the following equations (obtained from (8) and (9) by neglecting the heat transfer from the bars against the heat released by chemical reaction):

$$\frac{d\theta}{d\xi} = \frac{\lambda}{\xi_L} f(Y_1,\theta)\exp(-\theta_a/\theta) \qquad (30)$$

$$\frac{dY_1}{d\xi} = -\frac{d\theta}{d\xi}$$

thus we have

$$\theta + Y_1 = \theta_t + 1$$

and therefore

$$\frac{d\theta}{d\xi} = \frac{\lambda}{\xi_L} f(1+\theta_t - \theta,\theta)\exp(-\theta_a/\theta)$$

and finally

$$\frac{\lambda}{\xi_L}\xi = \int_c^{\theta} \frac{\exp(\theta_a/\theta)}{f(1+\theta_t-\theta,\theta)}\, d\theta$$

the integrating constant c being chosen so that the solution matches with equation (28).

IV. Ignition conditions

Equations (19) and (29) read

$$\theta_t = \theta_G + E_1(\nu, \xi_L, \varepsilon) \tag{31}$$

$$\lambda = \frac{\xi_L \nu}{f(1,\theta_t)} E_2(\nu, \xi_L, \varepsilon)\exp(\theta_a/\theta_t) \tag{32}$$

where

$$\varepsilon = \xi_t/\xi_L \qquad (0 \leqslant \varepsilon \leqslant 1)$$

$$E_1 = \frac{\nu}{(4+\nu^2)^{1/2}}\left[\exp(\sqrt{4+\nu^2}\ \xi_L(1-\varepsilon))-1\right]\frac{\exp(\sqrt{4+\nu^2}\varepsilon\xi_L)-1}{\exp(\sqrt{4+\nu^2}\ \xi_L)-1} \tag{33}$$

$$E_2 = \frac{1+r_1^2(\nu)\exp(\sqrt{4+\nu^2}\xi_L\varepsilon)}{1+r_1^2(\nu)}\ \frac{\exp[\sqrt{4+\nu^2}\xi_L(1-\varepsilon)]-1}{\exp(\sqrt{4+\nu^2}\xi_L)-1}\ . \tag{34}$$

It is easy to show that E_1 is symmetric in ε with respects to $\varepsilon=1/2$ increasing from zero at $\varepsilon=0$ to a maximum at $\varepsilon=1/2$, furthermore $E_1 \leqslant 1$ everywhere and $E_1=1$ only if $\nu \to \infty$ and $\varepsilon \neq 1$, $\varepsilon \neq 0$. On the other hand E_2 decreases monotonically from unity at $\varepsilon = 0$ to zero at $\varepsilon = 1$.

We now substitute equation (31) in (32) and arrive at

$$\lambda(\xi_L, \nu, \varepsilon) = \frac{\xi_L \nu}{f(1,\ \theta_G + E_1)} E_2 \exp\left(\frac{\theta_a}{\theta_G + E_1}\right) \tag{35}$$

Let us now define

$$\lambda_o \equiv \lambda(\varepsilon = o) = \frac{\xi_L \nu}{f(1,\ \theta_G)} \exp(\theta_a/\theta_G) \tag{36}$$

$$\lambda_{1/2} \equiv \lambda(\varepsilon=1/2) = \frac{\xi_L \nu E_2(\varepsilon=1/2)}{f\left[1, \theta_G + E_1(\varepsilon=1/2)\right]} \exp\left[\frac{\theta_a}{\theta_G + E_1(\varepsilon=1/2)}\right]. \tag{37}$$

For all ε, $\lambda(\varepsilon) < \lambda_o$

If either $\xi_L \nu$ or ν are small, E_1 is everywhere small, and $\lambda(\varepsilon)$ decreases monotonically from λ_o to zero as ε goes from zero to unity. On the other hand if neither $\xi_L \nu$ nor ν are small, $\lambda(\varepsilon)$ decreases from λ_o to zero, presenting relative minimum near $\varepsilon = 1/2(\lambda_{1/2})$ and maximum (below λ_o).

The above result, it sould be understood, does not imply the plainly absurd conclusion that for $\lambda > \lambda_o(\xi_L, \nu)$ there is no solution to Eqs.(7)-(9). Notice that as λ_o approaches λ_o from below ($\xi_t \to o$), hydrazine burning occurs closer and closer to the bars origin. At $\lambda=\lambda_o$, we have $\xi_t=0$, and from Sec. II,

$$\begin{aligned} A_2 &= 0 \\ \theta_t &= \theta(\xi < 0) = \theta_G \\ \theta(\xi > 0) &= 1 + \theta_G \\ \theta_B(\xi) &= 1 + \theta_G \ ; \end{aligned}$$

thus the chemical heat release and the heat transfer terms in Eq.(8) would be equal to each other right at the start. The point is the clear: for λ comparable to λ_o, the analysis of Secs. II and III breaks down because there is <u>no</u> region enclosing the origin where chemical heat release may be neglected. In fact for $\lambda >> \lambda_o$, the heat transfer

term should be neglected until burning does occur if at all; then from Eqs.(7)-(9) one would obtain

$$\frac{d\theta}{d\xi} = \frac{\lambda}{\xi_L} f e^{\theta_a/\theta} , \quad Y_2 + \theta = 1 + \theta_G , \quad \theta(\xi = 0) = \theta_G \tag{38}$$

in a thin, ignition layer at the origin, while for $\xi > 0$

$$\theta = \theta_B = 1 + \theta_G , \quad Y_1 = 0. \tag{39}$$

As λ becomes larger and larger, the ignition width becomes smaller and smaller.

The criterion to determine whether burning does or does not occur, is related to the width of the ignition layer in (38) and in Sec. III. The hypothesis underlying Eqs. (38) and (39), and the analysis of Secs. II and III is that the width of the ignition layer be small compared with the bars length. Now, in Sec. IV that width is given by $\Delta\xi \sim 1$, so that the analysis breaks down unless

$$\Delta\xi \sim \frac{\theta_t^2}{\theta_a \theta_t'} << \xi_L$$

or |using Eq.(29)|

$$\lambda >> \frac{\theta_t^2 \exp(\theta_a/\theta_t)}{\theta_a f(1,\theta_t)} ; \tag{40}$$

Equation (38) yields similarly

$$\lambda >> \frac{\theta_G^2 \exp(\theta_a/\theta_G)}{\theta_a f(1,\theta_G)} . \tag{41}$$

It is then clear that a rough criterion for burning to occur would be condition $\lambda > \lambda^*$, where

$$\lambda^* \equiv \frac{2\theta^2}{\theta_a f(1,\theta)} \exp \frac{\theta_a}{\theta} , \tag{42}$$

with $\theta = \theta_G$ for $\lambda > \lambda_o$ [see Eq.(41)] and $\theta = \theta_t$ for $\lambda < \lambda_o$ [see Eq. (40)] where θ_t is a function of λ through Eqs.(31) and (32). The factor of 2 arises from setting $\Delta\xi/\xi_L = 1/2$; although the thin ignition layer hypothesis would then not be valid, the criterion should give the minimum λ for burning within a factor of 2 (or 1/2). Clearly, it is implied that for $\lambda < \lambda^*$ there is no burning.

It follows then that, given ξ_L, ν and θ_E, the necessary and sufficient condition for burning to occur is that

$$\lambda > \lambda_{min}(\xi_L, \nu, \theta_G); \tag{43}$$

λ_{min}/λ^* has been drawn in fig. 13. Since $\theta_t > \theta_G$ from equation (31), $\lambda^*(\theta_t) < \lambda^*(\theta_G)$, so that in all cases

$$\bar{\lambda}_{min} < \bar{\lambda}^*(\theta_G) = \frac{2\theta_G^4}{1.8\theta_a} e^{\theta_a/\theta_G} ; \tag{44}$$

we took $f(1,\theta) \sim 1.8/\theta^2$ from equation (29) of Chapter II, and thus $\bar{\lambda}$ should be used everywhere from now on. To obtain $\bar{\lambda}_{min}$ we first consider the case $\bar{\lambda}_o > \bar{\lambda}^*(\theta_G)$. Given θ_G, ξ_L and ν, we let ε vary from zero to unity to find the epsilon rate, and thus the minimum value of λ, λ_{min}, for which

$$\bar{\lambda}(\xi_L, \nu, \varepsilon) > \bar{\lambda}^*(\xi_L, \nu, \varepsilon),$$

making use of equation (31) for $\theta_t(\theta_G, \xi_L, \nu, \varepsilon)$. We then notice that as $\xi_L.\nu \to o$, $\theta_t \to \theta_G$, and therefore $\overline{\lambda}^* \to \overline{\lambda}^*(\theta_G)$; now, since $\overline{\lambda}_o = \overline{\lambda}^*(\theta_G)$ for $\xi_L.\nu << 1$, it follows that there is no special need to discuss separately the case $\overline{\lambda}_o < \overline{\lambda}^*(\theta_G)$ (and thus neither the case $\overline{\lambda}_o \sim \overline{\lambda}^*(\theta_G)$). Notice that for $\theta_G = \theta_w$, $\overline{\lambda}^*(\theta_G)$ is less than $\overline{\lambda}_{cr}$ of chapter II, by more than an order of magnitude.

CHAPTER V

GENERAL DISCUSSION

Authors

Prof. J.R. Sanmartín*
Dr. E. Fraga

*Presently at the School of Aeronautics Polytecnic University of Madrid.

Chapter V

GENERAL DISCUSSION

We shall review here the results obtained in this report, emphasizing their practical application in a real case. We shall stress in particular those criteria that allow to decide under which conditions an electrothermal hydrazine engine would work.

In Chapter I we obtained overall reaction rate and stoichiometry valid for relatively low temperatures (700° to 1000°K), the condition of interest to study ignition. These results are only required for the quantitative analysis in Chaps. II and IV, and therefore need not be detailed here. We notice that the overall kinetics is obtained from the Eberstein-Glassman scheme, and thus the quantitative results of Chaps. II and IV are dependent on the validity of that scheme (although the formal analysis there would remain valid for quite different overall kinetics).

In Chapter III we studied the vaporization process and the transient effects developing after the start of the engine assuming homogeneous conditions inside the chamber, in connection with the well stirred reactor model of the engine considered in Chapter II. We first obtained the droplet vaporization time both in the rate limited limit

$$t_{(\gamma=o)} \sim r_{so} \frac{\rho_L(T^e)}{P_v(T^e)} \sqrt{\frac{2\pi RT^e}{M_1}} \qquad (1)$$

and in the diffusion limited limit

$$t_{(\gamma=o)} \sim r_{so}^2 \frac{\rho_L(T_s)C_p(T_s)}{2M_1\kappa(T_s)I(T_\infty,T_s)} \qquad (2)$$

where r_{so} is the initial radius, M_1, P_v, ρ_L, C_p and κ the molar mass, vapor pressure, liquid density and gas molar specific heat and thermal conductivity of hydrazine respectively; I is a certain integral close to unity, and T^e is the entrance temperature. The dependency on T_s and T_∞ is weak; one may thus take T_∞ equal to the temperature at the grids and chamber walls, T_w, and T_s equal to the boiling temperature at the chamber pressure P. A criterion follows immediately: in a pulsed regime the pulsed duration τ must satisfy

$$\tau >> t_{(\gamma=o)} \qquad (3)$$

where the largest of times (1) and (2) must be used; for $r_{so} > 10^{-5}$ cm, time (2) is the largest and we arrive at condition

$$\tau(\text{sec}) >> 2.10^3 r_{so}^2 \ (\text{cm}) \qquad (3')$$

having used $T_s \sim 500°K$, and $T_\infty \sim T_w \sim 800°K$.

Secondly, we obtained the rate of vaporization and thus, the liquid hydrazine mass fraction at the chamber exit, Y_{1L}. The obvious requirement $Y_{1L} << 1$ leads to the condition

$$\frac{2}{5} \frac{t_{(\gamma=o)}\dot{m}RT}{M_1 PV} << 1 \qquad (4)$$

where $\dot{m}$ is the mass flow rate and V the chamber volume.

Next we estimated the time required for gas filling of the chamber t_f

$$t_f \sim \left[\frac{4}{3} \frac{V}{\dot{m}} \frac{M_1 P}{RT} t_{(\gamma=o)} \right]^{1/2} ; \qquad (5)$$

again the condition

$$\tau >> t_f \qquad (6)$$

should be satisfied for a pulsed regime.

A final, obvious requirement is that the wall heat capacity C_w be much larger than the heat capacity of the gas inside the chamber, so that the grids and walls heat the gas without showing noticeable thermal depletion:

$$\frac{PV}{RT} \frac{C_p}{C_w} << 1. \qquad (7)$$

The main results of this Report are those contained in Chapters II and IV. In Chapter II a well stirred reactor model was considered. We discussed both, the pulsed regime

$$\tau << \frac{M_1 C_w}{\dot{m} C_p} , \qquad (8)$$

and the steady regime

$$\tau >> \frac{M_1 C_w}{\dot{m} C_p} . \qquad (9)$$

For the first case, the results derived for the hydrazine molar fraction and dimensionless temperature (defined in Eq. 24 of Chap. II) at the exit, X_1 and θ, as functions

of $\bar{\lambda} \propto VP^2/\dot{m}$, (defined in Eq. 29), T^e, T_{wo} and $\sigma-1 \propto K/\dot{m}$ (defined in Eq. 23) (where K is the energy transfer from walls to gas per unit time and unit degree of temperature difference) are shown in Figs 2-6. From the figures we concludedthat there is a function of T^e, T_{wo} and σ, called $\bar{\lambda}_{ign}$, such that if

$$\bar{\lambda} > \bar{\lambda}_{ign}$$

near full combustion occurs, while for

$$\bar{\lambda} < \bar{\lambda}_{ign}$$

there is almost no combustion; $\bar{\lambda}_{ign}(\sigma, T^e, T_{wo})$ is given in figures 9 (or figures 10). Notice that for σ less than about 5, $\bar{\lambda}_{ign}$ becomes extremely large and that there is a minimum value of $\bar{\lambda}_{ign}$, called $\bar{\lambda}_{cr}(T_{wo}, T^e)$, which is given in Fig. 12. The minimum value of σ for which $\bar{\lambda}_{ign} = \bar{\lambda}_{cr}$, called $\sigma_{inf}(T_{wo}, T^e)$ is given in Fig. 11. Clearly the range of interest for σ is

$$5 < \sigma < \sigma_{inf} ;$$

to increase the heat transfer, so that $\sigma > \sigma_{inf}$, yields no benefits. In fact, too efficient heat transfer should be avoided, since assuming that burning occurs, θ decreases as σ increases. Obviously, λ_{cr} may be lowered increasing T_{wo}, or (more weakly) T^e. Notice that $\bar{\lambda}$ increases with pressure and volume and decreases with the mass flow rate.

For steady regime, X_1 and θ are shown in Figs. 8 as function of $\bar{\bar{\lambda}} \propto PV/\dot{m}$ (defined in Eq. 30 of Chapter II), T_{wo} and T^e, the dependence on σ being negligible. Again near full combustion occurs for $\bar{\lambda} > \bar{\lambda}_{ign}$ and no combustion for $\bar{\lambda} < \bar{\lambda}_{ign}$,

Use of the results of Figs. 2-6 and Figs. 8 allow to compute the thrust of the engine, for pulsed and steady regimes respectively.

In Chapter IV, we considered the hydrazine engine as a plug-flow reactor, as both an alternative and a complementary analysis to the study of a well-stirred reactor model carried out in Chapter II. This model has shown that an engine working purely as a well-stirred reactor presents serious inconvenients: the minimum value of λ for burning, $\lambda_{cr}(T_{wo}, T^e)$ may be too high to be acceptable; the strong thermal coupling of walls and grids to the gas (large σ) required to avoid large values of λ_{ign} leads to a low burn-out temperature in a pulsed regime, furthermore, the large capacity of chamber walls required to avoid thermal depletion of the walls in a pulsed regime, may lead to an unacceptable long time for achievement of a steady regime (steady wall temperature).

In the plug-flow model we assumed a steady plug-flow along solid bars (thermaly isolated from the walls), that conduct heat from a regime downstream where burning occurs, to the origin upstream, where the hydrazine arrives unburned and at a temperature T_G.

We find that burning occurs if $\bar{\lambda} > \bar{\lambda}_{min}(T_G, \nu\xi_L, \nu)$ where λ_{min} is given in Fig. 13; ν and ξ_L are defined in equation (6) k_B, S_B and L are the bars heat conductivity, total cross section and length respectively. We find that $\bar{\lambda}_{min}$ is at least an order of magnitude smaller than λ_{cr}, and for appropriate ν and ξ_L may be substantially smaller. We find also that if $\lambda \gtrsim \lambda_o \equiv (\xi_L \nu \theta_G^2/1.8)\exp(\theta_a/\theta_G)$, there is no need for bars in the plug-flow model. In addition for a pulsed regime, T_G may be taken near to T_{wo}, the temperature mantained in walls and grids in the well stirred part of the reactor, where hydrazine is vaporized and heated, and the

burn-out temperature is high; clearly the bars should have a low heat capacity. For a steady regime, however, part of the thermal energy of the burned gas living the chamber must be used to vaporize and heat the entering hydrazine since otherwise thermal depletion would lead to a lowering of T_{wo} (and T_G).

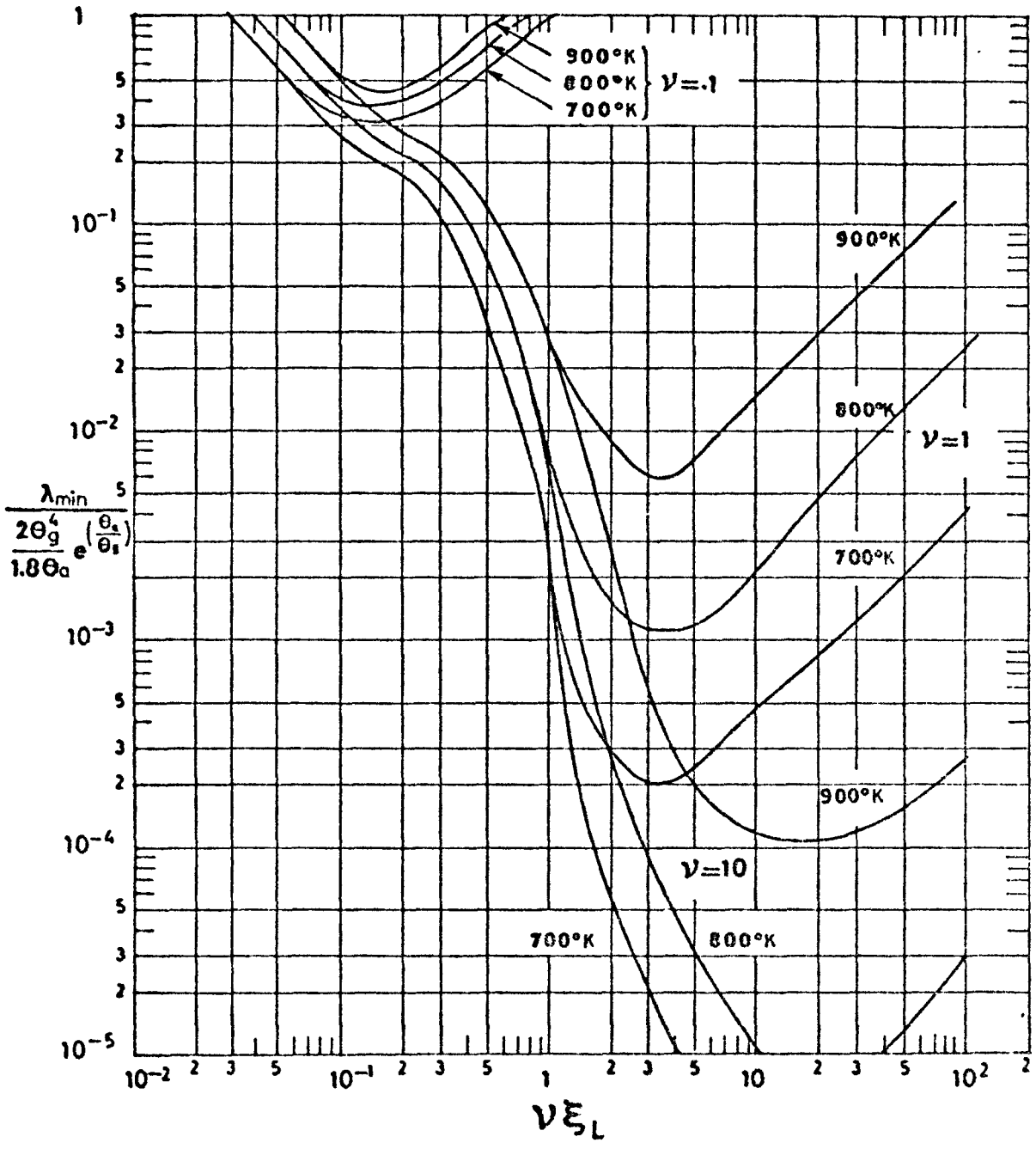

Fig.13 $\overline{\lambda}_{min}$, value of λ at which burning occurs, versus $\nu\xi_L$, for several values of ν and T_G.

List of symbols appearing in the figures

C_{pn}	Middle value of the hydrazine molar heat capacity at constant pressure.
K	Heat transfer constant between the mixture and the chamber.
$\dot{m}$	Mass flow rate.
P	Pressure.
P_v	Vapor pressure.
Q	Molar heat of reaction at constant pressure, Eq. (19), Chapter II.
T	Temperature.
T_b	Boiling temperature.
T^e	Entrance temperature.
T_G	Temperature at which the mixture leaves the well stirred-reactor part when there is a well stirred-reactor followed by a plug flow; $\simeq T_{wo}$.
T_{wo}	Steady state mean temperature of grid and walls Eq.(11), Chapter II.
X_1	Hydrazine molar fraction.
X_{cr}	Defined in Eq.(37a), Chapter II.
θ	Non-dimensional temperature, Eq.(24), Chapter II.
θ_a	Non-dimensional activation temperature.
θ_G	Non-dimensional temperature corresponding to T_G.
θ_{wo}	Non-dimensional temperature corresponding to T_{wo}.
$\bar{\lambda}$	Defined in Eq.(29), Chapter II, proportional to $\frac{VP^2}{\dot{m}}$ (V chamber volume).
$\bar{\lambda}_{cr}$	Minimum value of $\bar{\lambda}$ for burning to occur defined in Eq.(37b).

$\bar{\lambda}_{ign}$ Value of $\bar{\lambda}$ for ignition to occur p. II. 15.

$\bar{\lambda}_{max}$ Maximum value of $\bar{\lambda}$.

$\bar{\lambda}_{min}$ Minimum value of $\bar{\lambda}$.

$\bar{\bar{\lambda}}$ Defined in Eq.(30), Chapter II, proportional to $VP/\dot{m}$.

ν Defined in Eq.(6), Chapter IV, proportional to $\frac{\sqrt{k_B S_B k}}{\dot{m}\sqrt{L}}$ k_B, S_B and L are the heat conductivity, total cross-section and length of the bars.

ξ_L Defined in Eq.(6), Chapter IV, proportional to $\frac{KL}{(K_B S_B)^{1/2}}$

σ Defined in Eq.(23), σ-1 proportional to $\frac{K}{\dot{m}}$.

σ_{inf} Value of σ for which $X_1(\bar{\lambda})$ presents an inflexion point.